UNIVERSIDADE FEDERAL DE MINAS GERAIS

ESCOLA DE ENGENHARIA

THE ELECTRICAL ENGINEERING GRADUATE PROGRAM

BRUNO DE ÁVILA SBAMPATO

COMPARATIVE ANALYSIS BETWEEN MONO-Si AND OPV PHOTOVOLTAIC DEVICES: ACCELERATED AGING EXPERIMENTS APPLIED TO LCA AND LCOE

Belo Horizonte

2017

BRUNO DE ÁVILA SBAMPATO

COMPARATIVE ANALYSIS BETWEEN MONO-Si AND OPV PHOTOVOLTAIC DEVICES: ACCELERATED AGING EXPERIMENTS APPLIED TO LCA AND LCOE

ANÁLISE COMPARATIVA ENTRE DISPOSITIVOS FOTOVOLTAICOS DE MONO-Si E OPV: EXPERIMENTOS DE ENVELHECIMENTO ACELERADO APLICADOS A ACV E LCOE

Master's thesis presented to The Electrical Engineering Graduate Program of School of Engineering of Federal University of Minas Gerais.

Supervisor: Prof. Dr. Wadaed Uturbey da Costa

Co-supervisor: Prof. Dr. Davies William de Lima Monteiro

Belo Horizonte

2017

DEDICATION

À mudança, à transformação, à evolução. À persistência nessa busca, à retomada após cada queda. A cada queda.

Ao rompimento das barreiras e dos limites. Ao conhecimento... do meio ambiente, da eletricidade, dos materiais, de si mesmo, da Engenharia, do ICB, da FAFICH, da Música, do ICEx, do IGC, etc.

À derrubada das fronteiras da visão humana. À técnica. À técnica aplicada ao humano.

Aos propósitos, aos sonhos, aos objetivos nobres. Ao SOL, que brilha para todos!

ACKNOWLEDGEMENTS

À minha família que me deu condições de chegar até ao mestrado e me apoiou em todos os sentidos durante todo este percurso.

À minha orientadora, Professora Dra. Wadaed Uturbey da Costa, que aceitou o desafio deste trabalho multidisciplinar, acreditou na proposta e me acompanhou de perto nesta trajetória.

Ao meu co-orientador, Professor Dr. Davies William de Lima Monteiro, que primeiramente me acolheu no PPGEE e me abriu as portas do OptMA^{lab} que levarei com carinho em todas as fases futuras de minha vida.

Aos colegas do OptMA^{lab}, que sempre demonstraram um espírito de grupo muito forte dividindo conhecimentos e se apoiando mutuamente e também aos colegas orientados pela Wadaed com os quais troquei valiosas experiências.

À Anne Lisboa que colaborou com este trabalho através de suas atividades de iniciação científica.

Aos demais colegas do PPGEE que dividiram esses momentos comigo e que muitas vezes ofereceram ajuda sem esperar nada em troca.

Ao Dr. Anderson Lima e ao Dr. Diego Bagnis do CSEM Brasil pelo fornecimento das amostras de Organic Photovoltaics, disponibilização dos equipamentos de envelhecimento acelerado e pelo aprendizado a respeito desta tecnologia.

À Prof. Dra. Izete Zanesco, ao Prof. Dr. Adriano Moehlecke, ao Dr. Moussa Ly e ao Prof. Dr. Sérgio Boscato do NT-Solar da PUCRS pela disponibilização da estrutura e de pessoal para laminação das amostras de silício monocristalino.

À Prof. Dra. Luciana Pedrosa pelo apoio e compreensão no momento mais difícil.

E aos amigos do Engenheiros da Alegria, do skate e do Coltec pelo suporte e pelos momentos de descontração.

ABSTRACT

Nowadays, the electrical energy matrix diversification as well as the intensification of the use of renewable sources of energy makes the study of photovoltaics (PV) very relevant. In this work, an emerging technology is compared with a benchmark one, namely, organic photovoltaics (OPV) devices and monocrystalline silicon (mono-Si) devices. The comparison includes environmental aspects, done through Life Cycle Assessment (LCA) methodology and costs characteristics, analyzed using the Levelized Cost of Energy (LCOE). In both calculations, the amount of energy generated by a PV module is very important, and it depends on the device efficiency and degradation through time, hence tests of electrical performance with accelerated aging were held. For LCA, the impact categories analyzed were Global Warming Potential (GWP), Cumulative Energy Demand (CED), Human Toxicity Total, Ecotoxicity total and Metal Depletion Potential (MDP). Besides that, Energy Payback Time was calculated. Experimental data from the accelerated aging tests are used to estimate the amount of energy that would be produced by modules of each technology and makes it possible to calculate values of Life Cycle Impact Assessment having kWh as reference unit. For the LCOE, DC power plants of 3 kWp on rooftops were considered in a time horizon of ten years, one with OPV modules and the other with mono-Si ones. Again, the information of energy generated through time was used as input data. As a result, OPV had smaller values for CED, EPBT and GWP, but they were higher for MDP, Human Toxicity Total, Ecotoxicity total and it also had a higher LCOE, demonstrating to have a worst performance than mono-Si, in general.

Keywords

Solar energy, organic photovoltaics, life cycle assessment, levelized cost of energy, accelerated aging test**.**

RESUMO

Atualmente, a diversificação da matriz energética elétrica, bem como a intensificação do uso de energias renováveis, torna o estudo de fotovoltaicos (FV) muito relevante. Neste trabalho, é feita a comparação de uma tecnologia emergente com um benchmark, especificamente, dispositivos fotovoltaicos orgânicos (do inglês, OPV) e dispositivos fotovoltaicos de silício monocristalino (mono-Si). A comparação inclui aspectos ambientais, feita através da metodologia de Avaliação de Ciclo de Vida (ACV) e características de custos, analisadas usando-se o Custo Nivelado da Energia (do inglês, LCOE). Em ambos os cálculos, a quantidade de energia gerada por um módulo FV é muito importante. Ela depende da eficiência do dispositivo e de sua degradação ao longo do tempo, então, testes do desempenho elétrico com envelhecimento acelerado foram realizados. Para a ACV, as categorias de impacto analisadas foram o Potencial de Aquecimento Global (PAG), Demanda Acumulada de Energia (DAE), Toxicidade humana total, ecotoxicidade total e Potencial de Depleção de Metais (PDM). Além disso, o Tempo de *Payback* Energético (do inglês, EPBT) foi calculado. Dados experimentais oriundos do teste de envelhecimento acelerado foram usados para estimar a quantidade de energia que seria produzida pelos módulos de cada tecnologia e tornou-se possível calcular valores de Avaliação de Impacto de Ciclo de Vida tendo o kWh como unidade de referência. Para o LCOE, usinas DC de 3 kWp instaladas em telhados foram consideradas em um horizonte de tempo de dez anos, uma com módulos OPV e a outra com mono-Si. Novamente a informação de energia gerada de acordo com o tempo foi usada como dado de entrada. Como resultado, o OPV teve valores menores de DAE, EPBT e PAG, mas valores maiores para PDM, Toxicidade humana total e Ecotoxicidade total e também teve um LCOE mais elevado, demonstrando ter uma performance geral pior que o mono-Si.

Palavras chaves

Energia solar, fotovoltaica orgânica, avaliação de ciclo de vida, custo nivelado da energia, teste de envelhecimento acelerado.

FIGURE INDEX

TABLE INDEX

LIST OF ABBREVIATIONS, SYMBOLS AND ACRONYMS

ADP	Abiotic Depletion Potential
AP	Acidification Potential
CED	Cumulative Energy Demand
CSS	Continuous Solar Simulator
EP	Eutrophication Potential
EPBT	Energy Payback Time
EPE	Equivalent Primary Energy
ETL	Electron Transport Layer
EVA	Ethylene Vinyl Acetate
FAEP	Freshwater Aquatic Ecotoxicity Potential
FF	Fill Factor
GWP	Global warming potential
HOMO	Higher Occupied Molecular Orbital
HTL	Hole Transport Layer
HTP	Human Toxicity Potential
IMI	ITO-Metal-ITO
Im	Current on maximum power point
Isc	Short Circuit Current
ITO	Indium Thin Oxide
IV curve	Curve of current against voltage
Wp	Watt peak
LCA	Life Cycle Assessment
LCI	Life Cycle Inventory
LCIA	Life Cycle Impact Assessment
LCOE	Levelized Cost of Energy
LUMO	Lowest Unoccupied Molecular Orbital
MAEP	Marine Aquatic Ecotoxicity Potential
MDP	Metal Depletion Potential
MG-Si	Metallurgical Grade Silicon
Mono-Si	Monocrystalline Silicon
ODP	Ozone Depletion Potential
OPV	Organic Photovoltaics
PCOP	Photochemical Oxidation Potential
PR	Performance Ratio
PV	Photovoltaic
PV curve	Curve of power against voltage
R2R	Roll to roll
STC	Standard Test Conditions
TEP	Terrestrial Ecotoxicity Potential
Vm	Voltage on maximum power point
Voc	Open Circuit Voltage

TABLE OF CONTENTS

1 INTRODUCTION

Photovoltaic (PV) solar modules are devices capable of converting solar radiation into electricity. This energy conversion technology is gaining more and more space in a scenario of necessity of avoiding greenhouse gases emissions and of importance of electrical energy matrix diversification.

Despite the low environmental impacts during a PV power plant operation, the same cannot be stated about its silicon modules production process (FILHO, 2013). Therefore a broad analysis of those impacts may conduct to an energetic planning more adequate and to a more complete vision of a power conversion technology.

Figure 1 illustrates the development of PV technologies through time. As can be seen, there are many types of them at different levels of maturity. They have different efficiencies (since 10.6% until 46% nowadays) and started being developed at different moments (since 1976 until 2017).

Figure 1 - Best Research-Cell Efficiencies

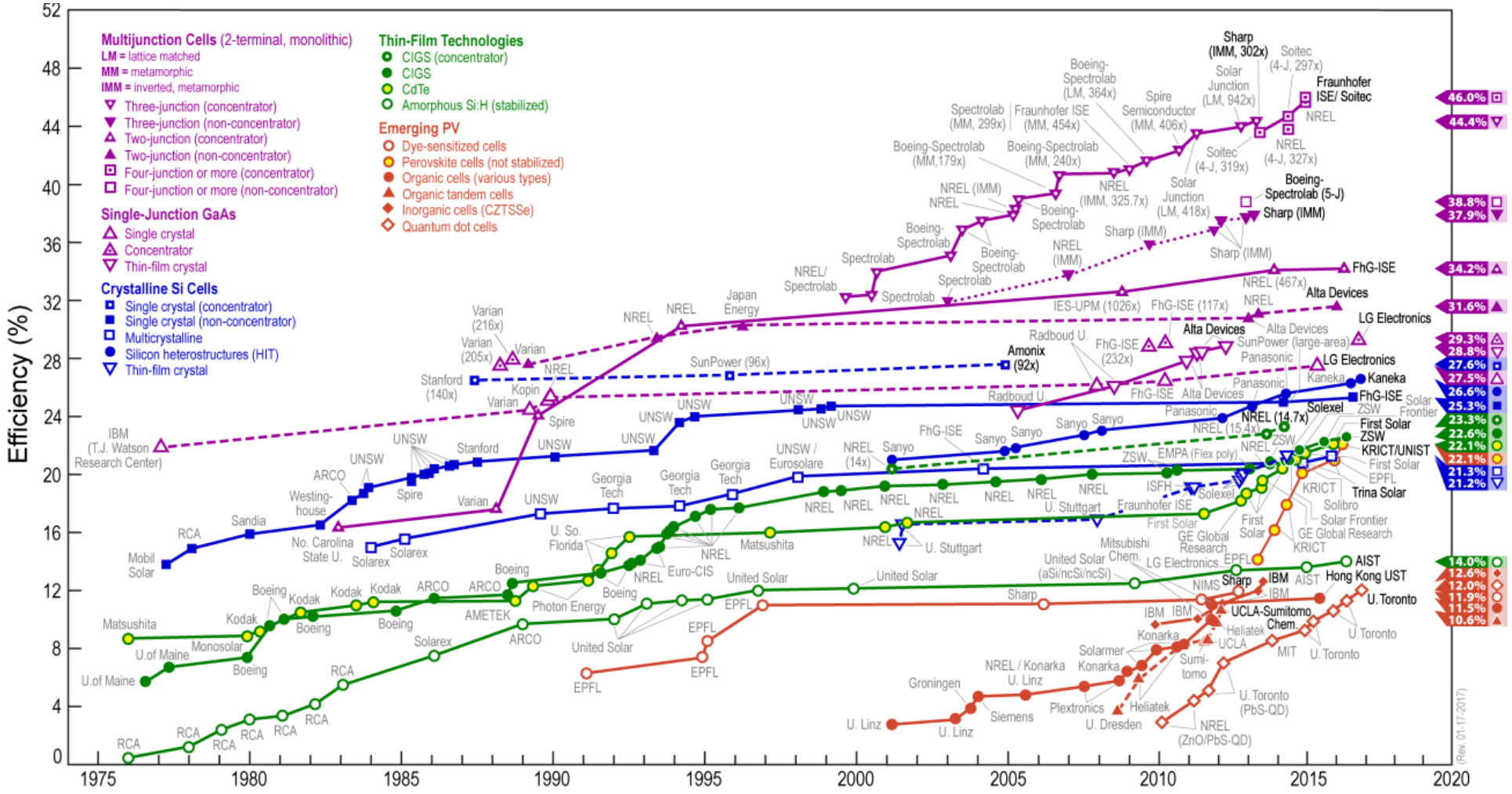

Source - NREL, 2017

In this chapter, there is a section dedicated to the motivation of this study, another clarifying its aims and then one explaining how the other four chapters of the master's thesis are structured.

1.1 Motivation

New PV modules technologies arise as time goes on bringing new applications, higher efficiencies or lower costs. One of those emerging technologies is the organic photovoltaic (OPV). Based on organic polymers, solar panels may be built on flexible materials, semitransparent, lightweight and through a process which requires less energy expenditure. It had a rapid development in the last few years and then deserves attention. Besides that, Belo Horizonte, Brazil, has one of the few OPV manufacturers in the world. Since it is a relatively new technology, it is important to better understand its capabilities and limitations.

Due to the variety of PV technology options that is available, it becomes necessary to have a systematic way to compare them considering a variety of aspects of energy generation through photovoltaics. It is worth stating that even among the OPVs a variety of types is possible. Very important characteristics of each of those technologies are the environmental impacts and the cost.

This matter interests the photovoltaics and LCA community in general, academics, decision makers related to energy planning, electric sector regulator and industry. It allows the sector to better understand the environmental impacts of its activities.

The present study differs from others LCA based research, because it integrates this methodology with a cost analysis, besides using experimental data to estimate energy generation.

1.2 Aims

This aims of the study are further clarified dived into general and specific ones.

1.2.1 General aims

The general aim of this master's thesis is to compare two PV technologies, namely, mono crystalline silicon (mono-Si) and organic photovoltaics (OPV) through a joint analysis of costs and environmental impacts originated from production of those PV module technologies. In order to do so, an estimate of energy generation is demanded.

The first is a well known technology and widely used, taken as reference, while the second is a less mature technology with differentiated applications.

1.2.2 Specific aims

Part of the specific aims of this study is the application of two methodologies. One of them is the Life Cycle Assessment (LCA), seeking to quantify environmental impacts of both technologies production. The other one is the Levelized Cost of Energy, in order to obtain the energy unitary cost of OPV as well as mono-Si.

The other specific aim is related to the experimental part of the study, because an estimate of degradation through time is necessary to predict the energy generated by each technology, which is input for LCA and LCOE. Then, the devices are used on the accelerated aging test. Besides that, prior to this test, the sample preparation is required, it is, the lamination of the mono-Si solar cells.

1.3 Master's thesis structure

This master's thesis is structured in order to compare organic solar cells and silicon photovoltaics based on Life Cycle Assessment and Levelized Cost of Energy. Then, in the next chapter there are Basic Concepts and Literature Review, regarding the photovoltaic solar energy technologies, the Life Cycle Assessment methodology, the Levelized Cost of Energy, the accelerated aging tests and the measuring systems. On chapter 3 the master's thesis methodology is described in terms of the analysis of each technology performance and how LCA and LCOE were applied. On chapter 4 the results are presented, since the lamination process done for mono-Si, going trough

visual inspection, the electrical performance, LCOE, LCA and lastly a global discussion. Finally, on the last chapter, conclusions are drawn and further work is recommended.

2 BASIC CONCEPTS AND LITERATURE REVIEW

This chapter starts explaining how the two PV technologies analyzed work and how they are manufactured. Later the equipment used to measure electrical performance is described. The third section concerns the levelized cost of energy and then the life cycle assessment methodology and the computational tools that assist on its application are presented. Finally, there is a section dedicated to accelerated aging tests.

2.1 The two technologies under analysis in this study

2.1.1 Mono Crystalline Silicon

Monojunction photovoltaic cells are semiconductor devices composed by a p-n junction in which the photovoltaic effect happens. This effect is the conversion of photons in electrical energy due to their absorption inside the solar cell. In this case an electron is excited from the valence band to the conduction band, creating an electron-hole pair. A built-in electric field is established in the region around the p-n junction and it is responsible to separate those photogenerated carriers that can be created inside itself (drift current) or out of it and diffusing until this region (diffusion current). The accumulation of electric carriers on the different sides of the cell causes a difference on the electric potential between the electrodes of the cell and a photogenerated current, which depends on the light intensity (SBAMPATO *et al.*, 2016).

In this study, mono crystalline silicon cells were used. Commercially, silicon devices are the most used, mainly as polycrystalline structure, also known as multi-crystalline.

Part of the silicon used to be originated from the scrap of microelectronics industry, however, with the fast PV market growing, the metallurgical silicon (MG-Si) started being more and more used to produce single crystalline silicon. (MARKVART AND CASTAÑER, 2003).

One of the most used processes to obtain the single silicon crystal is known as Czochralski. It consists of introducing a seed of silicon crystal attached to a rod on a recipient containing liquid silicon. In the sequence, the rod is slowly

suspended rotating while more atoms join the solid piece being formed according to the original crystal orientation. Its diameter is defined by the rotating speed. Later, the ingot is sliced into several rather thin wafers (350 to 750 µm) and shaped as a pseudo-square (TOM MARKVART AND LUIS CASTAÑER, 2003).

After that, the wafer is processed to become a cell. It may be additionally etched superficially in order to texturize it and hence improve optical confinement. It has to be cleaned prior to starting the junction formation, when phosphorous is added as a dopant to the wafer through diffusion in order to create an n-region on the wafer that is already p-type due to Boron added in-situ still during the Czochralski process. Then, the front surface is passivated with hydrogen and an antireflection coating is added, the back side surface receives an aluminum paste containing silicon. This creates a plain surface of conductor while on the front surface a silver grid is added through screen printing. Figure 2 shows an illustration of a mono-Si cell structure.

Figure 2 - Mono-Si PV cell parts.

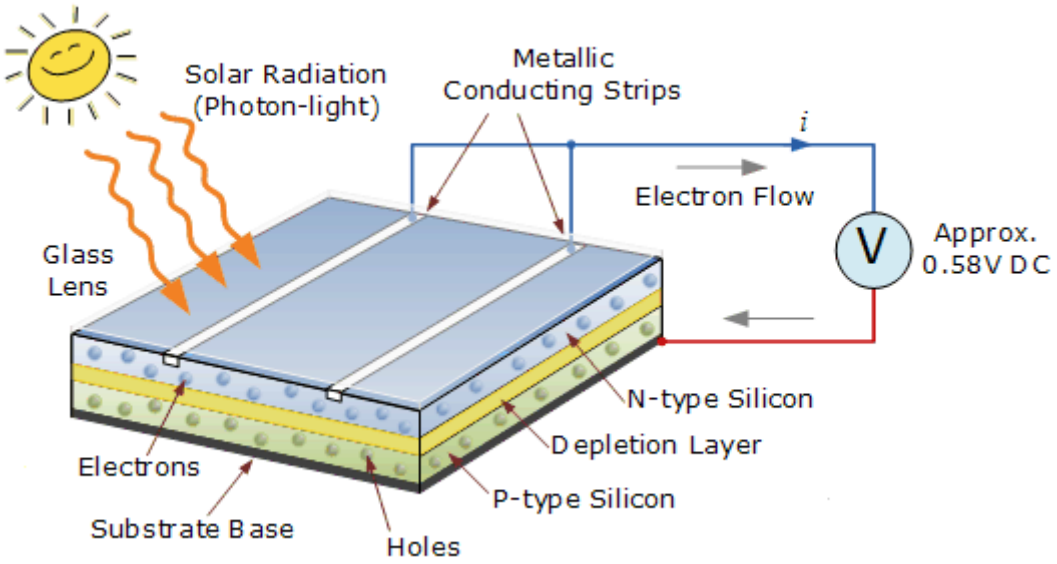

Source – adapted from http://www.alternative-energy-tutorials.com/solar-power/photovoltaics.html accessed on 10/08/2017

To construct a solar panel, those cells are connected in a suitable combination of parallel and series associations and go through lamination. Since the

lamination process was made during this study to prepare the samples used, it will be better explained on section 3.1.2.

2.1.2 Organic Photovoltaic

The other technology under study is the organic photovoltaic. It is an emerging technology based on polymers. Those solar panels may be made of flexible materials, semitransparent, light and through a process which does not include temperatures as high as the process of crystalline silicon. In Belo Horizonte, Brazil, there is a company named CSEM Brasil which is a research center seeking to make the manufacturing process of this kind of module viable, due to the perception that this is a market niche in which the country may act on the state of the art. CSEM Brasil enabled this study through providing the samples of this technology besides allowing the use of aging equipments.

The LCA is very important to assess the developing organic technologies. In this kind of study, many assumptions may be taken into account, then there are several of them which have to be reported such as the irradiation, the module rated efficiency, system's performance ratio, type of system (roof top or ground mounted), expected life time, besides others aspects that are common to all types of LCA study, which will be further explained.

Organic modules are made of an active layer that has donor and acceptor polymers, each of them have a highest occupied molecular orbital (HOMO) and a lowest unoccupied molecular orbital (LUMO) with different energy levels that an electron may have. It is worth stating that donors have highest HOMO level as well as highest LUMO level. Besides that, the cathode has an energy level lowest than the acceptor's LUMO and the anode's energy level is higher than the donor's HOMO, as illustrated on figure 3. Hence if an electron-hole pair is photogenerated and it reaches the interface between both polymers, they will be separated by the electric field and the electron will be transported through the described energy cascade, going to lower energy levels. In the meanwhile the hole has the opposite behavior reaching higher energy levels, therefore going to the other direction in the module (ANCTIL; FTHENAKIS, 2012). In order to have all this working, an usual device starts with a substrate which is transparent and has an also transparent conductor, then an electron transport

layer is printed, followed by the active layer, the hole transport layer and finally a metal conductor.

Figure 3 - Organic solar cell structure and active layer energy levels

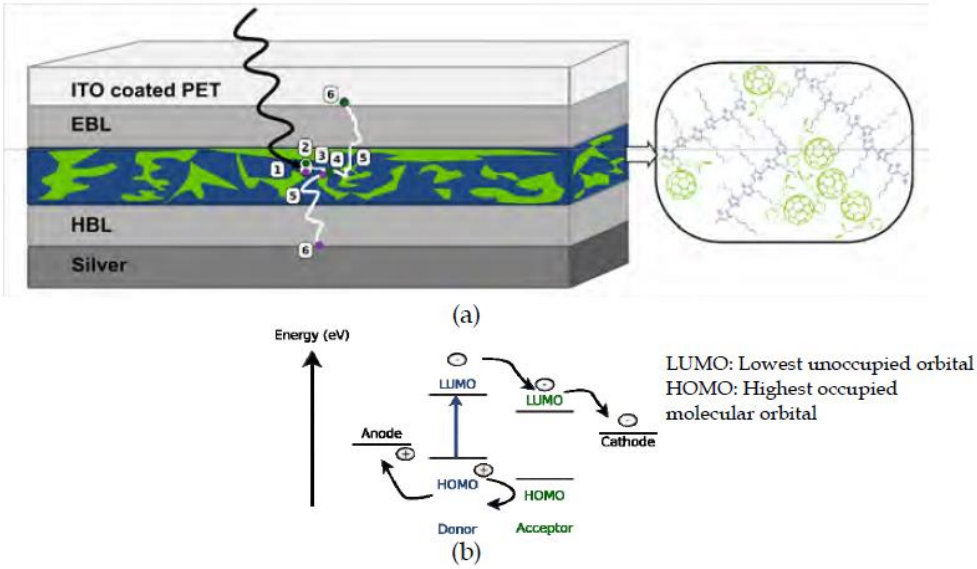

Source - ANCTIL; FTHENAKIS, 2012.

It is possible to improve the efficiency of the cell through lowering the band gap of the active layer polymers and also having a stack with more than one active layer, so that different light wavelengths may be absorbed, those are named tandem cells. Besides that, tuning the hole transport layer's work function is another way to extract more energy from this type of device (CHENG *et al.*, 2015).

Life cycle inventory data may be obtained from manufacturers whenever possible. However this type of data is scarce even in data bases and only fullerenes production have few information available (ANCTIL; FTHENAKIS, 2012).

2.2 Measuring systems

One of the main characteristics of a PV cell is its IV curve. It is, current and voltage pairs are measured in a certain range and plotted. The main region to operate solar cells is positive voltage and negative current, although the graph is usually flipped so that the curve is fitted on the first quadrant. A power versus

voltage curve (PV curve) of a PV cell is also very common. Each voltage is multiplied by the corresponding current and plotted against itself.

As illustrated on figure 4, the curve has a short circuit current value (where it crosses the I axis) and an open circuit voltage value (where it crosses the V axis). However, its operation point is neither of them, since power is null on both, because either current or voltage is null. The curve has two sections, one close to a current source and another similar to a voltage source. Between them, there is the part named “knee”. There, the maximum power point will be found for the best combination of current-voltage product (Bueno, 2016).

Figure 4 - The IV curve

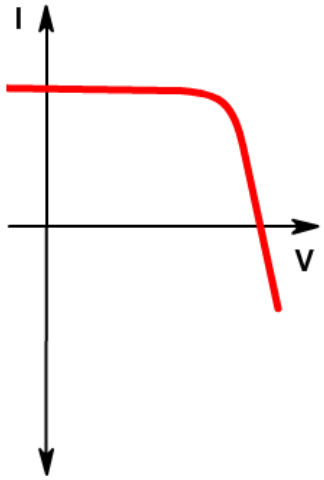

Source - http://www.pveducation.org/pvcdrom/iv-curve

In order to extract the solar cells’ IV curves a continuous solar simulator (CSS) was used as well as a source-meter. The first is designed to offer an irradiance very similar to the sun with 1000 W/m^2, according with AM 1.5 standard with a cooling system set to 25 ºC, according to the Standard Test Conditions (STC) (LAS, 2009). It means that air mass is 50% thicker than when the sun’s light is going across the atmosphere perpendicularly. Aiming the characterization, the Keithley’s source meter 2612B was used (KEITHLEY INSTRUMENTS, 2012[1]; KEITHLEY INSTRUMENTS, 2012[2]). In this case, it was a source of current in a certain range and it measured both, voltage and current, enabling the IV curve plotting.

2.3 Economic viability index

The economic viability index used is the Levelized Cost of Energy. This metric considers the life-cycle cost of a power plant, including its installation, operation and maintenance, as well as the total amount of energy that this plant will produce during this period, regarding its efficiency loss. It is given as the price per unit of energy. According to NREL (2017), LCOE calculation departs from the definition on eq. 1.

$$\sum_{\mathbf{n=1}}^{\mathbf{N}} \frac{\mathbf{LCOE_n \cdot Q_n}}{\mathbf{(1+d)^n}} = \sum_{\mathbf{n=0}}^{\mathbf{N}} \frac{\mathbf{C_n}}{\mathbf{(1+d)^n}} \quad (1)$$

In eq. 1, Q_n is the amount of energy generated per year, n is the year, N is the total PV system lifetime, d is the discount rate and C_n is the cost on each year including installation on the year it happens and operation and maintenance. Rearranging eq. 1 and considering LCOE a constant value per year, eq. 2 is obtained.

$$\mathbf{LCOE} = \frac{\sum_{\mathbf{n=0}}^{\mathbf{N}} \frac{\mathbf{C_n}}{\mathbf{(1+d)^n}}}{\sum_{\mathbf{n=1}}^{\mathbf{N}} \frac{\mathbf{Q_n}}{\mathbf{(1+d)^n}}} \quad (1)$$

This index is very used for the called “grid parity”, that refers to the comparison of LCOE with the electricity grid tariff of the place of implantation of the PV system. According to BRANKER et al., (2011), PV generation have reached grid parity in certain locations and as the systems escalate, it is expected that the technology will become advantageous in more geographical regions. There is not a single cost for certain generation technology, it depends on the location, prices of equipments used, taxes, subsidies, discount tax and etc.

The LCOE, as any other economic viability index, may be used together with other techniques, such as sensitive analysis and Monte Carlo simulations to define what are the most relevant parameters for its determination (DARLING et al., 2011).

2.4 Life Cycle Assessment

2.4.1 The LCA methodology

The Life Cycle Assessment is a methodology which quantifies environmental impacts related to the life cycle of a product or service. The use of resources such as energy and materials are accounted as well as solid, liquid and gaseous wastes generation and the manufacturing of products and by-products. Based on the quantification of those inputs and outputs of a process, a life cycle inventory is built. Then, through a methodology of Life Cycle Impact Assessment (LCIA), materials and energy reported previously are grouped by impact category and each type of substance that is responsible for a certain kind of environmental impact is accredited an impact factor to convert it into a category indicator. Energy employed may be converted into primary energy to measure the energetic expenditure.

The texts that standardize the methodology are the NBR 14.040 (2014), Environmental management – Life cycle assessment – Principles and framework, and the NBR 14.044 (2014), Environmental management – Life cycle assessment – Requirements and guidelines. They determine that the LCA is divided in four phases, as illustrated on figure 5. The first phase comprises the definition of goal and scope, the second phase is the Life Cycle Inventory (LCI) analysis and the third refers to Life Cycle Impact Assessment. The interpretation phase must be held after each of the other phases and the process is iterative. In that manner, the previous phases may be hold again in the case that they appear to be inadequate in the moment that a posterior phase is realized.

More details of this methodology may be found in (JUNQUEIRA, 2016) that describes the development of this methodology through time, several software and a variety of LCIA methods. The study goes deep on this third part of LCA.

Figure 5 - LCA structure

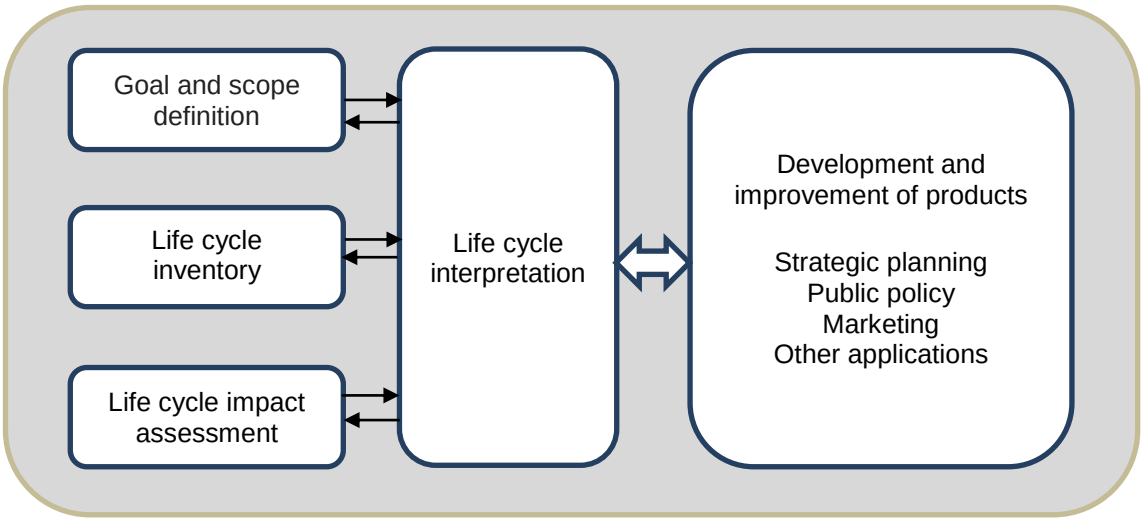

Source - BRAZILIAN TECHNICAL STANDARDS ASSOCIATION (ASSOCIAÇÃO BRASILEIRA DE NORMAS TÉCNICAS, 2014) - adapted by the author

The most complete life cycle assessment is known as “from-cradle-to-cradle” in which since the raw material extraction until the recycling of the product are considered, going through the manufacturing, transportation, assembling and use. This way, a study’s scope is defined with a very broad border. However other approaches are possible, for example, “from-cradle-to-gate”. In this type of assessment, the product is considered only until it is ready to use, it means that from the factory’s gate on is not included on the scope any more. The scope selected needs to be compatible with the study’s goals, it is, its applications, reasons, target audience and intention of comparison with other products.

Besides the border, other aspects of an LCA scope includes the functional unit, that defines in terms of which quantity the life cycle impacts will be calculated and the data quality requirements that will be necessary to reach the study goals.

According to the BRAZILIAN TECHNICAL STANDARDS ASSOCIATION (*ASSOCIAÇÃO BRASILEIRA DE NORMAS TÉCNICAS,* 2014)[1], LCA may be useful to identify aspects that may be improved in a process, inform decision makers, select environmental indicators and for marketing purposes. It is important to mention that only flows that cross the system boundaries are taken into account. Energy use is very relevant in this type of assessment, it may be

regarded considering the fuel type, energy sources, conversion efficiency, inputs and outputs associated with its generation. On those studies transparency is considered very important due to subjectivity in choices made during the work. Single scores indicators should not be used, because there is no scientific basis that supports this kind of summarizing. Interpretation should be coherent with the goal and scope, should take to conclusions, explain limitations as well as make recommendations.

Complementing the previous norm, BRAZILIAN TECHNICAL STANDARDS ASSOCIATION *(ASSOCIAÇÃO BRASILEIRA DE NORMAS TÉCNICAS,* 2014)[2] states that inputs are transformed in outputs in a process. Moreover, it is the set of elementary process that defines the product system, with elementary and product flows, carrying out one or more functions defined, which models a life cycle. The reference flow measures the process outputs, because it is the one that has the interesting product as output. It establishes that a LCI study should not be used isolated aiming to make comparisons to be publicly released, LCIA must be conducted in those cases and the equivalence between systems has to be assessed before results interpretation. The criteria used in order to define the system boundaries must be identified and explained and data quality is regarded. Data aggregation is adequate only if they refer to equivalent substances or environmental impacts. The environmental mechanism is defined as the sum of environmental process related to impact characterization, moreover, for some impact categories, time and space may be relevant in the mechanism. Comparisons should be conducted by category indicator and not in a general way.

There are three important concepts in LCA: Impact category, life cycle impact assessment method and impact category indicator. Impact categories refer to the classification of the innumerous environmental impacts that can be found, for instance global warming, fresh water ecotoxicity and soil acidification potential. Impact category indicators or simply category indicators allow quantifying the environmental impacts for each impact category, by using a method. Therefore a method is a set of procedures for quantifying impacts. A specific impact category may be calculated by different methods, because different authors have proposed their own ways to mathematically relate the

relevant substances to the value of the impact indicator. It is done through impact factors assigned to each relevant substance that multiplies its amount in order to convert it on the unit of the impact indicator, and then the results of each relevant substance in added to obtain the result. Several software is available to help on organizing data, calculating inventory and impact indicators as described on section 2.4.2.

Several studies have been conducted utilizing the LCA methodology to quantify the impact of silicon based PV technologies. The next step is to describe applications of LCA to PV environmental impact quantification. As stated by ROSA (2013), the environmental impacts associated to the electric power generation through photovoltaics are concentrated on the modules production phase and the LCA is a good methodology to assess PV technologies.

LCA applied on silicon PV - One example of LCA for silicon PV is YANG *et al.*, (2015), it used this methodology for photovoltaics polycrystalline silicon modules in China and also includes in the assessment scope the impacts carried on foreign territory originated from raw materials importation. The study distinguished the use of local and imported materials for multi-Si PV modules manufacturing. For instance, 52% of multi-Si and 74% of EVA comes from abroad for this type of Chinese industry. Between 2004 and 2010, an average of 93% of the country's production was exported. The software used was SimaPro 7.3. The LCIA method was CML 2001, which includes global warming potential (GWP, 100 years), abiotic depletion potential (ADP), acidification potential (AP), eutrophication potential (EP), human toxicity potential (HTP), freshwater aquatic ecotoxicity potential (FAEP), marine aquatic ecotoxicity potential (MAEP), terrestrial ecotoxicity potential (TEP), ozone depletion potential (ODP), and photochemical oxidation potential (PCOP). As can be seen on figure 6, in most of the impact categories considered in the study the majority of the impacts is attributed to China's territory, they are GWP, 100 years, ADP, AP, EP, HTP, TEP, and ODP. While only FAEP, MAEP and PCOP had lower category indicators values for abroad than for China. Hence, it concludes that it is important to take into account the international trade for those PV modules LCA. The negative environmental impacts of photovoltaics are mainly related with its manufacturing process. However, it is later exported and the positive

impacts occur abroad, for example, 82.4% of GHG emissions are due to exported modules. Finally, because of a less restrict Chinese environmental legislation, the PV panels have higher impacts during their production.

Figure 6 - Indicators for China's multi-crystalline silicon solar panels

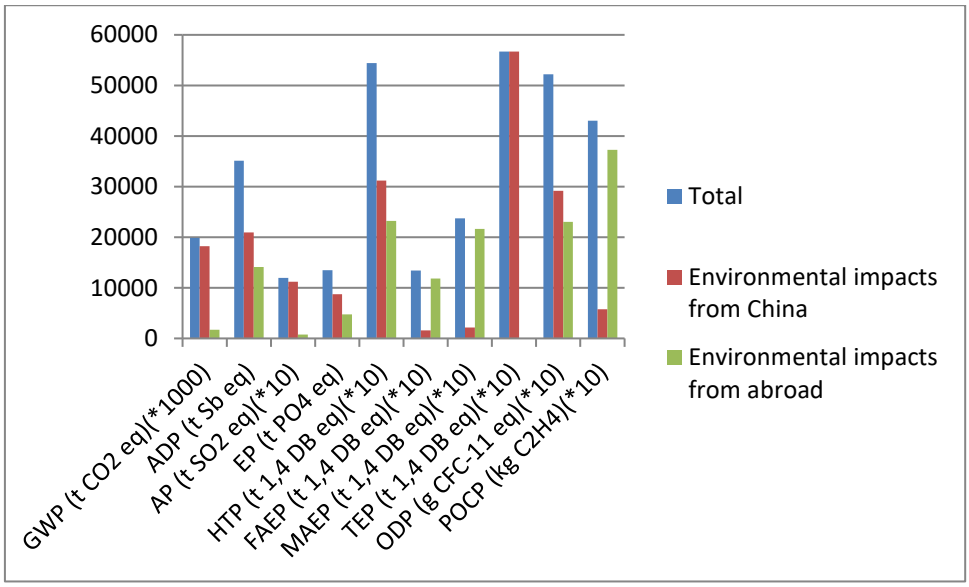

Source – adapted from YANG *et al.*, 2015

FTHENAKIS, VASILIS M *et al.* (2012) presents Cumulative Energy Demand (CED) and GWP for monocrystalline silicon photovoltaic systems. It compares the LCA considering modules produced by SunPower in Philippines (PH) and the process defined in ecoinvent. SunPower_NO/UTCE and Ecoinvent B are cases of MG-Si produced in Norway and the following steps of production considering the average European grid. Figure 7 presents the results for the LCA oh the PV cell. For CED, the Norway production of MG-Si causes an increase in the indicator and SunPower's process are less energy intensive than Ecoinvent in both cases. For GWP, the Norway production decreases amount of $CO_{2\text{-eq}}$ per cell in the case of SunPower, but it rises for Ecoinvent. Figure 8 shows results of LCA for modules. It can be noted that CED and GWP graph are approximately proportional and SunPower has the lowest result in both cases while Ecoinvent A has the highest.

Figure 7 - CED and GWP LCIA results for the cells

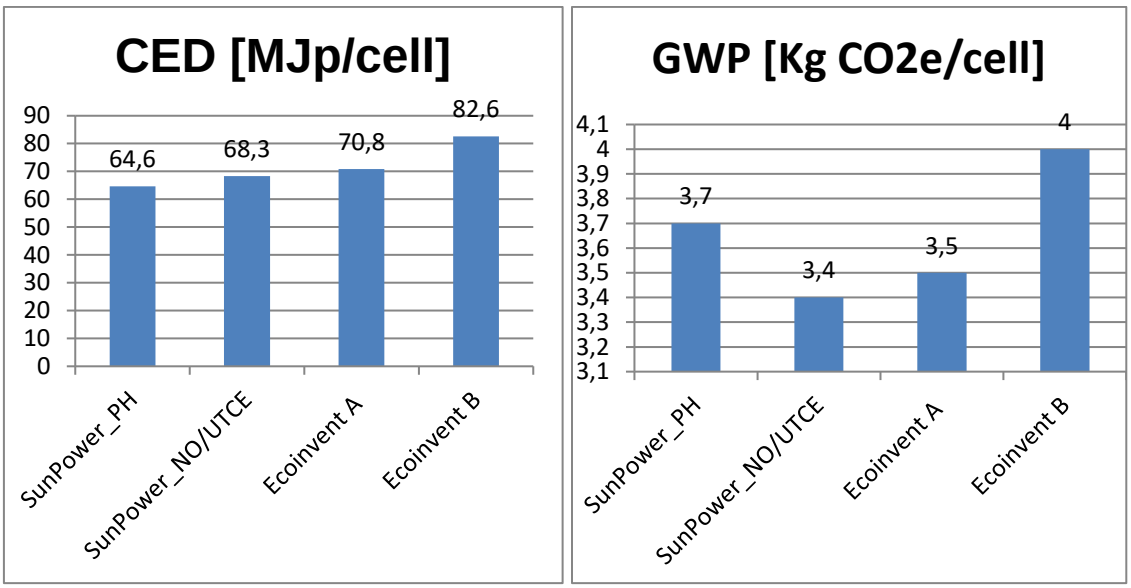

Source - FTHENAKIS, VASILIS M *et al.*, 2012

Figure 8 - CED and GWP LCIA results per Wp of module

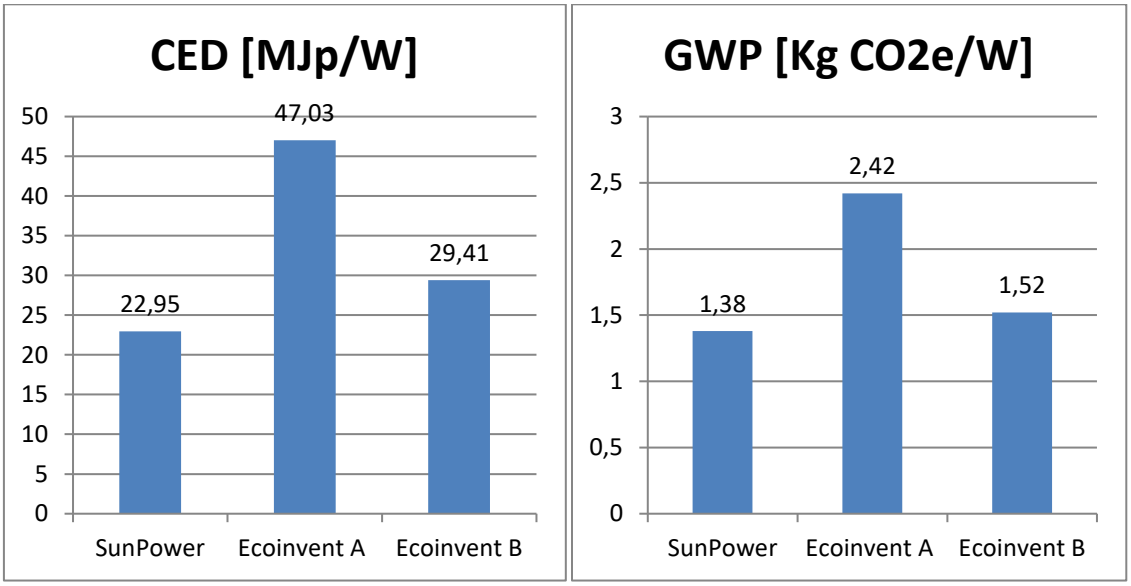

Source - FTHENAKIS, VASILIS M *et al.*, 2012

Moreover, through LCA it is possible to obtain the energy payback time of a PV module according to the electricity grids responsible to its production, taking into account the electrical grid in which the module will be connected to when operating as well, as described by ROSA (2013). Regardless the low environmental impacts during a photovoltaic plant operation, during the silicon module production there are relevant consequences to the environment. The Energy Pay Back Time (EPBT) is an index which may be calculated considering

the module efficiency, the location characteristics and the energy matrix used in the manufacturing process.

LCA applied on OPV - The development of technologies based on organic solar cells is considerably recent if compared with crystalline silicon. Any way, it is still possible to have access to LCA studies focusing on this kind of device and a few of them are analyzed below. Those studies are due to a very common concern nowadays of developing renewable electric power generation with low environmental impacts, not only on its operation, but in its whole production chain. This way, several groups that developed organic solar cells conduct LCAs in parallel to identify critical points on its process and define efficiency and life time goals that make OPV becomes more interesting than other alternatives.

ESPINOSA *et al.* (2011) conducted a LCA related to a roll to roll (R2R) process, it is, the substrate starts rolled on one side and is stretched until another roll, then it moves to this empty roll while is printed and later come back for the next layer printing and so on. The process is defined simply as ProcessOne, which carry all the steps under ambient conditions, except for the ITO (Indium Thin Oxide, a transparent conductor) application. It is worth noting that this layer is reported as the main cause of environmental impacts.

In ESPINOSA *et al.* (2011)‘s work, chemicals from a similar group according to its production categories were used in the cases that a specific chemical process was not available. Although databases are each time more complete, the lack of information is still a problem that this type of study is subject to, what imposes limitation on conducting LCA. The recycling of some materials was taken into account, for instance, the methanol. Hence, aware of the whole material inventory, it became possible to identify the most delicate aspects when up-scaling the production. The Energy Return Factor is used in this assessment, this metric is the ratio of energy produced by the device by the energy used for its production. The study considered 15 years lifetime for the system since it was according to the European Photovoltaic Technology Platform aims for organic photovoltaics until 2013, however it is now known that this lifetime has not been reached yet.

HENGEVOSS *et al.* (2016) develop a study based on tandem cells. The power conversion efficiency assumed is 8% and there are two lifespan scenarios, one considering 15 years and another of 20 years. As benchmarks for the comparison with others PV technologies, multi crystalline silicon and CdTe were considered. In that study, five impact categories were used, they are: global warming potential, cumulative energy demand, metal depletion by ReCiPe[1], Ecotoxicity according to USEtox[2] and energy payback time. It is noted that GWP for the tandem OPV is 50% higher than regular OPV and CED is 60% higher. This difference is attributed to a more complex design and additional features causing a production process composed by more steps. There were two scenarios for the performance ratio, 0.75 as conservative and 0.9 as optimist. Along with the environmental impacts, the levelized cost of energy was taken into consideration and this information was correlated with GWP in the graph shown on figure 9, in which can be noted that the amount of $CO_{2\text{-eq}}$ per kWh of generated energy is lower for the OPV technology compared with the first and second-generation benchmarks in any case. However, the cost of this energy may be considerably higher on the more pessimist scenarios. Data about the energy incidence considered basically shifts the points on the graph towards higher levels of both, cost and GWP values when this parameter reduces.

[1] ReCiPe is life cycle impact assessment method with 18 categories which is very used
[2] USEtox is another life cycle impact assessment method focused on toxicity

Figure 9 - LCOE and GWP of OPVs based on different scenarios regarding efficiency, lifetime, performance ratio and CdTe (efficiency of 11.9%) and multi-Si (efficiency of 14.1%). SE stands for Southern Europe with 1800-2000 kWh/(m^2.a) and CE means Central Europe with 1000-1200 kWh/(m^2.a)

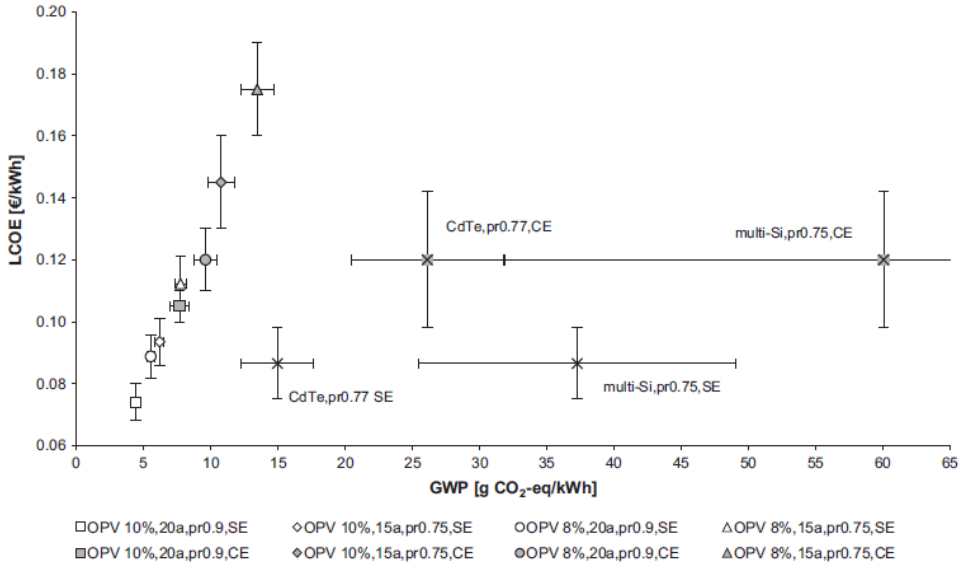

Source - HENGEVOSS *et al.*, 2016.

Besides those studies, the impact categories chosen by other authors studying PV LCA can be emphasized. TSANG et al. (2015) uses the whole method ReCiPe, it means that 18 categories are calculated. Besides this, CED is also calculated. In this study, a cradle-to-gate LCA is conducted using 1 watt-peak as reference unit. The energy payback time found is of 0.21 years and considerations of manufacturing routes may be focused using LCA aiming improvements in environmental, human health and ecotoxicity characteristics of OPV.

While that, ESPINOSA *et al.* (2012) uses only Energy Payback Time and Green House Gases, nevertheless it is suggested that more categories should be included in further studies. The study is based on the fact that indium is scarce and expensive and, since it is the main compound of ITO, the most successful transparent electrode, a replacement is considered, in the case, Al/Cr electrode. This takes to a relevant reduction in energy consumption for the OPV production. An EBPT of 10 year is found.

Finally, ESPINOSA; KREBS (2014) use three categories of CML 2001, global warming potential, acidification potential, and human toxicity, as well as ReCiPe

at the end point level. The LCA is about multi-junction organic solar cells, it is a stack of active layers in series. The larger number of materials and process has to be compensated by the efficiency improvement. Nevertheless, the conclusion is that single junction may be an advantage, mainly in situation that land use is not a limiting factor, because multi-junction solar cells would have to be at least 20% more efficient.

Other studies in this same area include DARLING; YOU (2013). In this study is shown that nowadays OPV still has strict niches. However as it improves life time and efficiency, more opportunities become available, mainly considering the climate change scenario that will demand great part of energy to be supplied by the sun. LIZIN *et al.* (2013) reviews studies regarding single-junction bulk heterojunction polymer solar cells with active layer made of P3HT/PC60BM. It takes into account the LCA of semi-industrial pilot lines in ambient surroundings. It recognizes that recent improvements in the manufacturing process have lowered environmental impacts associated to it and notes that lack of input data reduces the number of LCA studies of OPV. Finally, it emphasizes that environmental studies have to be kept being done to drive the technology in the right way.

One more study about LCA of OPV is by GARCÍA-VALVERDE; CHERNI; URBINA (2010). It also takes into account a typical bulk heterojunction organic solar cell and focus on the inventory in order to identify bottlenecks in a future supply chain for large industrial scale. The results found for EPBT and CO_2 emissions are considered satisfactory, because it is a emerging technology and a promising future is possible. ANCTIL *et al.* (2010) compares different active layers in OPV in terms of efficiency and LCA. The conclusion is that higher efficiencies are followed by higher EPBT. Finally, YUE *et al.* (2012) analysis LCA of OPV in Chicago, New York and San Francisco for near-term future and long-term future. Monte Carlos simulations are used and great potential of OPV is shown in terms of sustainability.

2.4.2 Computational tools

There are many options of LCA software available, such as Gabi, JEMAI-LCA Pro, Umberto, One Click LCA, among others. In Brazil, the most popular is

SimaPro. Besides those, there is OpenLCA (WINTER *et al.*, 2015), it is a free open source tool, besides being good software. Those tools help organizing data, structuring information and relating them.

They must be feed by two important items: data base in order to perform the inventory and methods to calculate the impact factors. NEEDS is one example of database, it focuses on renewable energy. Another database that is very popular is ecoinvent (BOURGAULT; WERNET, 2016; GMBH, 2016), which is considerably complete. Although it is not free, an academic version can be obtained without expenses. The methods can be obtained from the software developers in form of algorithms that can be imported in order to perform calculations. Eco-indicator 99, ReCiPe, USEtox and Cumulative Energy Demand are a few of the existing methods.

2.5 Accelerated aging tests

Accelerated aging tests are used for PV seeking to obtain initial data about the technology's life time. When developing a new kind of module or process, it is necessary to have an estimate of how long the device lasts, at least compared with others. It allows that the developers identify problems and, therefore, find solutions.

ASTM (2001) is a standard test method for PV modules. One test is a thermal cycling procedure, another is a humidity-freeze cycling procedure and the third is an extended duration damp heat procedure. The method does not intent to neither establish pass or fail levels nor determine photovoltaic module lifetimes, but states that the module's life time depends on its capability of withstanding the environmental conditions proposed. Forward-bias current is applied to simulate the maximum power point current of the module's operation and a frame is necessary to mount the modules so that air may circulate through the front and back surface. Visible effects as well as electrical performance are taken into account to be reported.

NDIAYE *et al.* (2013) reviews the literature searching for the main modes of failure of a PV module. Corrosion, breakage and mainly discoloration and delamination are found as causes for degradation. What takes to those process

are usually temperature and humidity. Anyway, it is still hard to predict how it occurs in field since long term studies are necessary. The mathematical models analyzed always present weakness to predict degradation over time, they come from a variety of factors, such as, excessive amount of assumptions, leak of similarity with reality, necessity of knowledge of materials intrinsic parameters and disregard of all degradation modes.

3 METHODOLOGY OF THE STUDY

This chapter describes the methodologies used in this work. In order to compare organic photovoltaic with silicon devices, two main aspects are considered. The first is related to the environmental impacts and the second is related to the technology's economic viability.

Environmental impacts are regarded through Life Cycle Assessment. In this methodology, the resources use as well as the emissions for soil, water and atmosphere along the PV module manufacturing process are accounted to perform a life cycle impact assessment. Considering a certain power plant, those impacts are quantified in relation to the production of a certain amount of energy and to one square meter of PV module.

The Levelized Cost of Energy is the parameter most used in the literature to compare economic viability of renewable sources. It takes into account the implementation, maintenance and operation costs of a power plant during a given time horizon of operation. In the sequence, all the energy produced by the power plant is calculated considering the efficiency loss. Notice that LCOE depends on plant location, which will affect the available irradiation, temperature, etc. Therefore, the cost per unit of produced energy can be calculated. A discount rate can be used to take into account the effect of time on the value of the resources; in this case, both costs and energy are discounted.

One can observe that technology efficiency and lifetime influence both the LCIA and the LCOE. This economic indicator and the impact category indicators are selected as indexes to assist decision-making while choosing among the technologies. In this study, the accelerated aging test is used to quantify the ratio between OPV degradation and mono-Si degradation, which is further used in the calculations of energy generation used for LCA and LCOE. Figure 10 illustrates the methodology adopted to compare the technologies.

Figure 10 - Master's thesis methodology

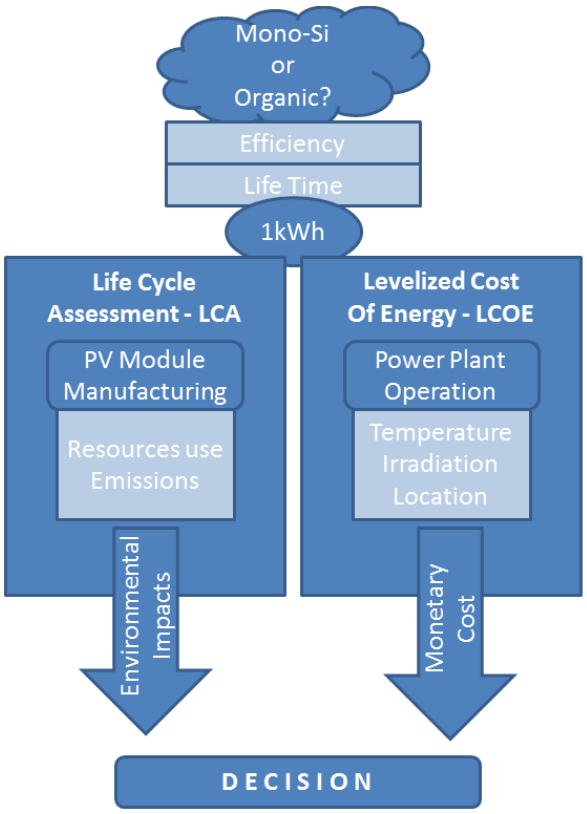

Source – Created by the author

Initially, the measurements procedure adopted to obtain electrical parameters over time is described, followed by the sample preparation, the aging tests and the comparison between LCOE and LCA, which are the indexes selected to compare and choose between the technologies. After that, some details of the application of LCOE and LCA methodologies are presented.

3.1 PV technologies performance

In order to conduct this study, the technology from Bosch and CSEM Brasil are considered for mono-Si and OPV respectively. The first one is an industrial and commercial cell manufacturing very well established. The model is Bosch Solar Cell M 3BB C4 1200 and further information may be found on its data sheet (BOSCH, 2012). The OPV module is made through a manufacturing process, which was originated, from R&D recent works and aims technological transfer.

3.1.1 IV curves extraction

According to section 2.2, the IV curve defines the maximum power that can be extracted from a cell or module. Depending on the irradiation that the device is exposed to and its area, the efficiency can be calculated, relating the input power in form of radiation and the output of electric power.

Environmental conditions influence the power conversion. One of them is temperature. If temperature rises, although the short circuit current (Isc) is slightly increased, Voc reduces considerably, hence the efficiency decreases. This type of correlation is noted mainly on mono-Si devices. Irradiation also changes a lot the IV curve, because Isc is approximately proportional to it and then the curve is basically vertically translated according to this parameter.

In this study, measurements are made with the continuous solar simulator (CSS) (ORBITAL Mod. AM15x100) under room temperature. Its spectrum is shown on figure 11. The air conditioner of the room in which the CSS is installed is set to 25 ºC, the cooling water pump is set to the same temperature pursuing to keep the cells on this temperature, as determined by the STC. The PV devices are exposed to irradiation only once and for the time necessary for the IV curve extraction. It takes 50 s for mono-Si and 10 s for organics.

Figure 11: Continuous Solar Simulator Spectrum

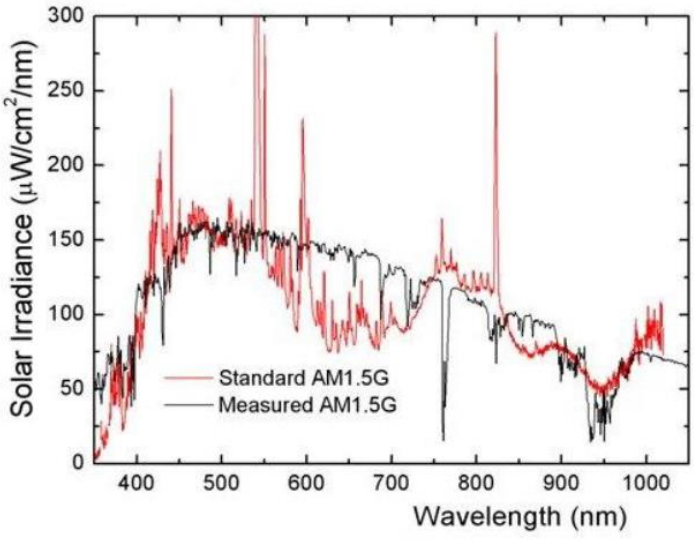

Source – “ANEXO A SIMULADOR SOLAR CONTÍNUO ORBITAL Mod . AM15x100 Características Técnicas Observações,” 2014

From previous experiments (Bueno, 2016), it is known that four-wire technique should be used. The first attempt is illustrated on figure 12-(a), the usual shape of an IV curve is obtained. Finally, connections are adjusted to decrease series resistance and the source current range is broadened so that the curve could reach the Isc values, as seen on figure 12-(b).

Figure 12 - Initial measurements for mono-Si on the source-meter software screen

(a) Four-wires

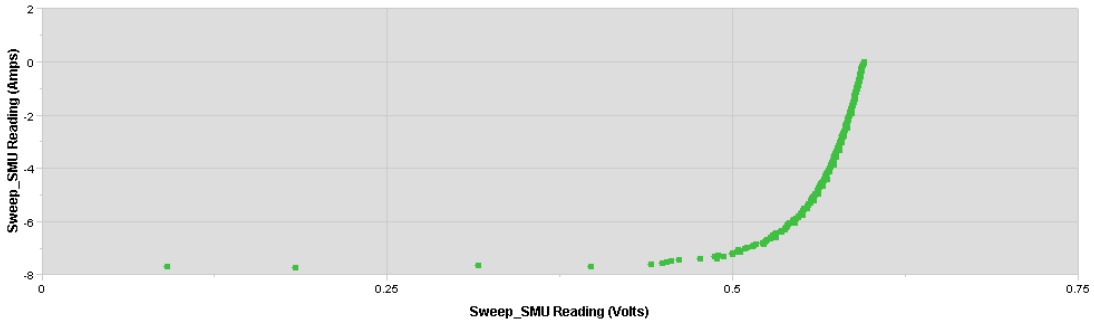

(b) Expected initial measurement

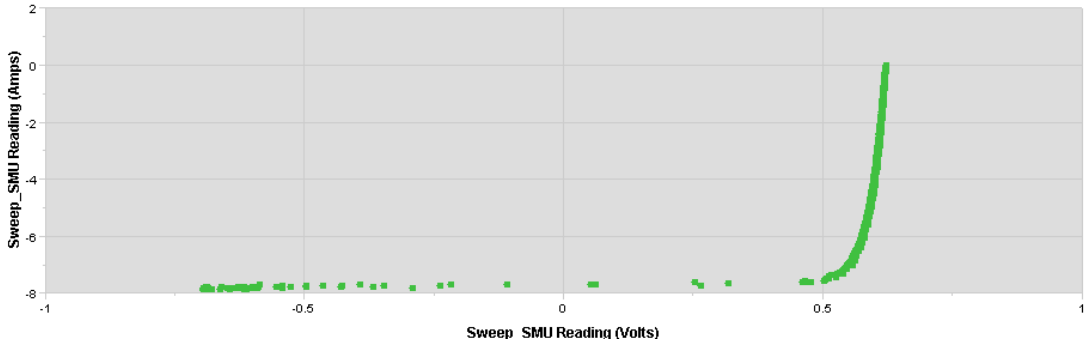

Source – Generated by the author

In the case of OPV devices, the difference between two-wires and four-wires is not very significant, because the current values in this case are much lower (around 80 times). Nevertheless, four-wire technique is also used so that it is compatible with the mono-Si measurements. Since the devices only have one connector for cathode and one for anode, the connectors are overlapped, as shown on figure 13 to reduce even more any possible voltage drop on the cables, the slight difference is illustrated on figure 14. Note that behind the OPV device there is a gold plate used to refrigerate the device, this metal part reflects irradiance that reaches on it back to the devices. In case of OPV, light may be absorbed from front and back surfaces and this may increase the generation of this technology.

Figure 13 – Connectors overlapped

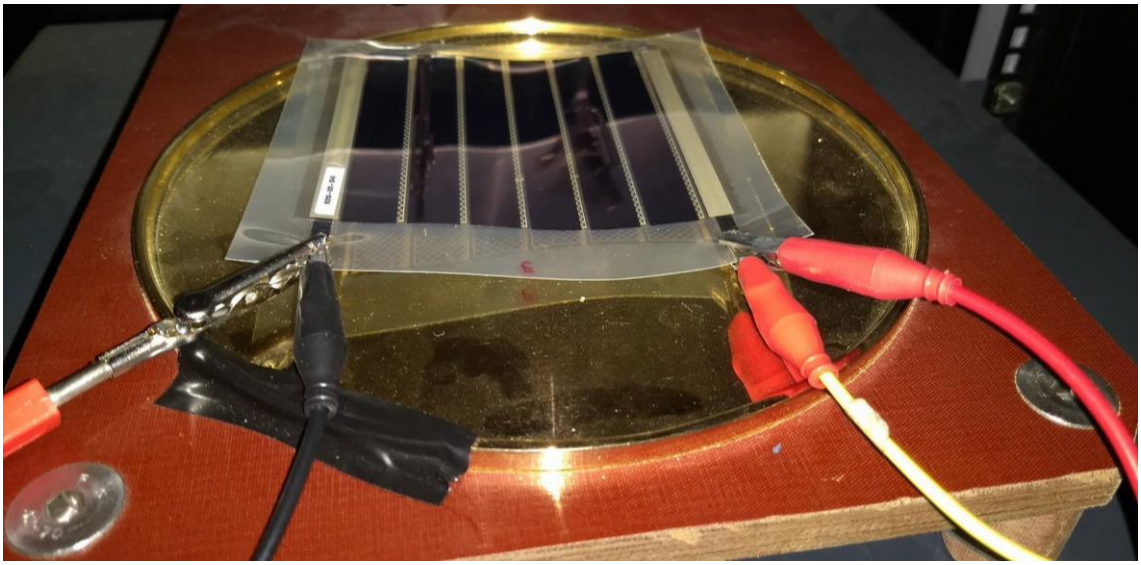

Source – Photographed by the author

Figure 14 - Initial measurements for OPV on the source-meter software screen

(a) Four wires with overlapping connectors over the OPV's contacts

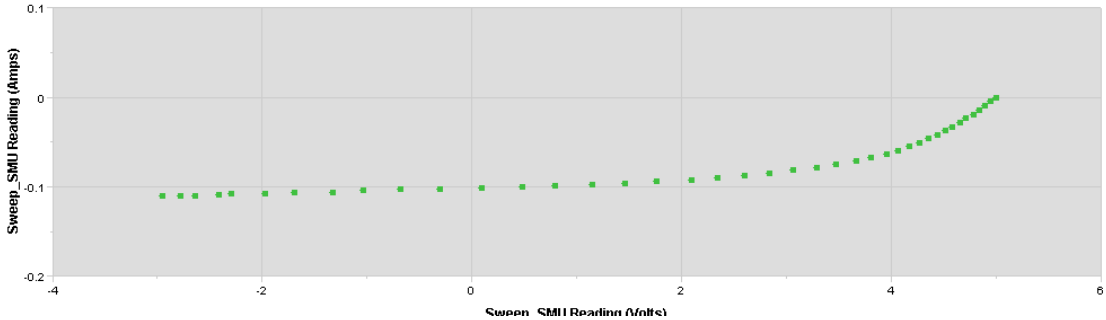

(b) Four wires measurement with two of them on the device's contact and the other two on the previous cables

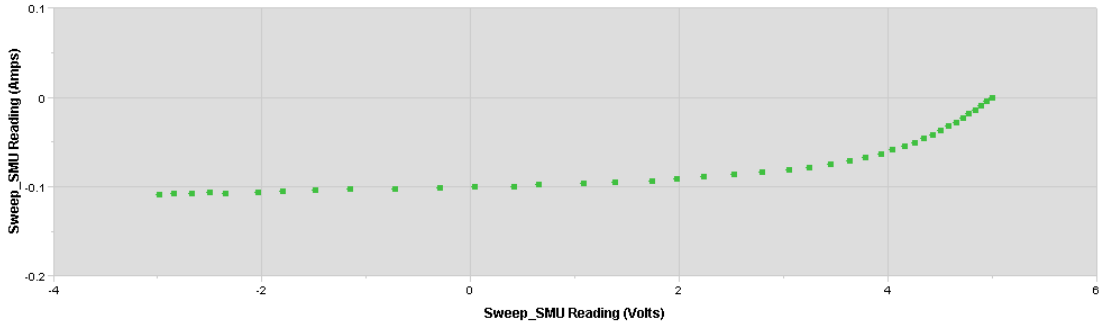

Source – Generated by the author

On figure 15 the configurations for measurements of each type of device are illustrated. On part (a) for mono-Si and on part (b) for OPV. Current ranges are

registered as well as number of points and time of measurements. The source and measure functions are shown too.

Figure 15 - Source meter software configurations screen for each technology

(a) Mono-Si measurement configuration

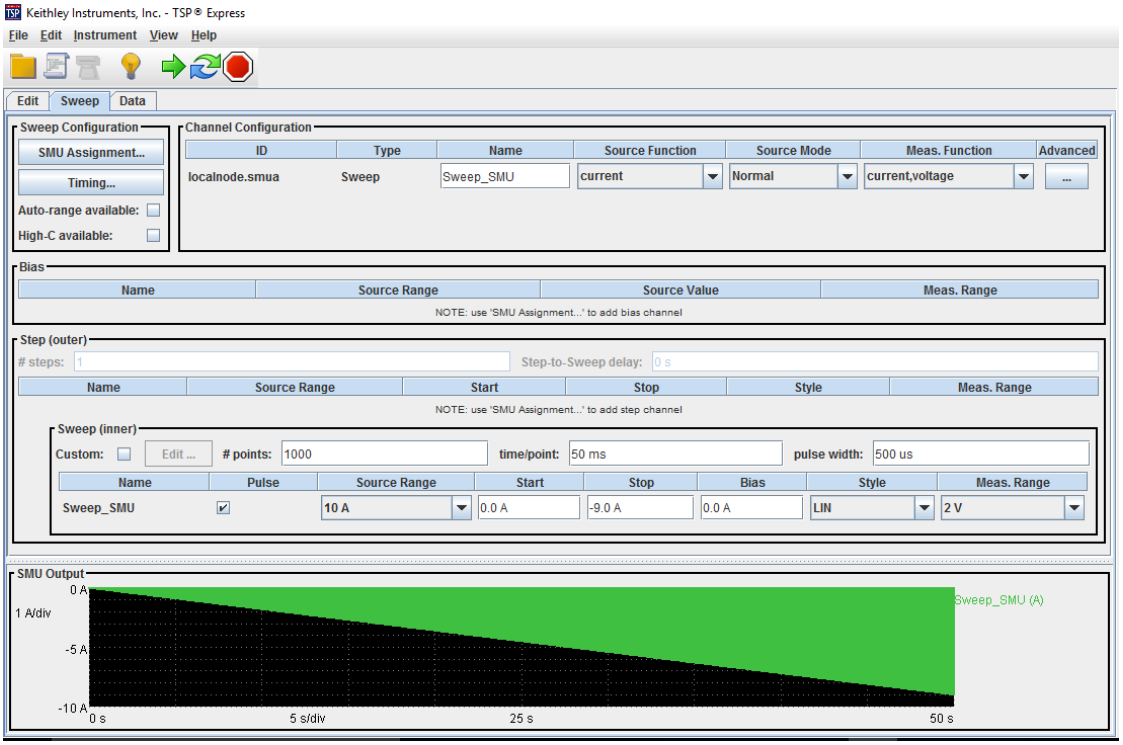

(b) OPV measurement configuration

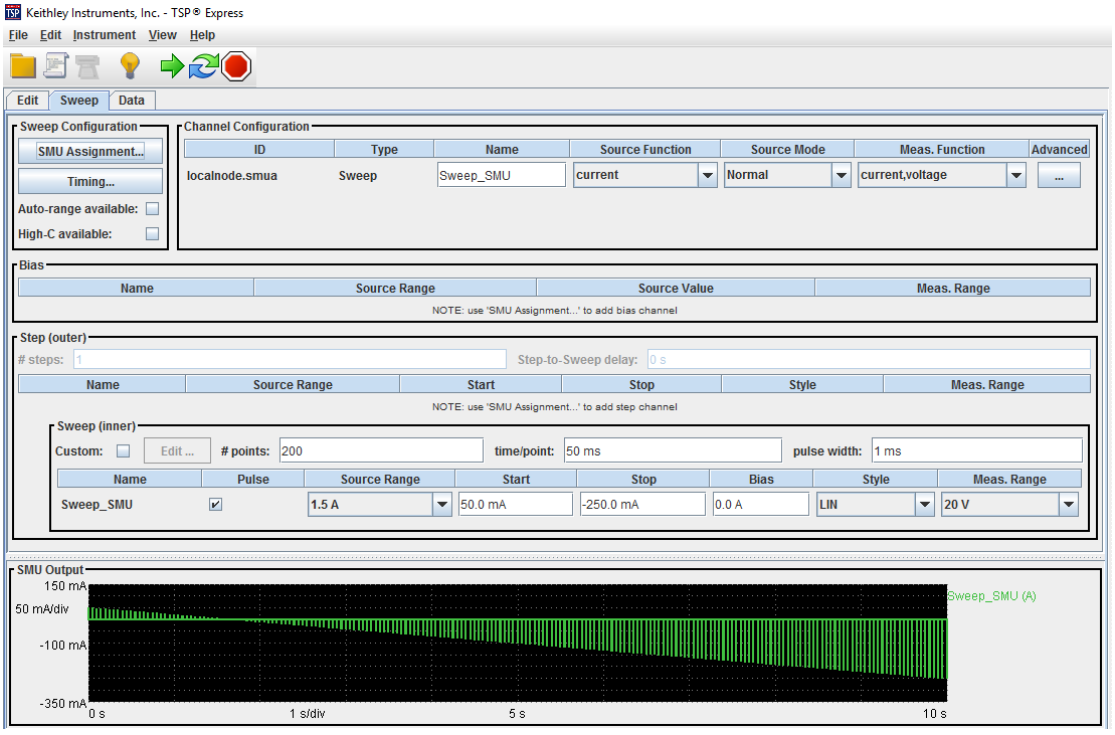

Source – Generated by the author

3.1.2 Sample preparation

In order to consider aging, the field conditions in which the photovoltaic technology will be exposed should be taken into account. Therefore, the comparison between OPV and crystalline silicon should be done considering the packaging that each type of cell would have after final assembly of the panel. The OPV samples are already encapsulated, but the silicon samples are cells without any protective layer. Therefore, it is important to prepare the samples for the experiment and obtain a structure similar to the one of a module. The mono-Si cells are involved between two layers of Ethyl Vinyl Acetate (EVA), covered with glass on the front side and with Tedlar on the backside, according to figure 16.

Figure 16 - Lamination sequence

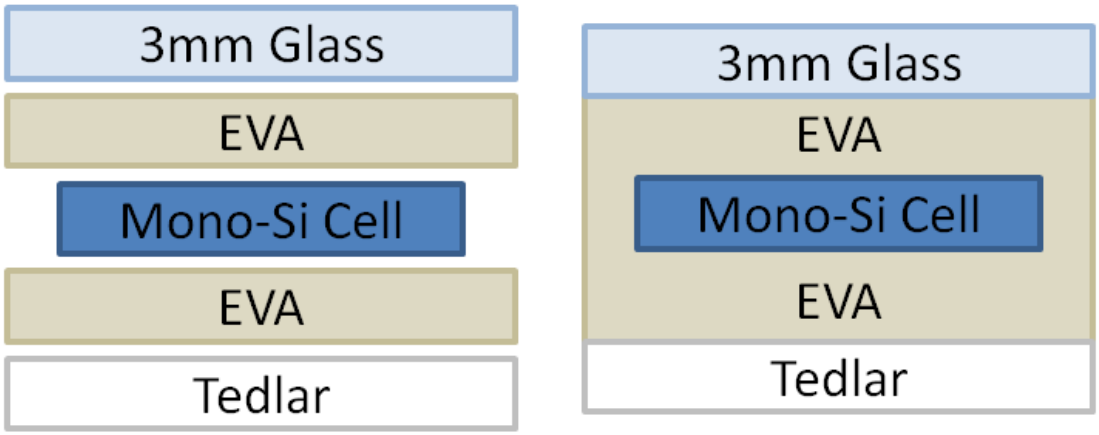

Source – Created by the author

This cell preparation was made in Technology Center in Solar Energy (*Núcleo de Tecnologia em Energia Solar* - NT-Solar) at Pontifical Catholic University of Rio Grande do Sul (*Pontifícia Universidade Católica do Rio Grande do Sul* - PUCRS). The type of glass used is soda with 3 mm of thickness, its transmissivity was measured at NT-Solar and is shown on section 4.1. Although usually photovoltaic 5 mm glasses are used, the thickness is reduced in order to increase transmittance, since photovoltaic glass, with proper transmittance, are very difficult to be acquired in unusual dimensions such the one required for this purpose. In this case, the shape was a square with 185 mm sides, since the cells are 156 mm wide. This dimension allows almost 1.5 cm of extra glass,

Tedlar and EVA on each side, protecting the cell from moisture, since the lamination did not include the aluminum frame, which has this same function.

The cells are measured before the lamination. After that, the glasses are cleaned with water and an appropriate soap free of sodium. Then they are dried and stored so that it is kept free of dirty. In the sequence, the busbars are welded on the cells and the sequence of layers is inserted on the laminator PENERGY model L150A, as illustrated on figure 17.

Figure 17 - Laminator used for samples preparation

Source - SANTOS, 2011

The processes are described by three graphs on figure 18. It starts with the chamber closure and a pre heating until 70 ºC, this turns the EVA into a gel. The lower part of the chamber has its pressure dropped to zero and the temperature rises to 90 ºC, besides that, the pressure on the upper part increases and press the device layers. After that, temperature goes to 150 ºC to cure the EVA. Later, the system is refrigerated with water until 75 ºC and, finally, it is connected to vacuum on the upper part to release the device from the membrane of the equipment.

Figure 18 - Temperature, lower chamber pressure and upper chamber pressure through cycles

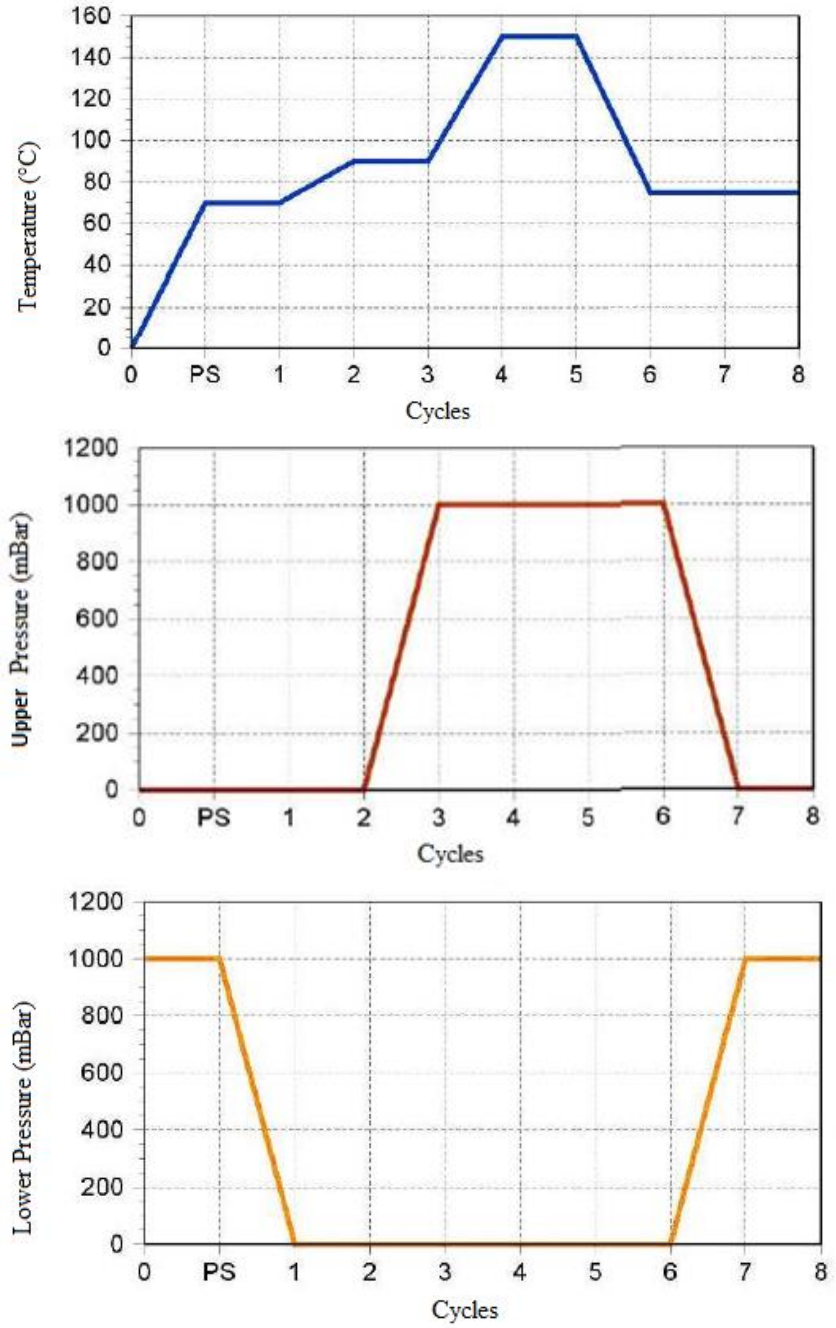

Source - SANTOS, 2011

This way, the laminated cells are ready and are measured again after the other layers are added.

3.1.3 Aging and efficiency reduction

Taking into account that mathematical models relating accelerated and natural aging conditions are very complex and uncertain, the strategy adopted was to design a comparative experiment. It means that, OPV and mono-Si devices are

put in the exact same conditions, so that the loss of efficiency over time could be analyzed.

For the present work, CSEM Brasil's equipment is used. One of them is the climatic chamber in which high temperature and humidity are present. During all the experiment, it operated with 65 ºC of temperature and 85% of relative humidity. The other equipment is the light stability chamber. In it, an irradiance of 1000 W/m^2 is applied through white and U.V. led lamps, such as the one determined by the Standard Test Conditions, however it is kept on 24 hours per day. It is important to differentiate the light stability chamber, which is aging equipment from the continuous solar simulator, which is used for IV curves extraction. It is worth stating that although the conditions on the aging equipment are reasonable, they are still arbitrary, since there are not exact values to be adopted and other combinations of temperature, humidity and irradiance could be used.

Then, a pair of devices, one of them of OPV and the other of mono-Si, is put side by side in the climatic chamber and another pair in the light stability equipment. To relate this aging under intense conditions to the one without the effect of temperature and humidity or irradiation, a third pair is kept in under room temperature, dark environment, protected from dust and moisture simply in a drawer. Measurements took place along 155 days. The frequency varied, three times on the first week, once a week during three weeks and every two weeks until the end of experiment. It was established according to previous experiences with this kind of test.

3.1.4 Comparison between LCOE and LCA

The devices efficiencies are later used for LCA and LCOE. Hence, scopes from both analyses have to be compatible. They are set as described on table 1.

Table 1 - Scope description for LCOE and LCA

LCOE	LCA
Generation costs (construction and operation) of an equivalent plant for each technology.	Environmental impacts associated with the manufacturing process of each technology.
The main difference between the power plants considered is the technology of the modules.	Define the product system for each technology.
Consider 10 years of power plant operation with modules degradation.	Consider the same energy generation for LCOE.
Consider the cost of the different structures for panel fixation according to each technology's weight.	Does not take into account the devices installation.
Land cost is not considered, because the power plant is built integrated.	Land use during power plant operation is out of scope of the from-cradle-to-gate LCA of the module.

Source – Created by the author

For the power plants, an installed capacity of 3 kWp and direct current generation is chosen. Modules are rooftop mounted and no inverter is used, in order to simplify the system. These assumptions are made to be compatible with household dimensions. One can observe that, since the installed capacity is defined, the generated energy during the ten years period with each technology is different. It is worth mentioning that this period is assumed keeping in mind a residential use that does not have a long term planning. Moreover, the OPV power plant will occupy a much larger area than the silicon based technology.

3.2 Economic viability index

From the methodological point of view, the LCOE calculation does not present any issues. One can observe that by definition it is a unitary cost, by unit of electricity generated, the fact that each system generates one amount of energy is indifferent. The cost of energy through each technology is calculated in terms of LCOE. According to item 2.3, the index is calculated for both technologies.

3.3 Life cycle assessment application

According to NBR 14.040 (ASSOCIAÇÃO BRASILEIRA DE NORMAS TÉCNICAS, 2014), the comparison of two LCA studies results is only possible if the assumptions and context of each of them are equivalents. Considering this, the scope is defined.

3.3.1 Goal and scope definition

This LCA goal is to compare the life cycle impacts of OPV modules manufacturing with those of monocrystalline PV modules fabrication. Since OPV is a very recent technology and that it has been developing very quickly in terms of efficiency and lifetime, new studies are frequently necessary. Besides that, many studies have been conducted about LCA of OPV (ESPINOSA *et al.*, 2012; HENGEVOSS *et al.*, 2016b; TSANG; SONNEMANN; BASSANI, 2014). This study adopts a different approach, there is a direct comparison with mono-Si and the efficiency decrease is taken into account using results from the accelerated aging test conducted.

This study concerns the photovoltaics community in general: decision makers in energy planning context, academics, as well as, industry, including manufacturers. They will be able to better understand the environmental impacts of their activities, identifying hotspots on the process, it is the parts of the process responsible for most of the environmental impacts, and improvements opportunities. The community related to LCA is also a target audience as well as the electric sector regulator.

The scope border comprises a “from-cradle-to-gate” approach. It is, since the raw materials extraction until the product (the PV panel) is completely manufactured. It was chosen because the environmental impacts of photovoltaics are attributed mainly to the production phase. The system function is to generate electrical energy, then the functional unit is a kWh and the reference flow is the number of panels necessary to generate this amount of energy. However, data used for both technologies takes to a LCA with square meter as functional unit, hence, results will be presented in terms of area as well like a intermediate step.

The impact categories are determined in accordance with the literature review presented on section 2.4.1, where there are two papers by ESPINOSA *et al.*, (2011 and 2012) and ESPINOSA and KREBS (2014) in which only a few impact categories are used. However, in the most recent one, the impacts categories become broader, since in the previous paper it was recognized that more aspects should be taken into account. TSANG et al. (2015) is too complex in terms of categories, since it uses the whole ReCiPe. This way, HENGEVOSS *et al.* (2016) shows the best choice of categories, because it is not too broad nor too simple and considers aspects very common in those types of studies.

Hence, the categories chosen for the present study are Global Warming Potential through IPCC method; Cumulative Energy Demand so that Energy Payback Time could be calculated; toxicity (human total and ecotoxicity total) through USEtox. Besides that, Metal Depletion Potential is also calculated through ReCiPe.

CED is very relevant in this case, because the products focus of the LCA are electrical energy generators and then the balance of energy production and consumption during manufacturing makes a lot of sense. Due to the same reasons, EPBT is also important, because it is a metric that relates generation capacity and the embedded energy. GWP is related to climate change, which is one of the main environmental issues nowadays and energy generation is one of the main causes of it. The two types of toxicities highlight the impacts of the toxic chemicals used in the processes and MDP is important, because of the conductors used, which consume metals, in some cases, rare types of them.

Data requirements include the production chain for mono crystalline silicon and organic photovoltaic modules. For silicon, ecoinvent database is used and, therefore, a general process is considered. For organics, ESPINOSA *et al.* (2011) process data is used as reference, because it takes into consideration a very common type of OPV that can be taken as example for this technology. Ecoinvent is still used in this case when inserting new raw materials so that the database can consider the previous process to obtain each new input.

Ecoinvent 3.3, which was the newest version by the time that the study was conducted, is used, so that the chance of finding each chemical was enhanced.

Furthermore, data quality requirements are not very strict since data is very scarce and then poor information also has to be used in some situations.

The limitations of this study include the different applications of the technologies. The categories defined on the scope also limits the LCIA, since it concerns only those impacts and cannot be seen as a complete assessment. One more relevant aspect is related to geography, because ecoinvent is a database very suitable for standard process globally, not including specificities of each region.

A specific critical review for this LCA is dismissed, since this whole work is presented on a master's thesis defense, which assesses, not only the LCA part, but also all the other aspects related to it in the complete study.

The main aspects of the goal and scope definition are summarized on table 2.

Table 2 - Summarized goal and scope definition for the LCA

LCA	
Goal	Compare OPV and mono-Si manufacturing process
Functional unit	kWh
Boarder	From-cradle-to-gate
Reference flow	Number of panels
Data requirements	Ecoinvent for mono-Si ESPINOSA (2011) for OPV

Source – Created by the author

3.3.2 Inventory analysis

In OpenLCA one process is created for each step with its several inputs, being one of them the output from the previous process and the others being linked through ecoinvent's process directly or considering its synthesis and therefore linking with the various chemicals needed, also through ecoinvent.

For LCI analysis, the software OpenLCA was used. The electricity spent by OPV was modeled according to the Brazilian electricity matrix and according to the Danish electricity matrix, since it is the one used by ESPINOSA *et al.*, (2011).

3.3.3 Impact assessment

On section 3.3.1, the impact categories were selected. Therefore, the indicators, which shall be used, are also defined. Then the impact assessment methods are chosen as specified on table 3. Calculations are done with OpenLCA as well.

Table 3 - Impact categories definition

Impact category	Initials	Category indicator	Methodology	Reference
Cumulative Energy Demand	CED	MJ_{Eq}	Own concept	(FRISCHKNECHT *et al.*, 2010)
Energy Payback Time	EPBT	Years	-	(FTHENAKIS, V. M. *et al.*, 2011)
Metal Depletion Potential	MDP	Fe_{eq}	ReCiPe (H - midpoint)	(GOEDKOOP; HUIJBREGTS, 2013)
Global Warming Potential	GWP	$CO_{2\text{-}eq}$	IPCC 2013	(IPCC, 2013)
Ecotoxicity total	-	CTU	USEtox	(ROSENBAUM *et al.*, 2008)
Human Toxicity Total	-	CTU	USEtox	(ROSENBAUM *et al.*, 2008)

Source – Created by the author

3.3.4 Interpretation

Based on the objective and scope, conclusions are taken, limitations are verified and recommendations are made. It is conducted through identifying significant issues based on LCI and LCIA. Figure 19 shows a schematic of interpretation connecting it with the other phases.

Figure 19 - LCA flowchart with detailed interpretation

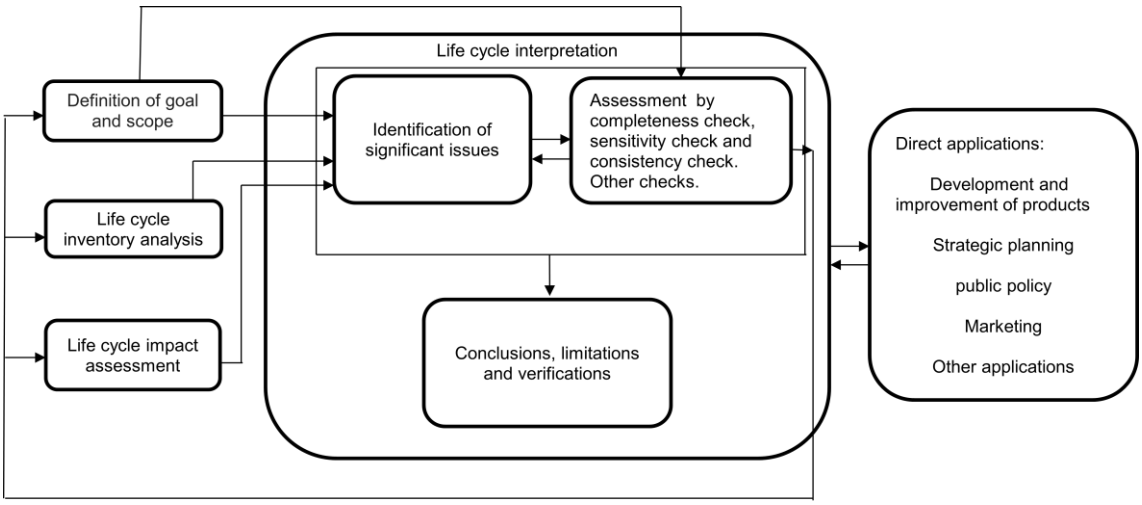

Source - BRAZILIAN TECHNICAL STANDARDS ASSOCIATION (ASSOCIAÇÃO BRASILEIRA DE NORMAS TÉCNICAS, 2014)[2].

4 RESULTS

This chapter presents the results obtained in the dissertation. As previously mentioned, a lamination process is conducted to protect the mono-Si devices from the environmental conditions, adding to them the same layers they have when building a module, while the OPV samples are already with all the layers, ready to face environmental conditions. Therefore, IV curves extracted right before and right after the lamination process are presented to show that the lamination occurred well and the samples are ready for the experiment. The transmittance of the glass used is also shown to verify that although it is not a proper PV glass, which has transmittance around 90%, the values found are considerably high. Afterwards, there is a section dedicated to the visual inspection, which is conducted to verify the devices prior to starting accelerated aging and after the end of the test to analyze the changes in its aspects.

On the sequence of this chapter, there is a very important part that presents the results of the accelerated aging test and the electrical performance of the devices during it. IV and PV curves are shown for different aging times and maximum power; besides several parameters are plotted through time, namely: short circuit current (Isc), open circuit voltage (Voc), current on maximum power point (Im), voltage on maximum power point (Vm), maximum power (Pm) and fill factor (FF). Finally, the ratio between OPV and mono-Si output power is presented as well as the relationship with aging on the natural environmental conditions. The information of this section is used for cost estimation on the next section and then for LCA on the following section. In the end, there is a general discussion to relate and compare information from the previous sections, completing all the results of the present work.

4.1 Lamination

As mentioned before, the mono-Si solar cells are laminated so that they are also protected from the environment conditions as the OPV cells are. Before starting this process, measurements are taken from the initial mono crystalline silicon cells, just before laminating and right after that. The IV curves extracted from the cells before the addition of other layers are presented on figure 20,

figure 21 and figure 22. The parameters extracted from them are present on table 4. Figure 23, figure 24 and figure 25 present the IV curves after lamination, with the respective parameters shown on table 5.

Figure 20 - IV curve for the 1st mono-Si cell

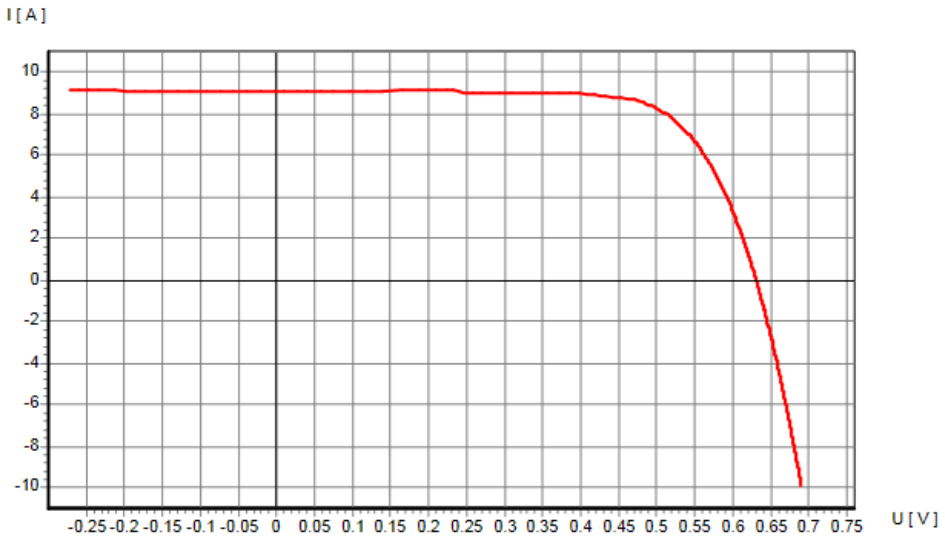

Source – Generated at PUCRS

Figure 21 - IV curve for the 2nd mono-Si cell

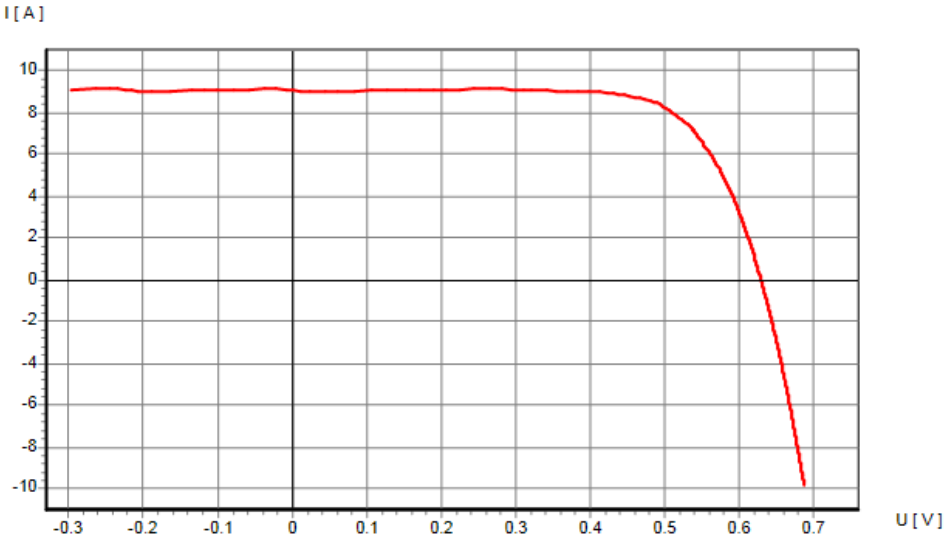

Source – Generated at PUCRS

Figure 22 - IV curve for the 3rd mono-Si cell

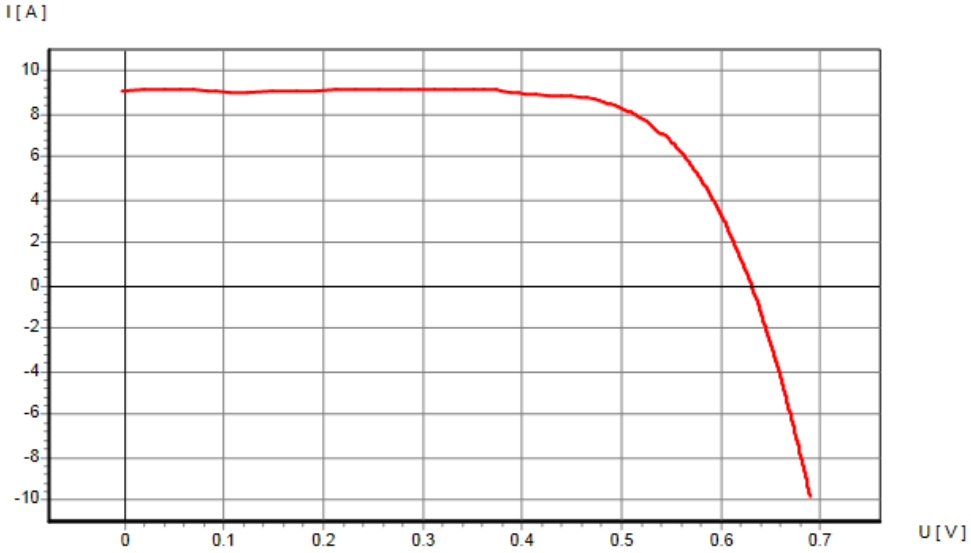

Source – Generated at PUCRS

Figure 23 - IV curve for mono-Si device A

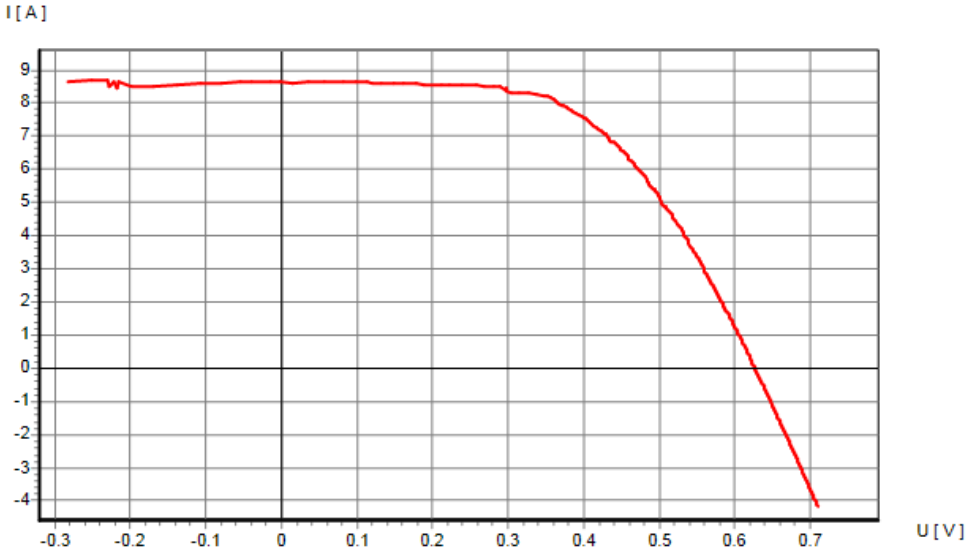

Source – Generated at PUCRS

Figure 24 - IV curve for mono-Si device B

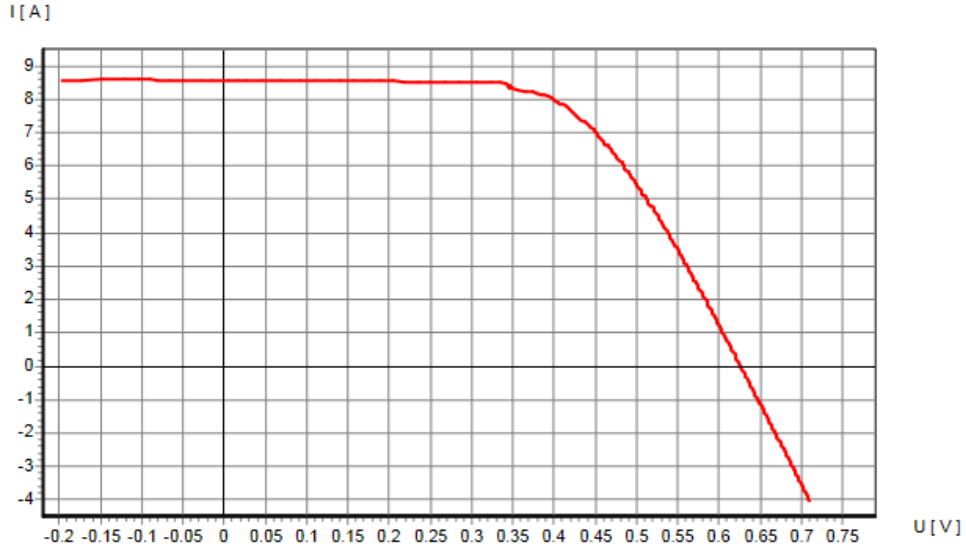

Source – Generated at PUCRS

Figure 25 - IV curve for mono-Si device C

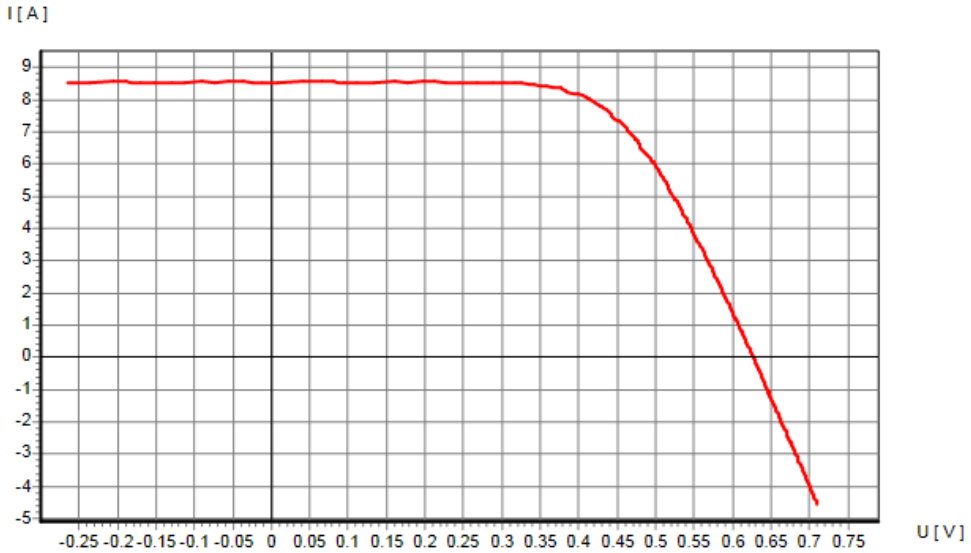

Source – Generated at PUCRS

Table 4 - Cells' parameters prior to the lamination process

	Mono 1	Mono 2	Mono 3	Average	
Voc	630.5	629.5	630.7	630.2	mV
Isc	9.073	9.072	9.128	9.091	A
Vm	491.6	489.1	490.5	490.4	mV
Im	8.404	8.438	8.438	8.427	A
Pm	4.13	4.13	4.14	4.13	W
FF	0.722	0.723	0.719	0.721	
Eff	16.50	16.43	16.40	16.44	%
Rs	8.0	7.8	7.9	7.9	m□

Source – Adapted from tables obtained at PUCRS

Table 5 - Devices' parameters after the lamination process

	Mono A	Mono B	Mono C	Average	
Voc	626.6	626.4	626.9	626.6	mV
Isc	8.617	8.564	8.513	8.565	A
Vm	412.5	415.7	432.2	420.1	mV
Im	7.348	7.740	7.723	7.604	A
Pm	3.03	3.22	3.34	3.20	W
FF	0.561	0.600	0.625	0.595	
Eff	12.11	12.86	13.34	12.77	%
Rs	21.2	21.3	18.8	20.4	m□

Source – Adapted from tables obtained at PUCRS

At this point, it is worth stating that unfortunately the identifications of the cells were lost during the lamination; therefore, it is not possible to directly relate the values for each device. At some point, it became so critical to preserve the samples integrity while removing them from the laminator membranes that the order of the labels were missed. Hence, the comparison is based on average values.

The average open circuit voltage (Voc) of 630.2 mV before the lamination drops to 626.6 mV after lamination, as can be seen comparing table 4 and table 5. It is explained due to the vertical shift occurred to the IV curve, because of the reduction of the photogenerated current due to additional layers and since it is exponential, it crosses the X-axis at lower values. The fill factor average starts with 0.721 and then it decreases to 0.595, what is justified by great drops on the Im and Vm values, much superior than the Isc and Voc reductions. Efficiency dropped from 16.44% in average to 12.77% and series resistance rose from

7.9 m□ to 20.4 m□. It is worth stating that before lamination the contact was done through a piece of equipment that touched the cells superior contacts on many points and on the backside of the cell, the whole area was touching a metal piece connected with the measuring system. After lamination, the contacts are done connecting wires on the busbars that were welded on the cells. This happened because of the welding of electrical conductors in series with the cell contacts. The shunt resistance was disregarded, because the values registered are not realistic.

Moreover, spectral transmittances of two samples of the spare glasses are measured on an ellipsometer and data are plotted on figure 26. One can observe that both samples behave in a very similar way and the curves are basically overlapping. Transmittance starts from approximately 83% for 1300 nm, slightly decreases, and then it reaches a maximum around 91% and presents a huge drop for wavelengths lower than 400 nm.

Figure 26 - Spectral transmittance for wavelengths from 360 nm to 1300 nm in percentage for two samples of the used glass

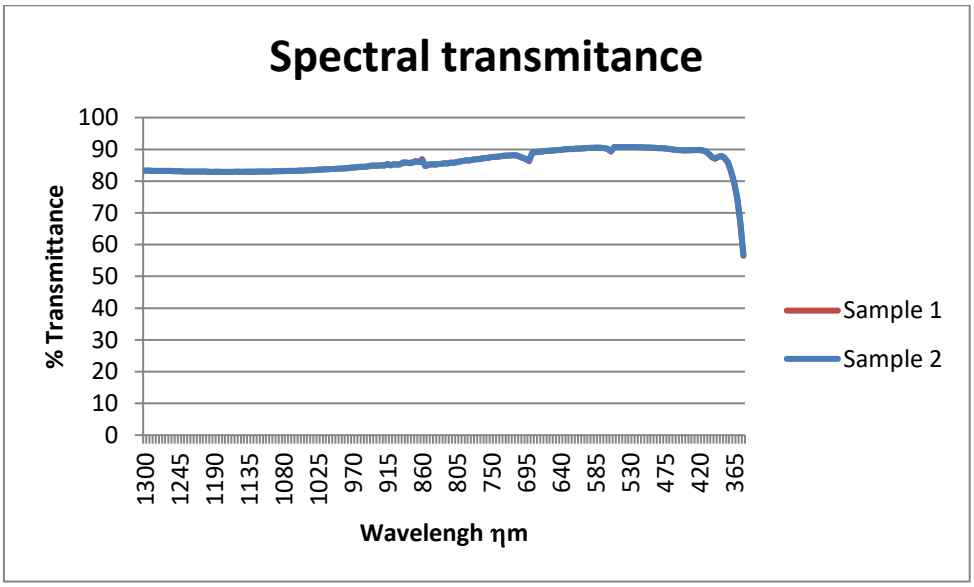

Source – Obtained from PUCRS

According to table 4, Isc values before lamination are between 9.072 A and 9.128 A. After analyzing figure 26, aware of an average transmittance of 85%, it is expected that Isc values would reduce at least 15%, since it is approximately

proportional to the irradiance on the cell. Nevertheless, according to table 5, Isc values range from 8.513 A to 8.617 A, what is around 94% of the initial values.

The increase of temperature of the cell could explain the Isc growth, but to be the only factor responsible to it, a variation of many degrees Celsius would be necessary. The glass' and EVA's refraction index combined could reduce the total reflectance as well as absorption. Besides that, the glass' thickness affects the constructive and destructive interferences and therefore the amount of light transmitted. Hence, it may be concluded that light angle, the layer combination and thickness and the reflection indexes may combine giving the observed results.

4.2 Visual inspection

The visual inspection is part of the accelerated aging experiments. Each time that measurements are done, the devices are observed looking for modifications on its visual aspects such as change of color, delamination, oxidation, bubbles formation, crack and similar artifacts. Figure 27 shows the mono-Si devices before the accelerated aging tests. It is worth reinforcing that almost 1.5 cm of glass, EVA and Tedlar is used extending beyond the cell edges on each side.

Figure 27 - Mono-Si laminated devices before the aging tests

Source – Photographed by the author

Figure 28 shows the device C of this type of technology when there was a problem with the climatic chamber and excess of humidity left some solute precipitated on its glass and how it was cleaned to continue the tests. It is important to highlight that modifications on the IV curve were minor. Finally, figure 29 shows those same devices when the experiments are concluded.

Figure 28 - Mono-Si device C cleaning when the climatic chamber had problems

(a) Device prior to cleaning and the appropriated wiper used to clean it

(b) Device after cleaning

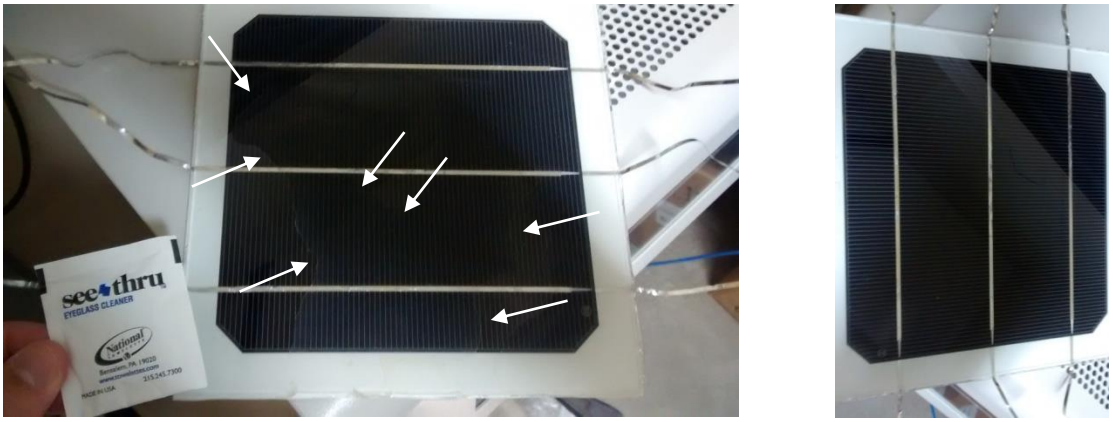

Source – Photographed by the author

Figure 29 - Mono-Si devices after the experiments

(a) Device A – light stability chamber

(b) Device B - drawer

(c) Device C – climatic chamber

Source – Photographed by the author

Unfortunately, the differences noticed are hard to be captured by a camera; anyway, they can be described. Device A, which was kept on the light stability chamber has a long delamination, but in only one of its corners. Device B, which was kept in the drawer without extreme conditions, has delaminations in all of its corners, but they cover small areas. Finally, device C, which was kept on the climatic chamber, has a small delamination on one of the corners and a clear stain over the glass. Those delaminations can be attributed, at least

partially, to sample manipulation. Since they are handled by the edges to avoid touching the glass over the cell area, many times layers are forced on the opposite direction of the glass, causing this type of damage. However, it is expected that delamination has small influence on electrical measurements, because it does not reach the cell area in any case. Discoloration is not a problem perceived and no cracks happened.

Figure 30 presents the OPV devices before the accelerated aging tests. Figure 31 shows the backside view of one of the devices where the metallic grid can be observed and figure 32 presents the OPV devices after aging. Finally, figure 33 illustrates how each stripe of active layer is connected on the OPV modules. There is a single sheet of IMI below all of them with one external contact attached to it and another IMI single sheet above all of them with another external contact. This way, all the OPV cells are connected in parallel.

Figure 30 - OPV modules prior to the aging tests

Source – Photographed by the author

Figure 31 - OPV-b backside view prior to aging tests

Source – Photographed by the author

Figure 32 - OPV devices after the experiments

(a) OPV device C - drawer

(b) OPV device D – light stability chamber

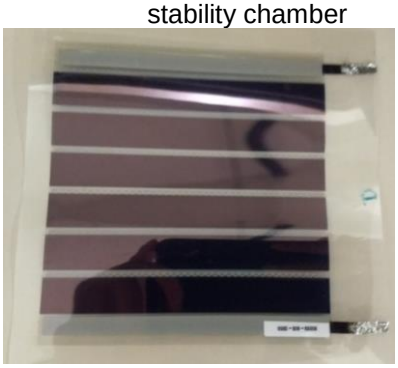

(c) OPV device E – climatic chamber

Source – Photographed by the author

Figure 33 - Schematic of the OPV module connections

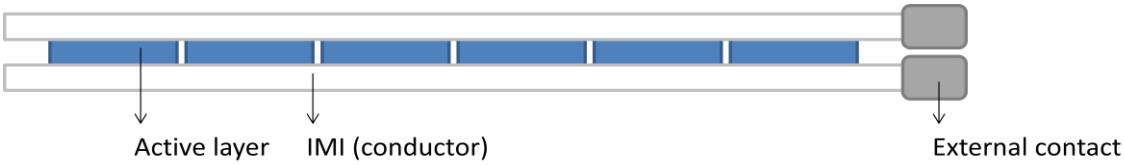

Source – Created by the author

Device C, on figure 32-(a), which was kept on the drawer without extreme conditions, has the external electrical contacts well attached to the plastic, a small delamination far from the active area and close to where the measuring wires are connected, indicating that they could have made this damage. Device D, on figure 32-(b), which was on the light stability chamber, only has the contacts partially loose. Lastly, device E, on figure 32-(c), which was on the climatic chamber, has loose contacts with the contact weld oxidized, a bubble is formed close to it. This one is the OPV device with the bigger delamination, but still far from the active area. All of the devices present the transparent conductor in a darker color while the lamination plastic is still very transparent merely with some scratches.

4.3 Electrical performance

This section is divided in four parts in order to present all the results of electrical performance. First, there are initial considerations about the measurements, showing the setup and presenting date, time and other details about each

measurement. In the sequence, one section for some IV and PV curves of OPV devices, followed by an analogue section for mono-Si. Finally, several data, for instance, maximum power and other parameters, is plotted through time.

4.3.1 Initial considerations about the measurements

This section shows the measurement setup on the Solar Continuous Simulator used at OptMA^{lab} (UFMG) and details of each measurement.

Figure 34 shows the setups as they are used to extract the IV curves during the accelerated aging tests. Label [1] indicates the mono-Si devices contact, label [2], the mono-Si device itself, label [3], the metal plate that is refrigerated, label [4], the OPV over lapping contacts, label [5], the OPV device itself and 6, the front panel containing the on/off switch, the switches for the lamps and ventilation and the voltage applied on lamps display.

Figure 34 - Measuring setups

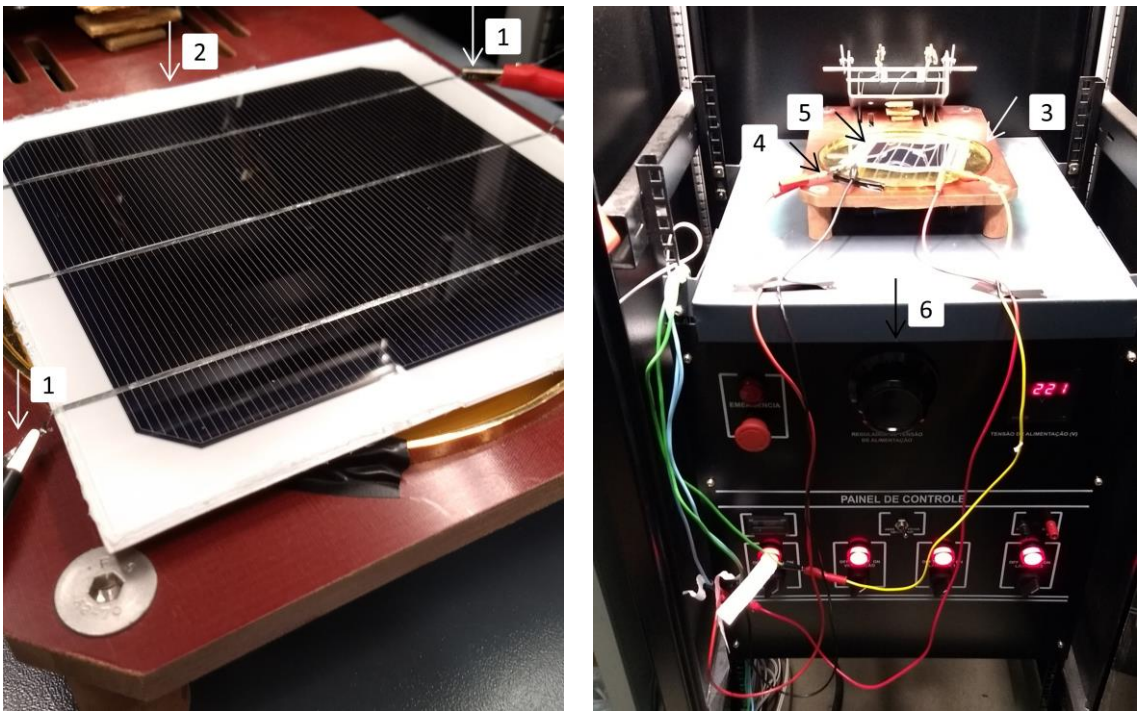

(a) Mono-Si (b) OPV

Source – Photographed by the author

The measurements were taken approximately on the same time of each day and they kept the devices out of the accelerated aging equipment for around 2:30 hours in average. Detailed information about each measurement is presented on table 6. Date, the time passed, the time that the devices were

picked up at CSEM, the start and end time of the Continuous Solar Simulator (CSS) and the time that the devices were returned. Besides that, the calibration voltage is shown, which is taken from the reference solar cell on open circuit to assure that the lamps are working properly and delivering the right irradiance. This cell comes with the CSS for the specific purpose of calibrating the equipment. In this case, values should be between 555.75 mV and 614.25 mV.

Table 6 - Accelerated aging tests measurements registration

Measurement	Date	Time (days)	Device pick up time	CSS working hours		Device return time	Calibration voltage (mV)
				Start	End		
0	28/11/16	0	-	16:06	17:11	18:05	602
1	30/11/16	2	15:15	15:56	17:29	18:15	601
2	02/12/16	4	15:33	16:17	17:17	18:00	595
3	05/12/16	7	14:40	15:20	16:20	17:05	600
4	12/12/16	14	14:30	15:05	16:05	17:00	600
5	19/12/16	21	14:20	14:55	15:55	16:40	599
6	03/01/17	36	14:05	14:39	15:39	16:30	595
7	18/01/17	51	14:30	15:01	16:01	16:45	596
8	02/02/17	66	14:25	14:55	15:55	16:55	598
9	17/02/17	81	13:35	14:05	15:30	16:20	599
10	06/03/17	98	14:20	14:57	15:57	16:50	595
11	20/03/17	112	15:20	15:36	16:43	17:50	595
12	03/04/17	126	14:10	14:50	15:50	16:40	596
13	17/04/17	140	14:40	15:17	16:43	17:35	597
14	02/05/17	155	14:30	15:13	16:31	-	597

Source – Created by the author

During the experiments, there were three problems with the climatic chamber, one between measurements 6 and 7, another between measurements 7 and 8 and the last one between measurements 8 and 9. While between 6 and 7 and between 7 and 8 the equipment stopped applying elevated humidity and temperature for an interval of time that cannot be determined, between 8 and 9 there was humidity in excess, as illustrated on figure 28.

After all those measurements, completing 15 at all, including the measurement 0, several graphs can be plotted. They cover IV and PV curves for different moments of the aging test and a series of parameters through time.

4.3.2 OPV devices: IV and PV curves

This section is focused on the OPV devices and shows three different moments of IV and PV curves. They are: right before starting the measurements, with 81 days of aging, which is the measurement closer to the middle of the experiment and then with 155 days, which is the last measurement.

Those curves are presented on figure 35 for the OPV device kept in the drawer. They reveal little modifications on the curves aspects and even a small increment in the maximum power can be observed on the last measurement. Isc values are close to 0.1 A, Voc approximates to 5 V and power is a bit lower than 0.20 W.

Figure 35 - Current versus voltage and power versus voltage curves for the OPV in the drawer device before the accelerated aging test, approximately on the middle of it (81 days) and on the last measurement (155 days)

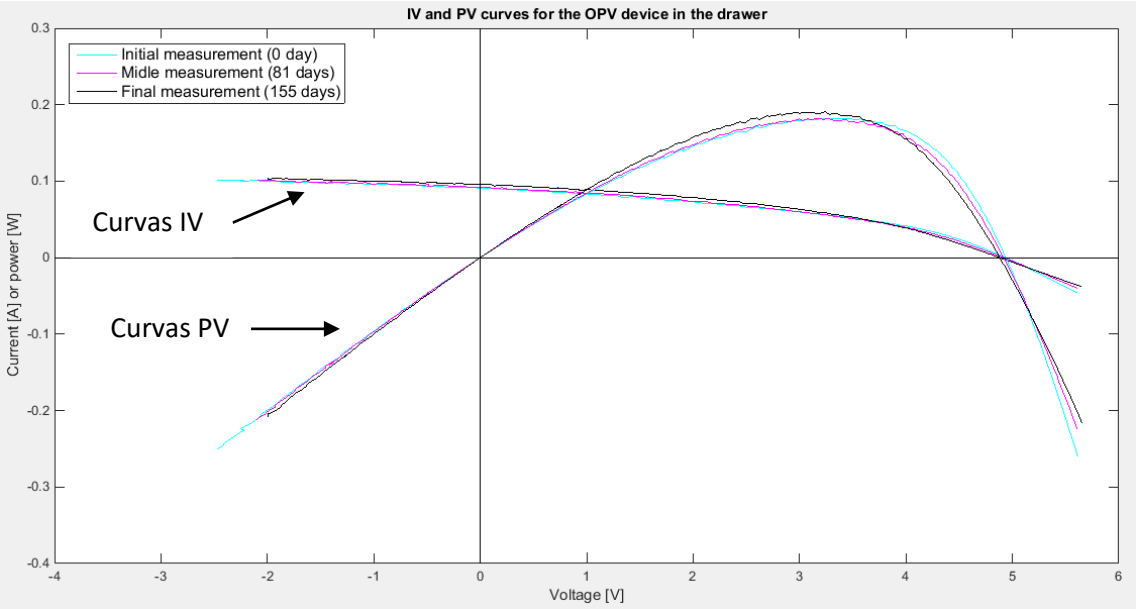

Source – Created by the author

Figure 36 shows both types of curves for the OPV device kept in the light stability chamber. Isc starts on the same value, however it drops to half of it on the last measurement, while Voc does not modify significantly. The curve covers a much smaller area on the first quadrant, but its shape is still similar to the initial one. Power, which is a little higher than 0.2 W at first, also drops to almost half of it.

Figure 36 - Current versus voltage and power versus voltage curves for the OPV device in the light stability chamber before the accelerated aging test, approximately on the middle of it (81 days) and on the last measurement (155 days)

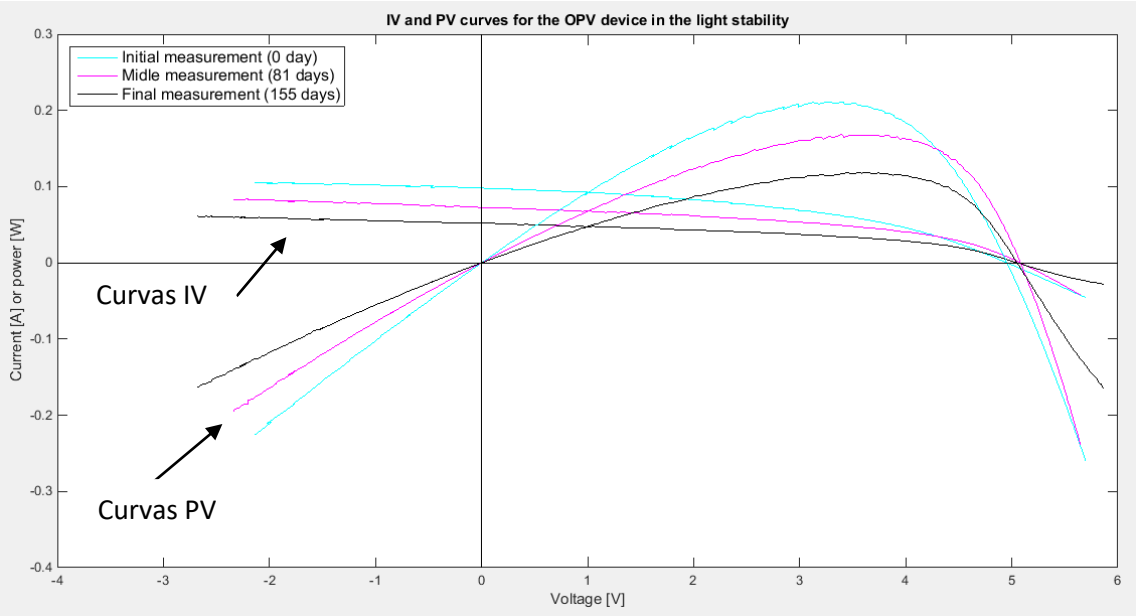

Source – Created by the author

The last OPV device is the one in the climatic chamber, shown in figure 37. The initial Isc, Voc and Pm are very similar to the previous devices; however, the IV curve shape is completely modified. It takes a shape similar to the letter “S” facing left. This shape may be attributed to the difference of degradation among the cells composing the OPV module, because it is expected that cells closer to the edge are more impacted by humidity. The decrement in Isc can be noticed, but is considerably small, while Voc reduces significantly. The modifications from the knee until Voc suggest an increase in the reverse saturation current that shifts this part of the curve to the left. Power becomes so low and also gets a different shape that it is important to keep attention to distinguish it from the IV curves, which are lower for each value between 1 V and Voc, and has higher values on the rest of the voltage range.

Figure 37 - Current versus voltage and power versus voltage curves for the OPV device in the climatic chamber before the accelerated aging test, approximately on the middle of it (81 days) and on the last measurement (155 days)

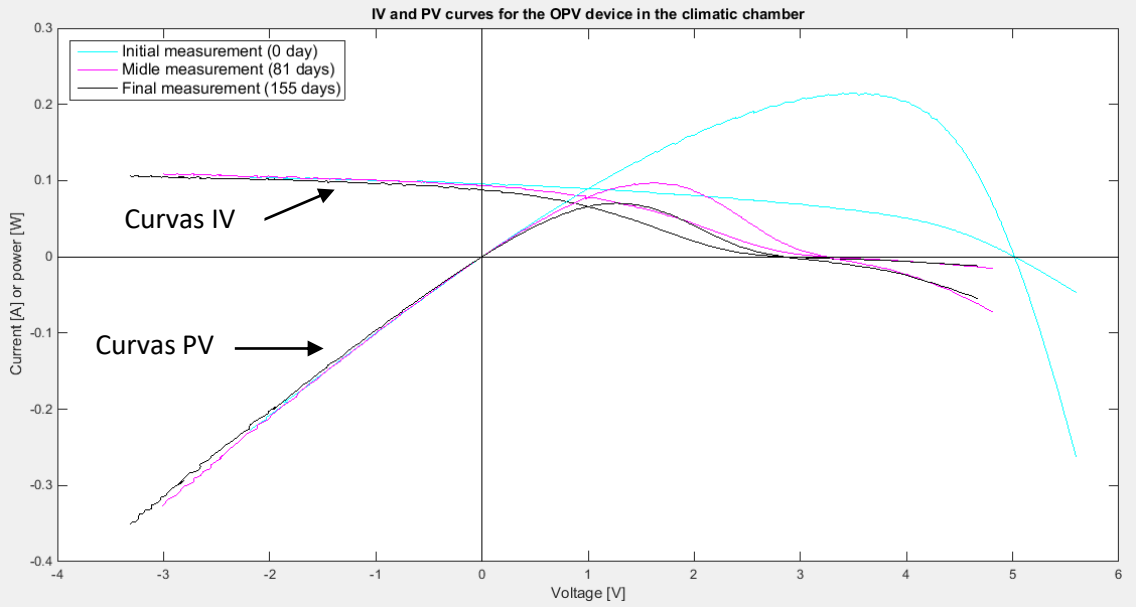

Source – Created by the author

4.3.3 Mono-Si devices: IV and PV curves

In this section the same type of graphs are shown, however for mono-Si in this case. There are still three IV and three PV curves for each sample of this type of technology and again the begging of the experiment (day 0), the approximate middle of it (81 days) and the last measurement (155 days) are presented.

In the case of mono-Si, changes on the curves can be also noted on the device in the drawer, as shown on figure 38. Isc values do not modify among measurements and Voc only reduces a bit. However, series resistance increases, it can be observed on the part of the curve that is similar to a source of voltage, which becomes more inclined through time, being that the difference between the initial and the middle measurement is much bigger than the difference between the middle and the final measurement.

Figure 38 - Current versus voltage and power versus voltage curves for the mono-Si device in the drawer before the accelerated aging test, approximately on the middle of it (81 days) and on the last measurement (155 days)

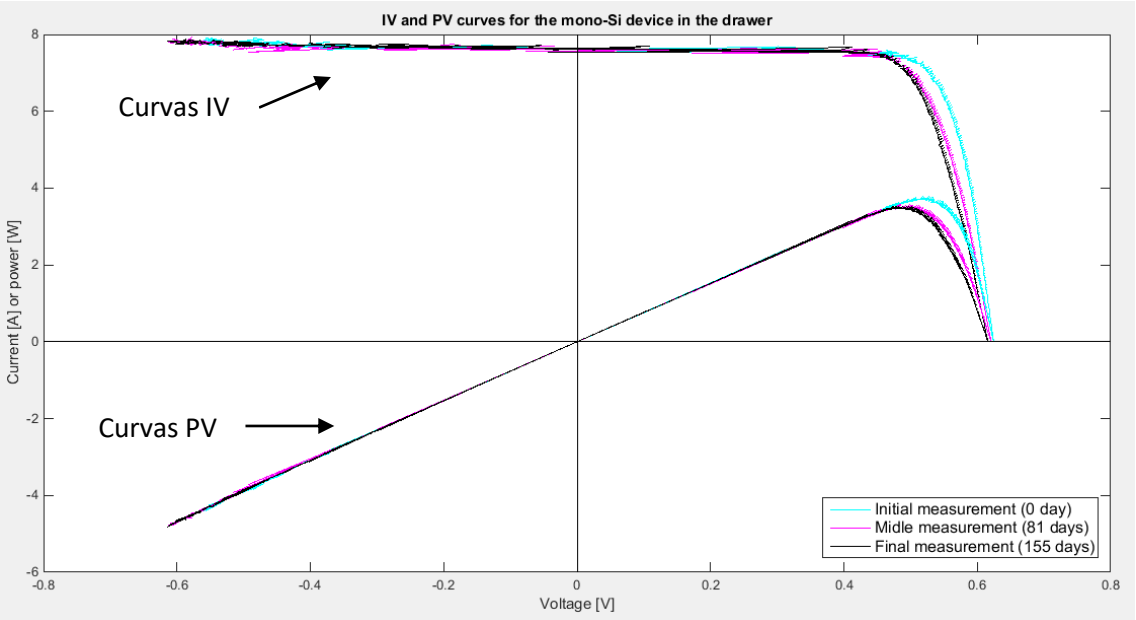

Source – Created by the author

In the case of the mono-Si device kept in the light stability chamber, presented on figure 39, modifications after the middle measurement are minor. Through time, Isc as well as Voc reduces a little and again the main modification is an increment of series resistance.

Figure 39 - Current versus voltage and power versus voltage curves for the mono-Si device in the light stability chamber before the accelerated aging test, approximately on the middle of it (81 days) and on the last measurement (155 days)

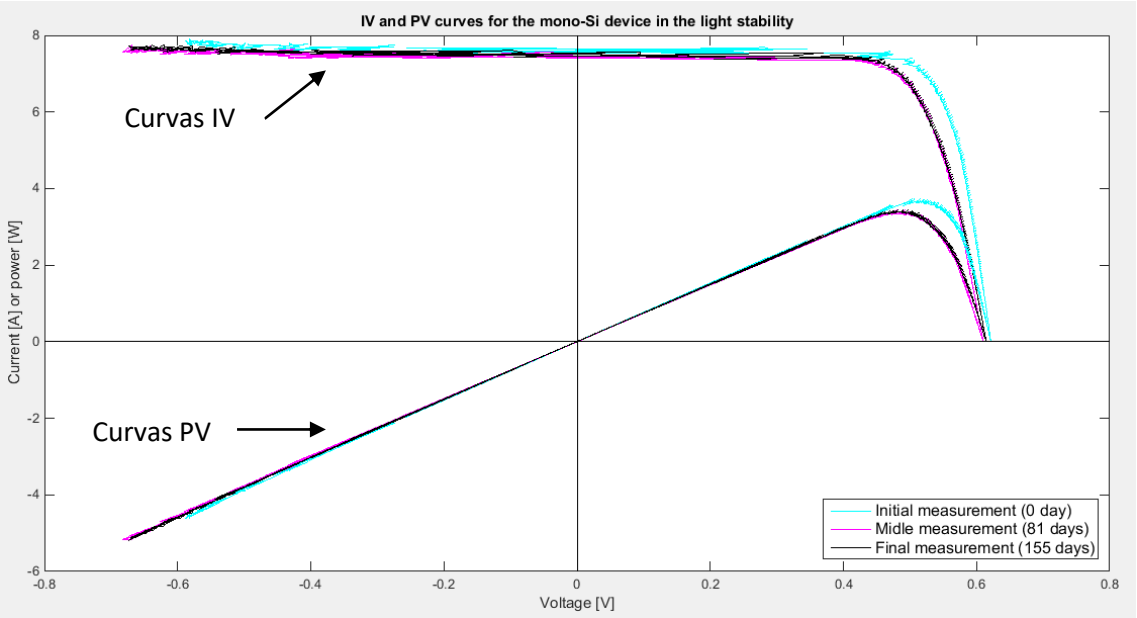

Source – Created by the author

Lastly, the IV and PV curves for the mono-Si device kept in the climatic chamber can be observed on figure 40. It presents the higher difference between the middle measurement and the last one, Isc values reduce and the power drop is the biggest among this type of technology.

Figure 40 - Current versus voltage and power versus voltage curves for the mono-Si device in the climatic chamber before the accelerated aging test, approximately on the middle of it (81 days) and on the last measurement (155 days)

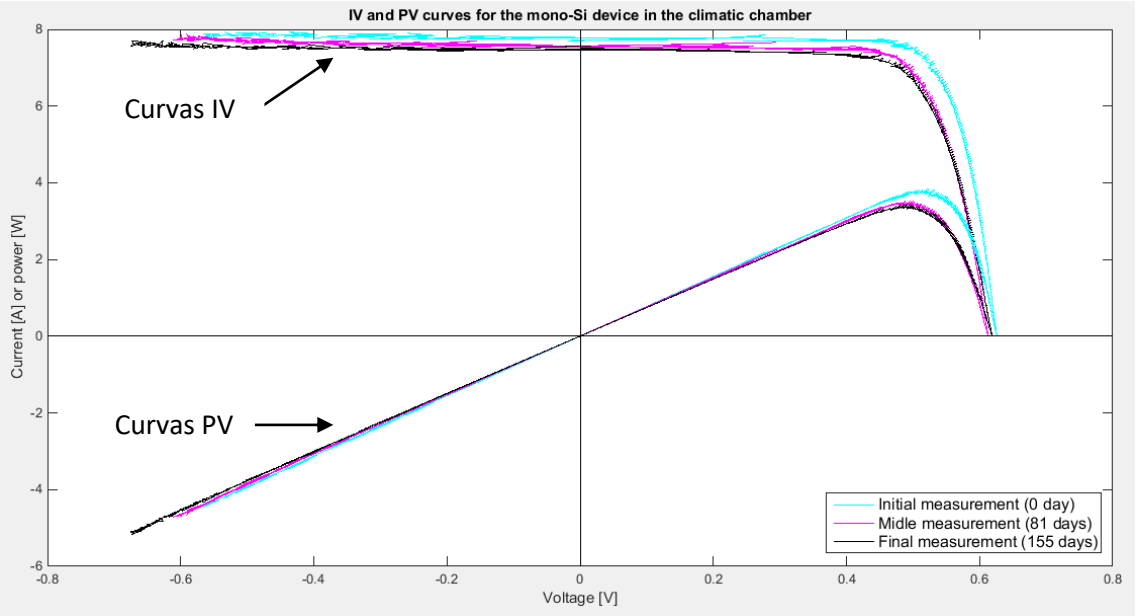

Source – Created by the author

4.3.4 Time evolution of maximum power and other parameters

In this section, several graphs are plotted to show the modifications on the devices over time. It starts with maximum power for OPV, followed by the maximum power for mono-Si and then several graphs showing both technologies together with normalized values, namely current on maximum power point, voltage on maximum power point, short circuit current, open circuit voltage and fill factor. Finally, the ratio of maximum power for OPV and mono-Si at each time is shown and two graphs are presented relating the accelerated aging with the value commonly found in the literature, one for climatic chamber and the other for light stability chamber.

Figure 41 presents the maximum power of each OPV device through time. The initial maximum power for the device kept in the drawer is considerably lower than for the other two devices and it rises as time passes. For all the devices, there is a part of the curve plenty of variations on the beginning of the tests interpreted as a stabilization time. The device in the climatic chamber presents an enormous drop on its maximum power and almost stabilizes close to 0.09 W while the device in the light stability chamber stabilizes around 0.16 W.

Figure 41 - Measurements results of maximum power through accelerated aging tests time for OPV devices

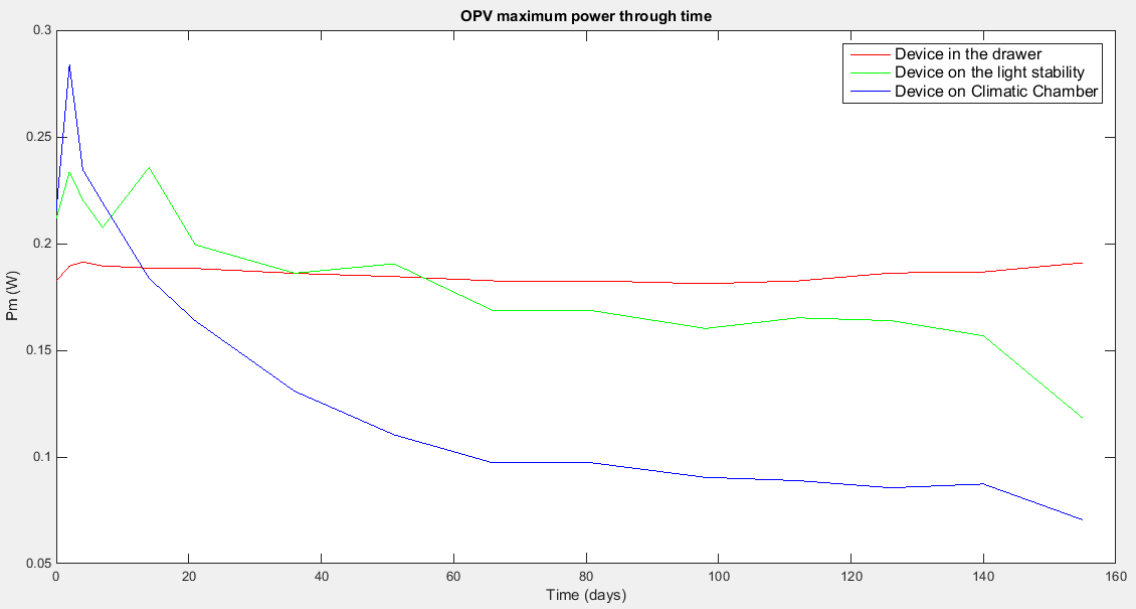

Source – Created by the author

An analogous graph is shown for mono-Si devices on figure 42. The highest initial maximum power is observed for the device in the climatic chamber, followed by the device in the drawer and then the device in the light stability chamber. One more time, greater variations are perceived on the beginning of the experiments. As it was predicted through the PV curves presented before, the device in the drawer also has a significant reduction on its maximum power. On day 81 the increment in the value referent to the climatic chamber can be associated with the fact that this equipment stopped working in this period. Nevertheless, on day 51 it can be inferred that some outer influence took place, because all of the measurements presents a local pick on the curve, even for the OPV device in the light stability chamber. On day 112, there is an unexpected behavior on the curve corresponding to the climatic chamber. This can be attributed to some deviation on the measurement, because later, on the next measurement, the curve restores the previous behavior.

Figure 42 - Measurements results of maximum power through accelerated aging tests time for mono-Si devices

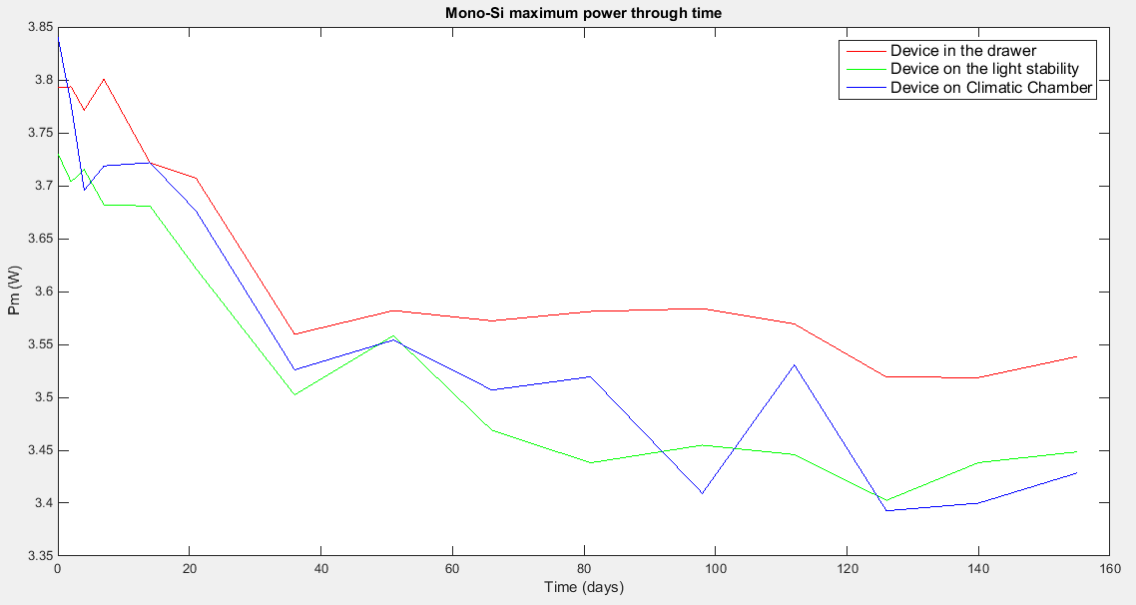

Source – Created by the author

In the sequence, maximum power for each measurement is normalized being divided by the initial maximum power on the first measurement of that same device and data is plotted on figure 43. By this way, the normalized power for all the devices is equal to 1 when time is equal to 0. With this kind of manipulation, it becomes evident that variations on mono-Si are much milder than on OPV, even in respect with the maximum power increase of the OPV device in the drawer.

Mono-Si with 126 days sums 21% of degradation (9% for light stability chamber + 12% for climatic chamber). OPV with 18.5 days also adds 21% of degradation (0% for light stability chamber – because in this case the device gained efficiency on the first days of experiment – and 21% for climatic chamber). Those values are highlighted, because 80% left of efficiency is usually the value that defines the end of life of a PV module.

Figure 43 - Normalized results of power through accelerated aging tests for both kinds of devices

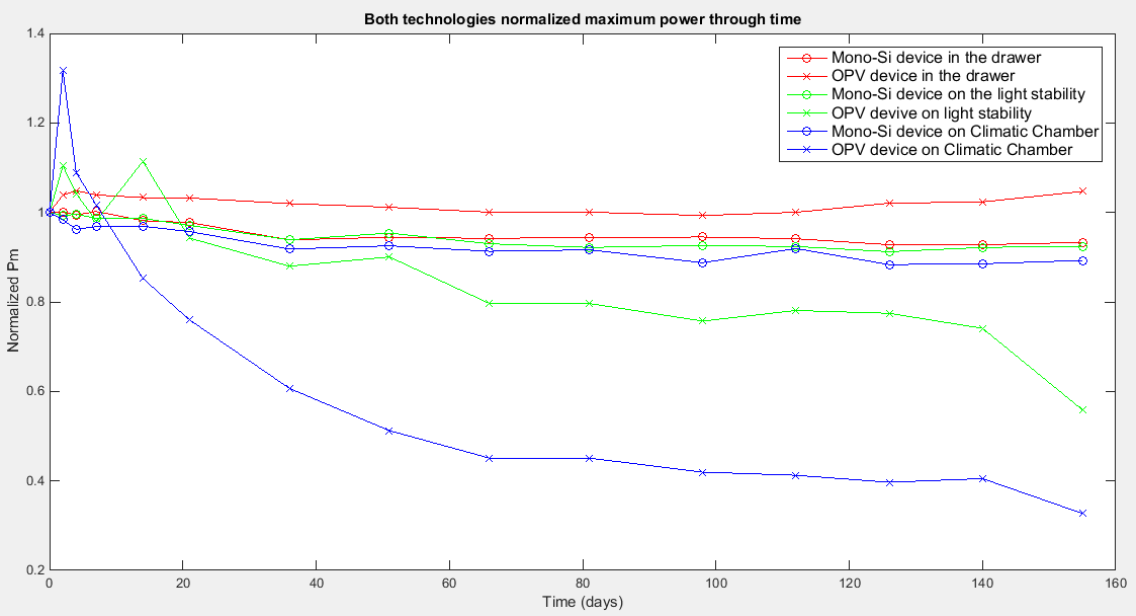

Source – Created by the author

After that, several parameters are extracted, normalized on the same way done for maximum power, and plotted through time. The first of them is the current on maximum power point, shown on figure 44. In this case, the OPV device in the light stability chamber has a drop of this parameter, which is much higher than any other device, their variations do not surpass 10%, while for this specific device it reaches 50%.

For mono-Si, the greater degradation is on the device from the climatic chamber.

Figure 44 - Normalized results of current on maximum power point through accelerated aging tests for both kinds of devices

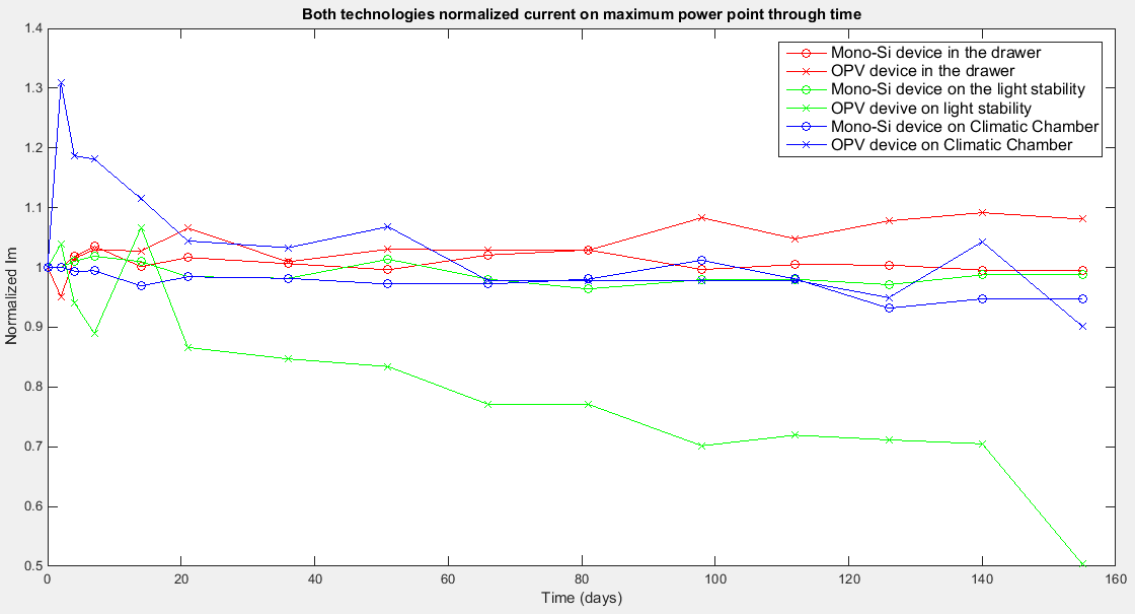

Source – Created by the author

On figure 45, voltage on maximum power point is plotted through time. In this case, the highlighted device is the OPV in the climatic chamber. The OPV device in the light stability chamber has an increase.

Figure 45 - Normalized results of voltage on maximum power point through accelerated aging tests for both kinds of devices

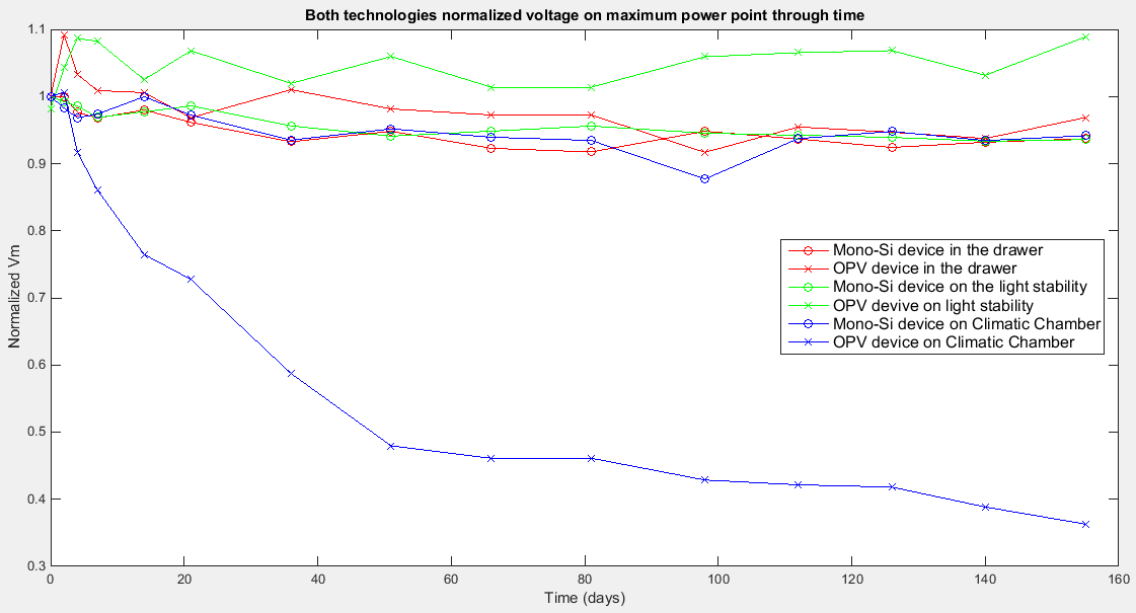

Source – Created by the author

As expected from previous experiences with OPV, the Isc value of the device in the light stability chamber had the greater degradation, almost reaching 50%, and the one on the climatic chamber reaches almost 10%. This can be seen on figure 46. For mono-Si, the device in this same aging equipment was the only one with Isc reductions.

Figure 46 - Normalized results of short circuit current through accelerated aging tests for both kinds of devices

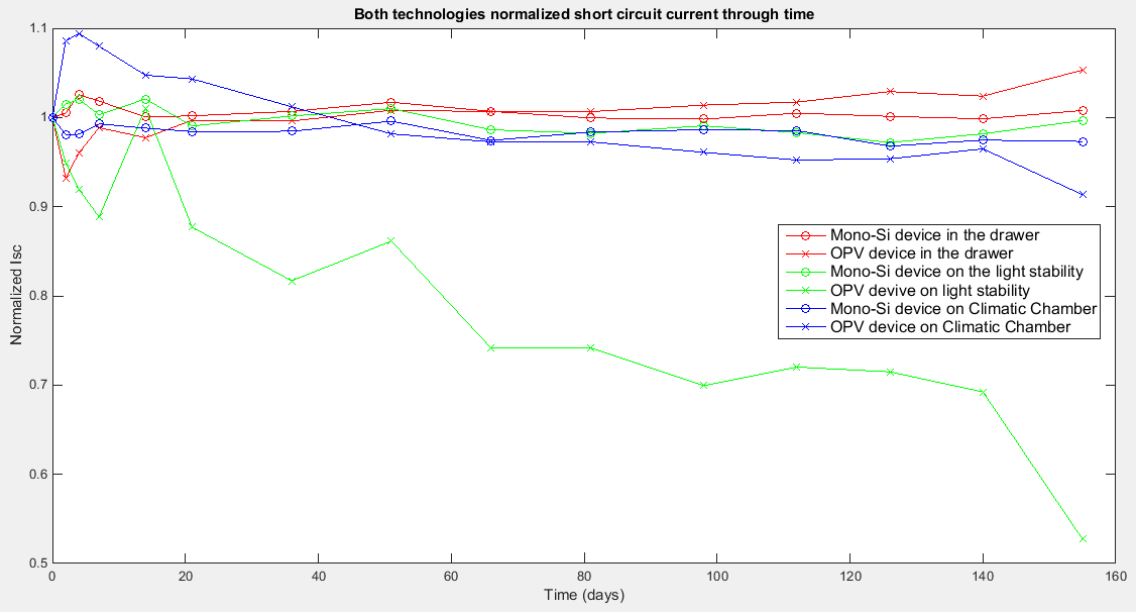

Source – Created by the author

Normalized open-circuit voltage through time is plotted on figure 47. For the mono-Si devices the reduction is very small and practically the same as well as for the OPV in the drawer. While that the OPV device in the light stability chamber has a small increment and the OPV in the climatic chamber has a huge drop of 40%.

Figure 47 - Normalized results of open circuit voltage through accelerated aging tests for both kinds of devices

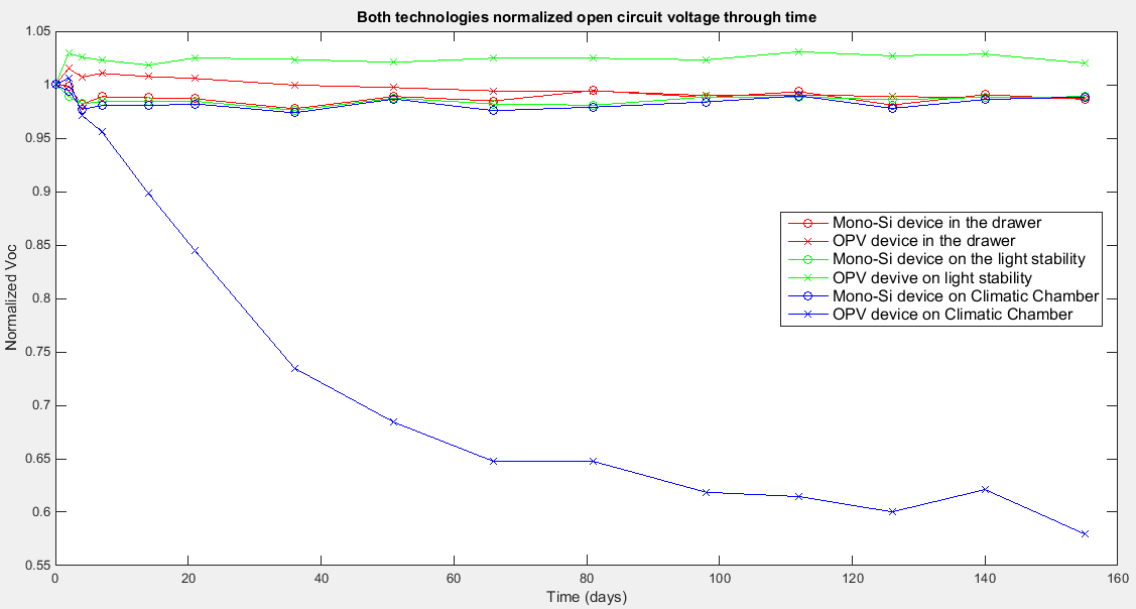

Source – Created by the author

On figure 48, the normalized fill factor (FF) is illustrated. It shows great increase for all the OPV devices on the first measurement what can explain the maximum power behavior on that moment. As time passes, the OPV device in the drawer gets back to a value very close to 1 and the OPV device on light stability chamber has a small increment on the FF. All the mono-Si devices have similar drops and the OPV in the climatic chamber drops almost 40%.

Figure 48 - Normalized results of fill factor through accelerated aging tests for both kinds of devices

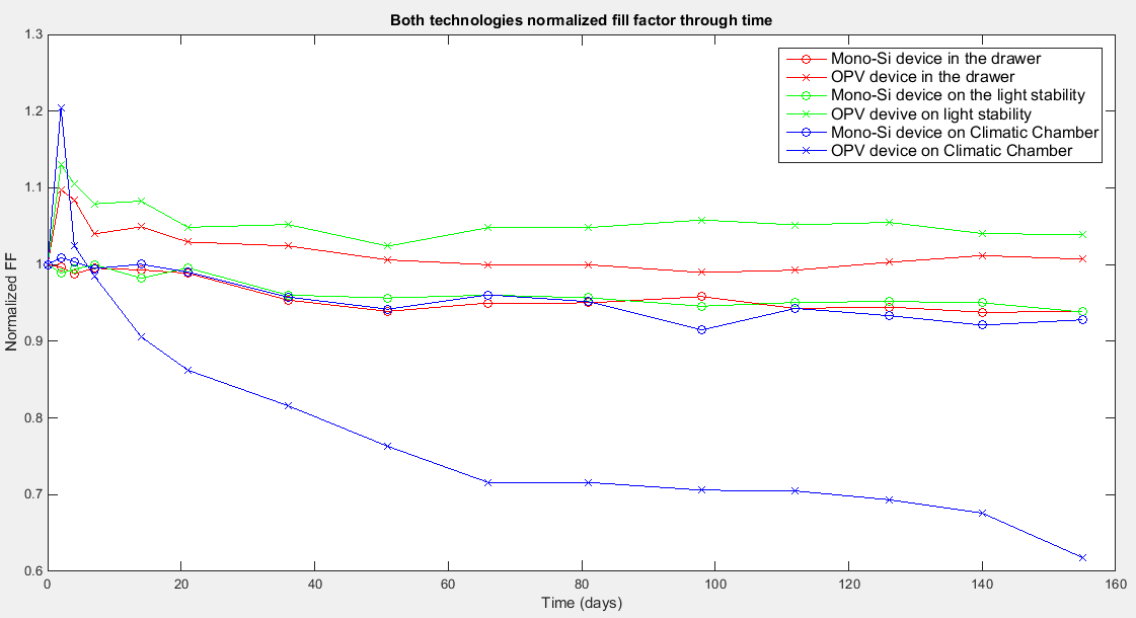

Source – Created by the author

While that, figure 49 shows a relationship between the degradation of both types of technology. For each time and type of aging equipment, the ratio between the maximum power for OPV and for mono-Si is calculated and then plotted through time. This way, the graph shows how much more the OPV degrades than the mono-Si in the climatic chamber (60% in the end of the period) and in the light stability chamber (40% on day 155).

Figure 49 - Ratio between the OPV normalized power and the mono-Si normalized power for each measurement through time

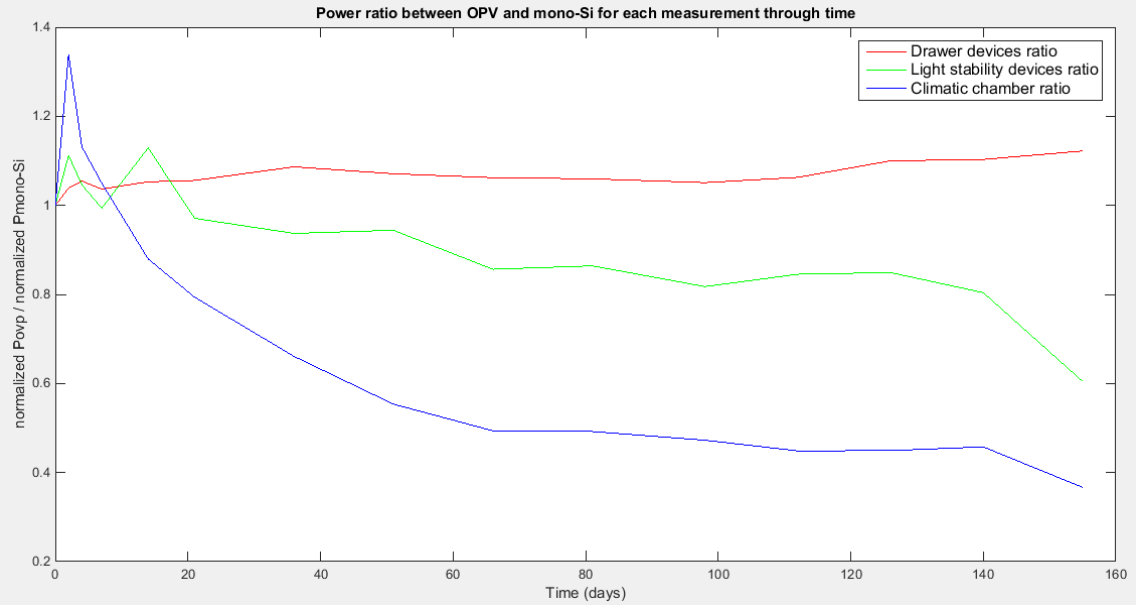

Source – Created by the author

Finalizing the electrical performance analysis, a theoretical degradation curve is plotted over the graph of normalized power versus time, it is presented on figure 50. This curve is made considering a degradation of 1% per year as presented by Diniz (2017) who got to this number based on literature review. However, the time values corresponding to each value of power is divided by 17 so that the degradation with 155 days is equivalent to the degradation in the light stability chamber in the end of the experiment. This suggests that the conditions in the light stability chamber equipment makes one day equivalent to 17 days in the natural environment.

Figure 50 - Mono-Si theoretical degradation curve with time axis compressed 17 times matching the final efficiency of the mono-Si device in the light stability chamber

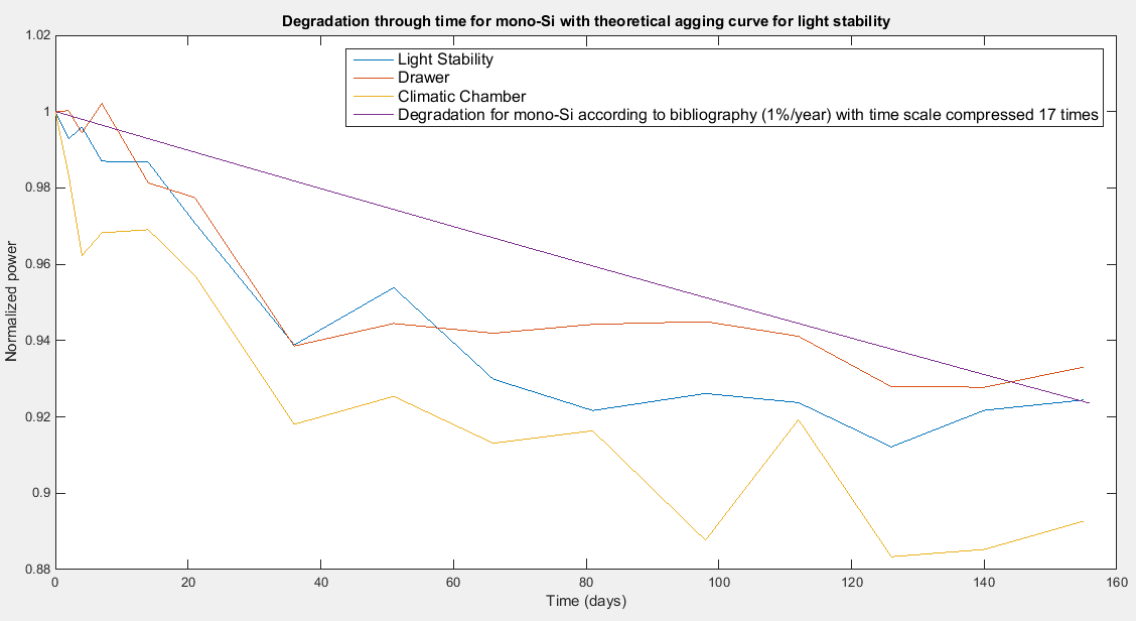

Source – Created by the author

Figure 51 is the analogous graph to match the final power of the device in the climatic chamber. In this case, the time axis has to be divided by 25, indicating that this equipment is more aggressive to the device in a way that each day of accelerated test is equivalent to 25 days in the natural environment and operation.

Figure 51 - Mono-Si theoretical degradation curve with time axis compressed 25 times matching the final efficiency of the mono-Si device in the climatic chamber

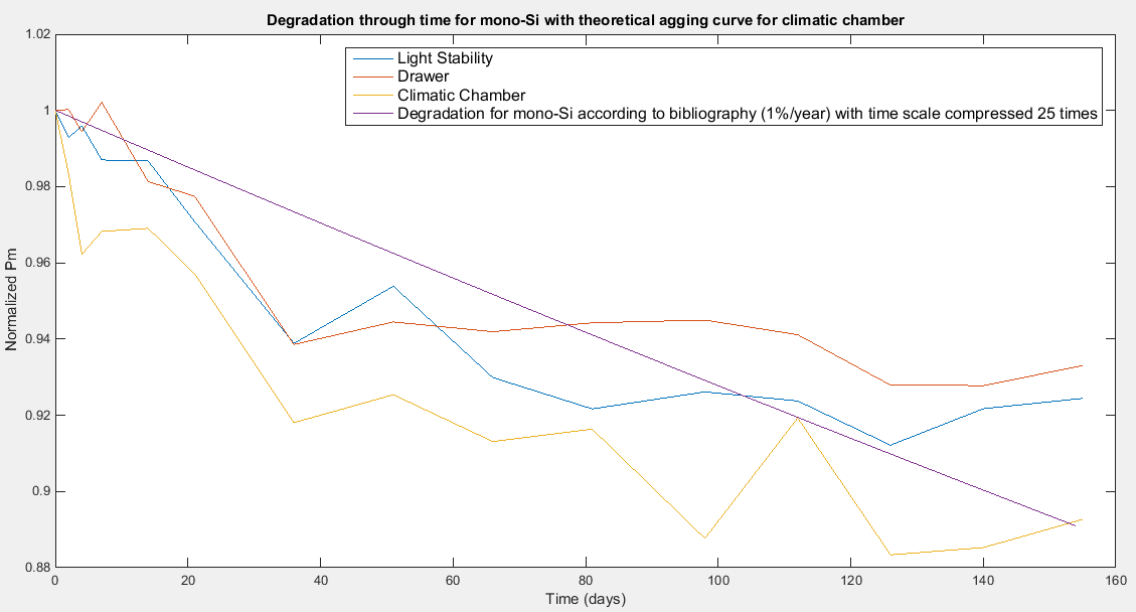

Source – Created by the author

When operating the combination of temperature, humidity and light is probably co-participaticipative and light is still partially responsible for temperature rose.

4.4 Economic viability index

As stated before, the levelized cost of energy is calculated to be used as economic indicator for both technologies. The power plant proposed is DC and 3 kWp.

The maximum output power of OPV considered is 20 W for a commercial module of 1 m^2, because it is considered the approximate measured initial Pm of 0.2 W for the 10 cm^2 sample devices. Mono-Si commercial modules are considered with 255 W, because this was the average of the 5 modules searched for cost. It defines the amount of modules needed for each type of power plant and the array for OPV is illustrated on figure 52 and for mono-Si is shown on figure 53.

Figure 52 - One-line diagram for the OPV array

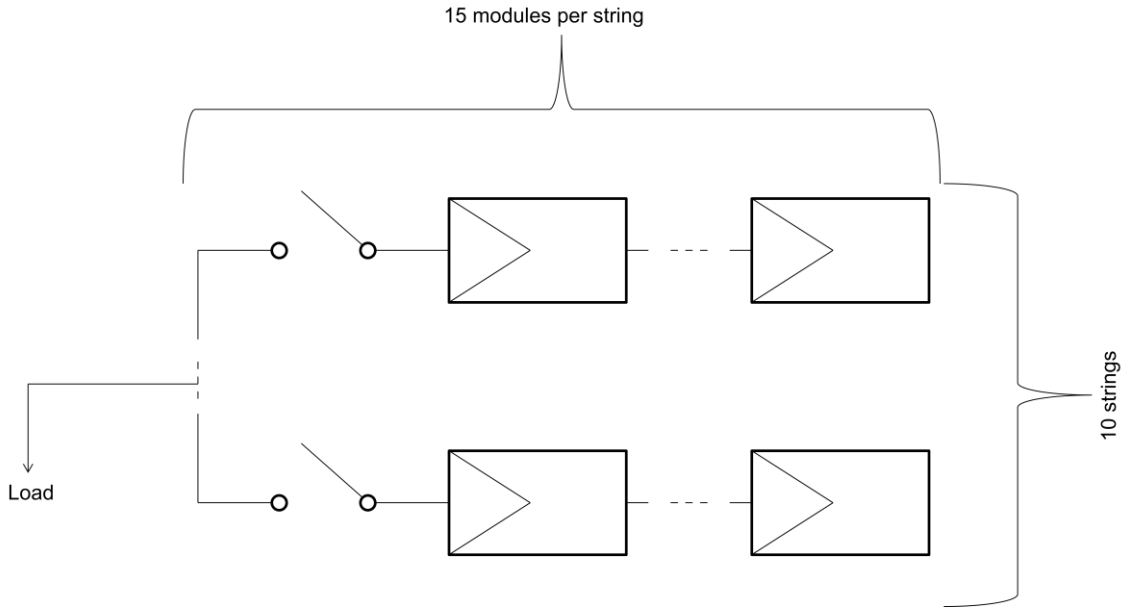

Source – Created by the author

Figure 53 - One-line diagram for the mono-Si array

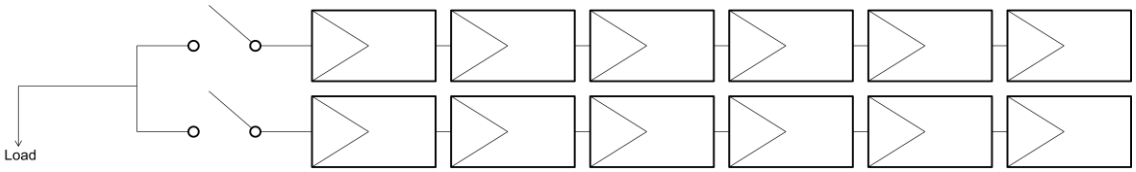

Source – Created by the author

In the case of OPV modules, three manufacturers around the world were contacted for prices, however commercial quotations are not available yet. Therefore, the search is done on papers that estimates its manufacturing cost according to the cost to build the factory, materials and process costs as well as the return of investment. Table 7 shows the costs calculated by several authors.

Table 7 - OPV module costs according to several sources

Authors	Price per Wp in foreign currency	Price per Wp in R$	Observation
Roes apud (MULLIGAN *et al.*, 2014)	2.8	R$ 10.42	5% efficiency, life time equals to crystalline silicon and glass substrate
(ESPINOSA *et al.*, 2011)	0.50-0.60 €	R$ 1.86-2.23	Forecast for 2013-2020
(MACHUI *et al.*, 2014)	4.28	R$ 15.92	37% of active area, 1.82% efficiency
(GAMBHIR; SANDWELL; NELSON, 2016)	US$ 0.23-0.34	R$ 0.72-1.06	Costs most sensitive to manufacturing scale, cell efficiency and module fill factor
Mulligan apud (GAMBHIR; SANDWELL; NELSON, 2016)	US$ 0.16	R$ 0.50	5% efficiency

Source – Created by the author

For the mono-Si power plant, module costs are searched online along with five different sellers. The modules nominal power ranges from 240 W to 275 W, then the price is calculated per Wp so that an average can be calculated, finding R$ 3.68/Wp with prices going from R$ 2.72/Wp until R$ 4.58/Wp.

Modules, mounting system, cables and switches costs are considered. Their amount and prices are specified on table 8. Average prices are registered for the modules. Mounting system is quoted for mono-Si. Considering that OPV modules weigh only 0.5 kg while the mono-Si weighs around 19 kg, the cost of OPV's mounting system is assumed to be proportional to its weight.

Table 8 - Prices per item for both power plants

	Mono-Si		OPV	
	Amount	Price (R$)	Amount	Price (R$)
Modules	12*255 Wp	3.68/Wp	150*20 Wp	5.96 /Wp
Switches	2	16.45	10	16.45
Cables	80 m	43.90	380 m	43.90
Mounting system	12	153.75	150	3.98

Source – Created by the author

Land costs are not taken into account, because it is considered that the area used will be rooftops of existing buildings. The annual operation and maintenance of the systems is set as 1% (MIRANDA, 2013). The discount rate taken into account is of 5%.

Mono-Si generation is calculated according to PVWatts Calculator (NATIONAL RENEWABLE ENERGY LABORATORY, 2017). The city of Belo Horizonte

radiation data is taken into account, more precisely the monitoring done in the Pampulha region. The module efficiency is set to 15% such as the average initial efficiency of the mono-Si samples.

Since the power plant is DC, there should not be any losses due to the inverter. Nevertheless, PVWatts Calculator does not allow ignoring this equipment or setting its efficiency to 100%, then the solution found is to set it to its maximum efficiency, which is 99.5% and reducing the system losses from 14% to 13.5%. By this way, the combined effect of both parameters is a reduction of approximately 14% in the output, as initially set by the software loss. It takes to a generation of 4788 kWh on the first year.

OPV generation is calculated for the same daily average radiation data used in PVWatts Calculator for mono-Si, according to eq. 3, in which E in the annual electrical energy generated, I is the annual irradiation (2054.95 kWh/m^2/year), A is total area of modules (150 m^2), Ef is the efficiency (3%), Act is the fraction of active area (0.67) and PR is the performance ratio (0.86).

$$\mathbf{E = I \cdot A \cdot Ef \cdot Act \cdot PR} \quad (\mathbf{3})$$

It takes to an initial generation of 5328 kWh on the first year. It is considerably higher than the first year for mono-Si, because the mathematical model used is much simpler and does not take into account many types of losses. For instance, the reflection for high angles of incidence. In spite of that, this value is still used considering that this type of technology works better with low levels of irradiation and angles of incidence far from the optimum.

A yearly degradation rate of 1% (Diniz, 2017) is taken into account and applied on the second year on for mono-Si. However, it is perceived from the section 4.3 that OPV degradation is much higher than mono-Si. Thus, according to figure 51 , that relates each day of accelerated aging test with 25 days of real degradation, each real year is treated as equivalent to 14.6 days of the test (25 multiplied by 14.6 days is equals to 365 days). In the sequence, according to figure 49, for each interval of 14.6 days until 146, what is equivalent to the ten years of the system considered, the ratio between the OPV normalized power and the mono-Si normalized power is registered. Later, it is discounted from the

original degradation that the system would have with the 1% rate as shown on table 9. The climatic chamber time relationship is used, because it is the equipment most aggressive to the devices according to the graphs seen on section 4.3.4, mainly figure 43, and in real environment conditions light would still be one more environmental factor collaborating with degradation. This additional degradation is regarded only for OPV devices, since mono-Si accelerated degradation was considered equivalent to the natural degradation reported by the bibliography and hence taken as reference.

Table 9 - OPV generation according to degradation

Time (Year)	Generation with mono degradation (kWh)	Ratio Popv/Pmono	OPV generation (kWh)
0	0	0	0
1	5328	0.87	4636
2	5275	0.72	3798
3	5222	0.61	3186
4	5170	0.52	2688
5	5118	0.49	2508
6	5067	0.48	2432
7	5016	0.47	2358
8	4966	0.45	2235
9	4917	0.45	2212
10	4867	0.42	2044

Source – created by the author

Conducting the whole LCOE calculation, the results presented on table 10 are obtained. According to the several modules costs obtained, minimum, average and maximum LCOE values are shown.

Table 10 - LCOE results in R$/MWh

	OPV	Mono-Si
Min.	1077	474
Avg.	2008	576
Max	3707	670

Source – Created by the author

4.5 Life Cycle Assessment

The last set of results presented in this section refers to the life cycle assessment of the PV modules. The study is conducted using OpenLCA and the ecoinvent database. Input data for the assessment of OPV modules is obtained from the literature and the processes are implemented by the author in OpenLCA. On the other hand, Mono-Si modules assessment is based on processes already implemented in the database.

4.5.1 LCA for OPV devices

Initially, the LCA of a generic OPV device is presented, based on ESPINOSA *et al.* (2011). The production process assessed is illustrated on figure 54 and table 11 contains the inputs for each of the steps presented on it together with the embodied energies of each material. Further information can be found on the reference paper. As previously mentioned, the software Open LCA is used. Although input data is the same, the study is different and has more impact categories, therefore some categories may be compared with the reference paper and others do not.

Figure 54 - Process considered for the LCA of OPV

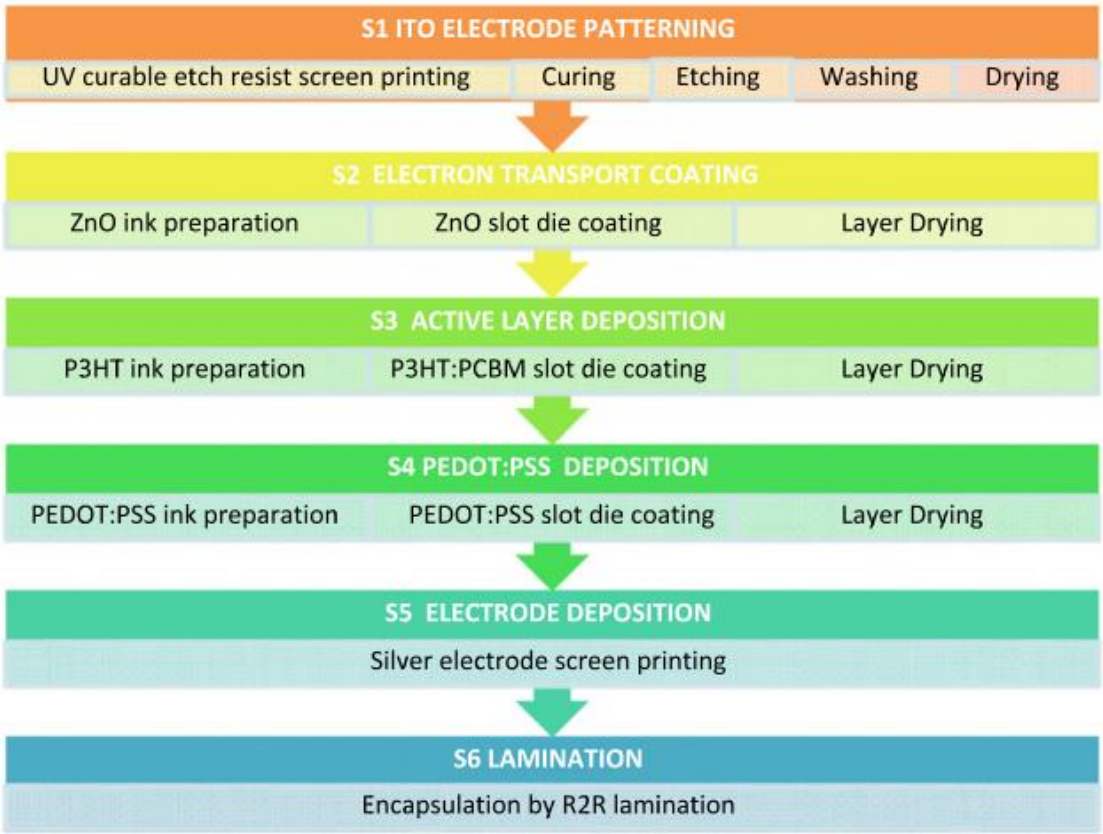

Source - ESPINOSA *et al.*, 2011

Table 11 - Material inventory for processing of 1 m² (active area of 67%) organic PV modules and their respective embodied energies in MJ (EPE - Equivalent Primary Energy)

	1 m² Processed surface (67% active area)	*Unit*	*EPE per 1 m² processed surface (67% active area) [MJ]*
S1 ITO electrode processing			
PET/ITO substrate	10,000.00	cm²	253.31
PET film	130.00	cm³	14.38
UV curable etch resist substance*	3.28	g	0.66
$CuCl_2$	0.25	g	0.02
Water	0.52	L	-
NaOH	1.66	g	0.04
Demineralized water	0.21	L	6.39E-07
S2 ET coating			
$Zn(OAc)_2$*	0.40	g	0.0131
KOH	0.20	g	0.25
MeOH	1.66	L	4.79E-02
Acetone	3.32	mL	0.17
Isopropanol	25.77	g	2.42
MEA*	0.04	g	0.15
S3 active layer deposition			
P3HT	0.10	g	0.18
PCBM	0.08	g	0.87
chlorobenzene	6.56	mL	0.51
S4 PEDOT:PSS deposition			
Isopropanol	40.52	g	Accounted before
PEDOT:PSS	29.51	g	4.70
S5 electrode deposition			
Silver ink(PV410)	19.67	g	4.13
S6 encapsulation			
3 M 467 MPF*	50.6	g	4.09
PET (2side)	72.75	g	5.87

* Missing materials

Source – Adapted from ESPINOSA *et al.*, 2011

Although ecoinvent is a very complete database, it does not have all the materials necessary for OPV manufacturing. Several of the inputs contained on the inventory had to be searched for its production process to later be inserted on OpenLCA. Besides that a very careful work is conducted to ensure that all data is correctly added. The missing materials when inserting the inventory in the software that could not even have its production process considered are the UV curable etch resist substance (step 1), $Zn(OAc)_2$ (step 2), MEA (step 2) and

3 M 467 MPF (step 6). Besides that, the silver ink synthesis is only partially added. It is made of silver acetate, which is made of silver nitrate and the other substances of the chemical reactions involving these two compounds are not introduced in the software. However, the amount of metallic silver that corresponds to the necessary to produce the silver ink used is inserted in OpenLCA. Anyway, the embodied energy corresponding to each of these materials is inserted on the software.

The study is conducted considering that the electrical energy needed is supplied by two different systems: the Danish electricity power system and the Brazilian electricity power system. The Danish power system is chosen, because it is the one used by ESPINOSA *et al.* (2011) and then the Brazilian power system, since the present study targets this country.

The product system created for OPV is illustrated on figure 55.

Figure 55: OPV product system

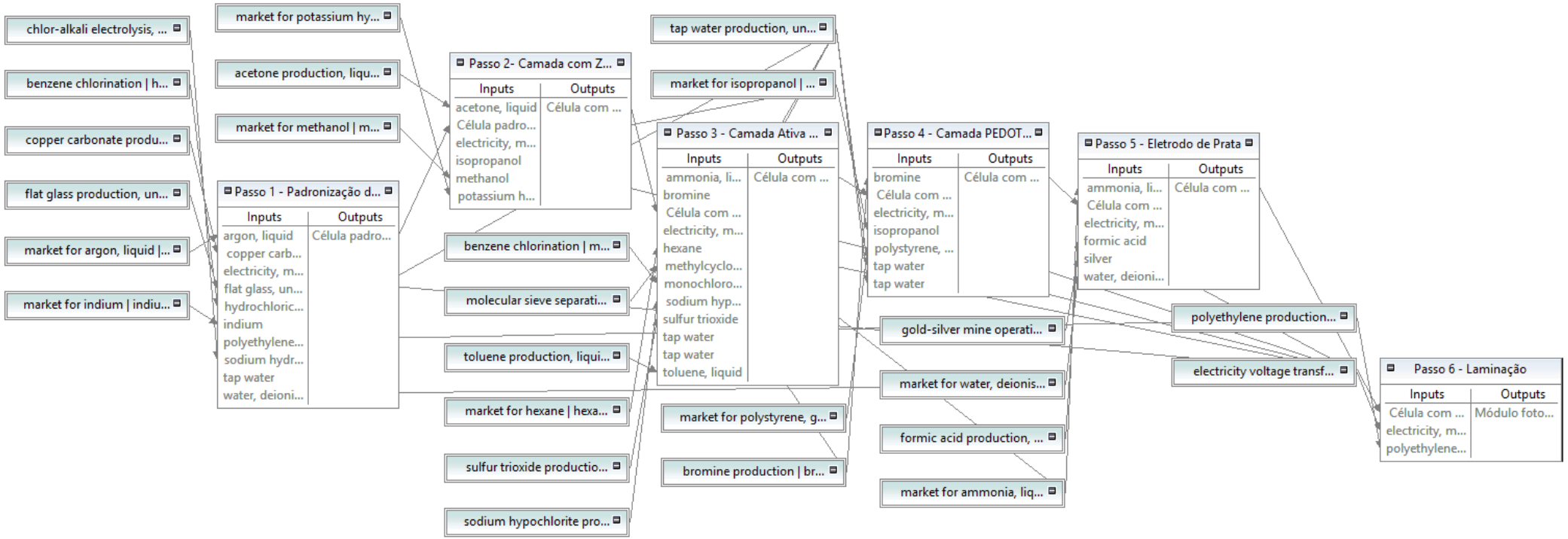

Source – Created by the author

Finally, the LCIAs are calculated for each of the impact categories previously determined. For CED calculation, the sum of all the primary sources of energy is done. Energy Payback Time is calculated according to eq. 4, in which I is the annual irradiation, Ef is the device efficiency, PR is the performance ratio of the power plant, A is the active area and 0.35 is the conversion efficiency for electricity production from the sun, as used by (ESPINOSA *et al.*, 2011). The values used are presented on table 12.

$$EPBT = \frac{CED}{I \cdot Ef \cdot PR \cdot A/0.35} \quad (2)$$

Table 12 - Values used for EPBT calculation

	EPBT calculation		
	Mono-Si	OPV	
Irradiation	2054.95	2054.95	kWh/m2
Efficiency	15	3	%
Performance Ratio	0.86	0.86	-
Active area	1.00	0.67	m2

Source – Created by the author

Table 13 presents the results obtained in OpenLCA with the Danish electricity matrix and the results from ESPINOSA *et al.* (2011) where only EPBT, GWP and CED are considered. Besides those categories, Metal Depletion Potential (MDP), Ecotoxicity total and Human Toxicity Total are taken into account. The first column is given by the software, in which the functional unit for PV module production is m^2. For the second column a generation scenario of 149.82 kWh per square meter is considered for the whole life time of the power plant according to the LCOE calculations, third column uses a scenario of 410.04 kWh according to ESPINOSA *et al.* (2011). Those values divide the impact indicators to transform the functional unit in kWh, according to the LCA scope. Following that, there is a column for what is given by the paper per m^2 and then per kWh.

GWP calculated through the software is lower than in the reference article, but still of the same order of magnitude. The difference is attributed to the missing materials in the inventory. The same happens to the CED. This fact, associated to the higher radiation, results in a smaller EPBT value. Since the difference

between energy calculated per square meter of module is considerably different when taking into account the article and according to what is calculated on the LCOE, then the impact indicators per kWh also reflect this modification depending on the way it is calculated.

Table 13 - Comparison between results from OPV inserted in OpenLCA with Danish electricity matrix and results from (ESPINOSA *et al.*, 2011)'s LCA of OPV that also uses this electricity matrix.

Impact category	Danish matrix in OpenLCA			ESPINOSA et al., (2011)		
	*/m^2	**/kWh	***/kWh	*/m^2	***/kWh	
MDP	6.363	0.042	0.016	-	-	kg Fe_{-Eq}
GWP 100a	7.852	0.052	0.019	15.49	0.038	kg CO_{2-Eq}
Ecotoxicity	747.316	4.988	1.823	-	-	CTU
Human Tox.	5.49E-05	3.66E-07	1.34E-07	-	-	CTU
CED	186.877	1.247	0.456	379.23	0.925	MJ_{-Eq}
EPBT		0.51			1.35	Year

* Impact indicator per m^2 of module

** Impact indicator per kWh of electrical energy generated according to what was calculated for LCOE for OPV (149.82 kWh)

*** Impact indicator per kWh of electrical energy generated according to what is considered by ESPINOSA *et al.*, (2011) (410.04 kWh)

EPBT is unique for any scenario

Source – Created by the author

Table 14 presents a comparison between the results from OpenLCA with the Danish electricity matrix and the Brazilian one. EPBT is lower for the Brazilian case as well as GWP and CED, while MDP, Ecotoxicity and Human Toxicity Total are technically the same, as expected.

Table 14 - Comparison between impact categories when using electricity matrixes inserted in OpenLCA, one from Denmark and the other from Brazil

Impact category	Danish			Brazilian			Unit
	*/m^2	**/kWh	***/kWh	*/m^2	**/kWh	***/kWh	
MDP	6.363	0.042	0.016	6.335	0.042	0.015	kg Fe_{-Eq}
GWP 100a	7.852	0.052	0.019	6.520	0.044	0.016	kg CO_{2-Eq}
Ecotoxicity	747.316	4.988	1.823	741.694	4.951	1.809	CTU
Human Tox.	5.49E-05	3.66E-07	1.34E-07	5.46E-05	3.64E-07	1.33E-07	CTU
CED	186.877	1.247	0.456	169.378	1.131	0.413	MJ_{-Eq}
EPBT		0.511			0.464		Year

* Impact indicator per m^2 of module

** Impact indicator per kWh of electrical energy generated according to what was calculated for LCOE for OPV (149.82 kWh)

*** Impact indicator per kWh of electrical energy generated according to what is considered by ESPINOSA *et al.*, (2011) (410.04 kWh)

EPBT is unique for any scenario

Source – Created by the author

Table 15 shows de CED results for 1kWh electricity in medium voltage for Brazil and Denmark. It shows that Brazil uses much less fossil and nuclear and much more water. This country also uses less wind.

Table 15 - CED results for both electricity mixes

	Brazil	Denmark
Fossil	1.76258	3.79073
Primary forest	0.04873	0.00061
Biomass	1.27629	1.54343
Solar	5.53E-06	1.52E-05
Geothermal	0.00013	0.00033
Wind	0.03784	0.98996
Water	3.04716	0.93440
Nuclear	0.39668	1.17532
TOTAL	6.56942	8.43480

Source – Created by the author

For a broader view of the LCA, results by impact category per process contribution are presented on figure 56, figure 57, figure 58 and figure 59 respectively corresponding to GWP, followed by Ecotoxicity, Human Toxicity Total and metal depletion. They are images captured from the OpenLCA screen. CED is not present since it is detailed into too many impact categories, one for each primary energy source, for example, solar, geothermal, hydro and

so on and that is not the focus of this study. A cut-off of 1% is used, it means that processes with less than this value of contribution are not presented.

In the case of GWP, as shown in figure 56 “electricity voltage transformation from high to medium” is the main contributor, it indicates that this process together with all the up flow process, like the electrical energy generation are included. Then there is the flat glass production and methanol, followed by other smaller contributions.

Figure 56 - Process contributions for climate change – GWP 100a of OPV production

Impact category: climate change - GWP 100a Cut-off: 1 %

Contribution	Process	Amount	Unit
30.12%	electricity voltage transformation from high to medium ...	1.96396	kg CO2-Eq
25.12%	flat glass production, uncoated | flat glass, uncoated | cut...	1.63787	kg CO2-Eq
12.17%	market for methanol | methanol | cut-off, S - GLO	0.79361	kg CO2-Eq
09.07%	gold-silver mine operation with refinery | silver | cut-off, ...	0.59133	kg CO2-Eq
07.67%	market for indium | indium | cut-off, S - GLO	0.50038	kg CO2-Eq
07.59%	polyethylene production, high density, granulate | polyet...	0.49509	kg CO2-Eq
05.14%	market for argon, liquid | argon, liquid | cut-off, S - GLO	0.33523	kg CO2-Eq
01.88%	market for isopropanol | isopropanol | cut-off, S - GLO	0.12283	kg CO2-Eq

Source – Obtained by the author

When considering Ecotoxicity only two processes contribute with more than 1%. They are gold-silver mine operation with refinery and market for indium.

Figure 57 - Process contributions for Ecotoxicity – total of OPV production

Impact category: ecotoxicity - total Cut-off: 1 %

Contribution	Process	Amount	Unit
96.65%	gold-silver mine operation with refinery | silver | cut-off, S - PE	716.88422	CTU
01.81%	market for indium | indium | cut-off, S - GLO	13.40719	CTU

Source – Obtained by the author

In the case of Human Toxicity, the same two processes appear as the main contributors for this impact category.

Figure 58 - Process contributions for Human Toxicity – Total of OPV production

Impact category: human toxicity - total Cut-off: 1 %

Contribution	Process	Amount	Unit
90.01%	gold-silver mine operation with refinery | silver | cut-off, S - PE	4.91152E-5	CTU
07.87%	market for indium | indium | cut-off, S - GLO	4.29597E-6	CTU

Source – Obtained by the author

Finally, for metal depletion, besides the same two process of the previous category, flat glass production is included.

Figure 59 - Process contributions for metal depletion – MDP – of OPV production

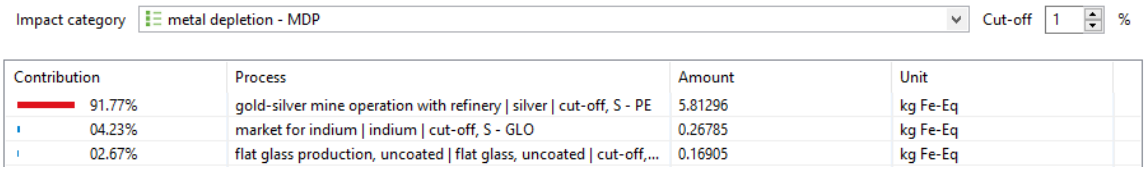

Impact category: metal depletion - MDP | Cut-off: 1 %

Contribution	Process	Amount	Unit
91.77%	gold-silver mine operation with refinery | silver | cut-off, S - PE	5.81296	kg Fe-Eq
04.23%	market for indium | indium | cut-off, S - GLO	0.26785	kg Fe-Eq
02.67%	flat glass production, uncoated | flat glass, uncoated | cut-off,...	0.16905	kg Fe-Eq

Source – Obtained by the author

The CED analysis takes to the conclusion that fossil, geothermal and solar are the only ones that do not have voltage transformation as main process contribution. If analyzing the process contributions when using the Danish electricity matrix, the same processes appear on the same order as for the Brazilian electricity matrix (the results presented above) with some variation on each percentage of contribution only.

4.5.2 LCA for Mono-Si devices

Mono-Si panel production LCA was done according to ecoinvent's database's process named "photovoltaic panel production, single-Si wafer | photovoltaic panel, single-Si wafer | cut-off, S - RoW", through which a product system is created. The electricity matrix is considered by ecoinvent according to an average of the global production of this good. On table 16, it is compared with the process for OPV inserted in OpenLCA for the Brazilian electricity matrix. For mono-Si, there is only one scenario for energy generation in order to calculate impact indicators per kWh, which is the energy calculated for LCOE. One can notice that for each indicator that OPV has a lower value than mono-Si, it would also be lower for OPV considering any energy matrix or ESPINOSA *et al.* (2011)'s study when comparing in terms of kWh and vice versa.

Table 16 shows that EPBT is higher for mono-Si as well as CED and GWP, however for the others impact categories indicators, OPV has higher levels, namely, Ecotoxicity, Human Toxicity Total and Metal Depletion Potential, but for this last one, the result is very close to the scenario for 410.04 kWh of energy generated by the module. In the case of Ecotoxicity, the values are also considerably similar.

Table 16 - Comparison between the OPV module in OpenLCA with Brazilian electricity matrix and the mono-Si from ecoinvent

Impact category	OPV with Brazilian matrix			Mono-Si		
	*/m^2	**/kWh	***/kWh	*/m^2	****/kWh	
MDP	6.335	0.042	0.015	25.813	0.014	kg Fe_{-Eq}
GWP 100a	6.520	0.044	0.016	282.350	0.150	kg CO_{2-Eq}
Ecotoxicity	741.694	4.951	1.809	3164.372	1.683	CTU
Human Tox.	5.46E-05	3.64E-07	1.33E-07	1.50E-04	7.98E-08	CTU
CED	169.378	1.131	0.413	4235.832	2.253	MJ_{-Eq}
EPBT		0.464		1.554		Year

* Impact indicator per m^2 of module

** Impact indicator per kWh of electrical energy generated according to what was calculated for LCOE for OPV (149.82 kWh)

*** Impact indicator per kWh of electrical energy generated according to what is considered by ESPINOSA *et al.*, (2011) (410.04 kWh)

**** Impact indicator per kWh of electrical energy generated according to what is calculated for LCOE for mono-Si (1879.98 kWh)

EPBT is unique for any scenario

Source – Created by the author

The complete inventory for both technologies is available at www.ppgee.ufmg.br/~wadaed

4.6 Discussion

This section discusses the results obtained. First, the experimental results are commented and, in the sequence, the result of the methodologies used are analyzed.

The procedures have been conducted in such way that humidity does not penetrate until the mono-Si cell (the use of 1.5 cm extra edge of glass, EVA and Tedlar, as described on section 3.1.2) were effective. It avoided that delamination reached the cell and then the lack of aluminum frame was not a problem in this experiment. In general, the visual modifications of the devices are minor and this is not an aspect that took evidence in the study.

On the electrical performance, the action of the climatic chamber is more intense than the one of the light stability chamber for both technologies, as can be observed from figure 43. Figure 46 shows that the device that decreases more the Isc value for OPV is the one in the light stability chamber and for mono-Si is the one in the climatic chamber. Analyzing figure 40 that brings IV

curves for the mono-Si device in the climatic chamber and together with figure 36 that shows the IV curves for the OPV in the light stability chamber, this same fact can be noticed. The Im value follows a similar pattern as can be observed on figure 44. Figure 47 shows that Voc only has significant decrease for the OPV device on the climatic chamber what can also be observed from figure 37 and the others figures on sections 4.3.2 and 4.3.3. Analogously, figure 45 shows similar results for Vm. figure 48 shows that all the mono-Si devices have similar losses of FF and the OPV on the climatic chamber have a huge drop on its FF value, it can also be observed on figure 37. Finally, figure 49 presents a similar behavior of figure 43 for OPV, because mono-Si devices are much more stable, then the ratio between them is predominated by the OPV values, it is worth noticing that the ratio for devices in the drawer increases through time.

OPV and mono-Si are compared considering the obtained results from LCOE and LCA studies. The results are summarized on table 17. It is possible to conclude that the main advantage of OPV is that it is a technology that consumes much less energy on its production, as can be seen on the CED values, what reflects on the EPBT and GWP, because energy generation is one of the main causes of this environmental impact. However, the others impact categories show worse results for this type of device, namely, MDP, Ecotoxicity and Human Toxicity Total. However, a quantitative analysis of the differences between those impact indicators for each technology is not conducted, because the OPV inputs have missing materials that would still increase some of its results. Besides that, its average LCOE is almost 4 times higher than for mono-Si, but it has to be taken into account that OPV is a much newer technology. One square meter of mono-Si produces more than 12.5 times more energy than one square meter of OPV during the time that the power plant proposed operates (ten years), according to section 3.1.4. In a general aspect, this emerging technology is not more interesting than the benchmark yet.

Table 17 - General comparison between OPV and mono-Si

	OPV	Mono-Si	
Total energy produced per m^2	149.82	1879.98	kWh
MDP	0.042	0.014	kg $Fe-_{Eq}$/kWh
GWP 100a	0.044	0.150	kg $CO2-_{Eq}$/kWh
Ecotoxicity	4.951	1.683	CTU/kWh
Human Tox.	3.64E-07	7.98E-08	CTU/kWh
CED	1.131	2.253	$MJ-_{Eq}$/kWh
EPBT	0.464	1.554	Year
LCOE	2.211	0.576	R$/kWh

Source – Created by the author

Besides that, a power plant with the same installed capacity made of OPV modules occupies a much larger area than one made of mono-Si. Therefore, an OPV system may have its installed capacity limited by the available area or its modules may have to be positioned on areas subject to be shaded or on parts of a building that do not favor the light incidence angle depending on the project.

At first, considering the area occupied by the power plant, MDP, Ecotoxicity, Human Toxicity Total and the amount of energy produced by each square meter of OPV modules, this technology seems to be a worse option. Nevertheless, there are characteristics that were not mentioned yet, but it is worth considering. It still has a great potential of improvement in efficiency and life time, taking into account that the technology is new and is in a development stage far below from mono-Si. It would increase the amount of energy generated per module and then decrease the environmental impacts per kWh as well as the price for each unit of energy.

Nowadays, the usage of OPV is related to specific situations when its specific characteristics make it the best or the unique technology possible (SUNEW, 2017). It may be due to the lightweight, so it can be installed in vehicles, roofs with weak structures, floating structures; to transparency and then it can be used in greenhouses and environments that demands natural light penetration as well or to design purposes, so it can assume different colors and shapes to be in harmony with any type of building. Another characteristic that favors

harmony with buildings or vehicles is the flexibility, because it can assume different shapes.

The comparison between both technologies was carried out, but one must be aware of its limitations. The mono-Si technology was used as a reference since it is a benchmark, allowing the comparison of indicators. Since both technologies have very different results for LCOE as well as LCA, it reinforces that they are technologies adequate for different applications. One technology does not replace the other and they occupy different niches.

Manufacturers have been working under demand and producing OPV modules for customized solutions (PÄTZOLD, 2017). In the near future, it may be possible to find OPV modules combined with different materials such as glass, concrete, steel or PV membrane (GRAFE, 2017). Furthermore, a company's option to purchase an OPV system may be related to its intention of making sustainable marketing. The literature signalizes that OPV brings more forms of solar energy use.

Finally, it is very important to emphasize that the study puts the two technologies in conditions as equal as possible to make the comparison fair in order to estimate the development gap between them. Thus, the tests and methods are applied on the same manner for both, anyway, when coming to real applications, specific characteristics of each type of device must be taken into account to define the project choice.

5 CONCLUSIONS

In this last chapter, conclusions are drawn in terms of technologies comparison and right after that, future work is recommended.

5.1 Technologies comparison

Many aspects related to PV technologies had to be understood to accomplish this work, such as how the cells and modules are structured, how to obtain the IV curves according to the Standard Test Conditions (STC), how to calculate the Levelized Cost of Energy (LCOE), how to conduct a Life Cycle Assessment (LCA) and how the accelerated aging tests are done.

This knowledge made it possible to develop a methodology to compare Organic Photovoltaics (OPV) and monocrystalline silicon (mono-Si). It considered their performance through time and used this information as inputs for LCA and LCOE, so that impact indicators and costs could be calculated in order to be used as decision criteria.

Despite the differences between OPV and mono-Si technologies, this study brought both to the same basis in order to establish a comparison, that is, both were laminated, they were left side by side on the same aging conditions, the LCA scope was equivalent for both technologies and the LCOE was calculated for power systems that the differences were only due to the module type.

The LCOE for OPV was twice as much than for mono-Si. Ecotoxicity Total, Human Toxicity Total and Metal Depletion Potential were also higher, emphasizing weaknesses of this technology. However, OPV had lower Cumulative Energy Demand, highlighting its manufacturing process as a less energy intensive process, which collaborated for a lower Energy Payback Time as well. Moreover, since most of the contributions to Global Warming Potential come from electrical energy generation, this impact indicator also showed a smaller value for OPV. As a general result, mono-Si has a better performance than OPV nowadays.

5.2 Future work recommendation

After concluding this study, it is possible to visualize some future work that would be suitable. One of them is to use a Life Cycle Impact Assessment (LCIA) method for monetary quantification of impacts in a way that the result could be summed with the LCOE for a unique final value.

Other interesting possibility is to conduct similar study with primary data for the LCI coming directly from an OPV manufacturer. This would enhance data quality and then LCA precision.

Finally, the same methodology applied in this master's thesis could be reproduced for any other emerging PV technology, for example, perovskite.

6 REFERENCES

ANCTIL, Annick *et al.* Life-cycle assessment of organic solar cell technologies. *Renewable Energy*, p. 742–747, 2010.

ANCTIL, Annick; FTHENAKIS, Vasilis. Life Cycle Assessment of Organic Photovoltaics. Third Generation Photovoltaics, n. March, p. 91–110, 2012.

ASSOCIAÇÃO BRASILEIRA DE NORMAS TÉCNICAS. ABNT NBR ISO 14040 Gestão ambiental - Avaliação do ciclo de vida - Princípios e estrutura. Associação Brasileira de Normas Técnicas, p. 1–22, 2014.

ASSOCIAÇÃO BRASILEIRA DE NORMAS TÉCNICAS. ABNT NBR ISO 14044 Gestão ambiental - Avaliação do ciclo de vida – Requisitos e orientações. Associação Brasileira de Normas Técnicas, p. 1–45, 2014.

ASTM. Standard Test Methods for Photovoltaic Modules in Cyclic Temperature and Humidity. ASTM Standard E 1171S, v. i, n. September, p. 1–5, 2001.

BOSCH SOLAR ENERGY. High performance – Stable yields . Bosch Solar Cell M 3BB. p. 3–4, [S.d.].

BOURGAULT, G; WERNET, G. Documentation of changes implemented in the ecoinvent. v. 3, 2016.

BRANKER, K.; PATHAK, M.J.M.; PEARCE, J.M. A review of solar photovoltaic levelized cost of electricity. *Renewable and Sustainable Energy Reviews*, v. 15, n. 9, p. 4470–4482, 2011.

BUENO, Poliana, H. Modelagem Analítica e Numérica Semiempírica de Células Fotovoltaicas. p. 1-135. Belo Horizonte, 2016.

CHENG, Jiaqi et al. Efficient Hole Transport Layers with Widely Tunable Work Function for Deep HOMO Level Organic Solar Cells. J. Mater. Chem. A, v. 0, p. 1–9, 2015.

DARLING, Seth B.; YOU, Fengqi. The case for organic photovoltaics. *RSC Advances*, v. 3, n. 39, p. 17633, 2013.

DARLING, Seth B; YOU, Fengqi; VELOSA, Alfonso. Environmental Science Assumptions and the levelized cost of energy for photovoltaics. Energy & Environmental Science, v. 4, n. 9, p. 3133–3139, 2011.

DINIZ, Jean. Metodologia para análise de investimento em sistemas fotovoltaicos considerando parâmetros de incerteza e métricas de risco. P 1-120. 2017.

ESPINOSA, Nieves et al. A life cycle analysis of polymer solar cell modules prepared using roll-to-roll methods under ambient conditions. Solar Energy Materials and Solar Cells, v. 95, n. 5, p. 1293–1302, 2011.

ESPINOSA, Nieves et al. Life cycle assessment of ITO-free flexible polymer solar cells prepared by roll-to-roll coating and printing. Solar Energy Materials and Solar Cells, v. 97, p. 3–13, 2012.

ESPINOSA, Nieves; KREBS, Frederik C. Life cycle analysis of organic tandem solar cells: When are they warranted? Solar Energy Materials and Solar Cells, v. 120, n. PART B, p. 692–700, 2014.

FILHO, Tiago. Ciclo de vida para estudo comparativo entre os impactos ambientais advindos de diferentes tecnologias de células fotovoltaicas. 2013.

FRISCHKNECHT, Rolf et al. Implementation of Life Cycle Impact Assessment Methods. Ecoinvent Report n.o3, v2.2, n. 3, 2010.

FTHENAKIS, V. M. et al. Methodology Guidelines on Life Cycle Assessment of Photovoltaic Electricity. 2011. v. IEA PVPS T.

FTHENAKIS, Vasilis M et al. Life cycle analysis of high-performance monocrystalline silicon photovoltaic systems: Energy payback times and net energy production value. 27th European Photovoltaic Solar Energy Conference and Exhibition, p. 4667–4672, 2012.

GAMBHIR, Ajay; SANDWELL, Philip; NELSON, Jenny. The future costs of OPV – A bottom-up model of material and manufacturing costs with uncertainty analysis. Solar Energy Materials and Solar Cells, v. 156, p. 49–58, 2016.

GARCÍA-VALVERDE, Rafael; CHERNI, Judith A.; URBINA, Antonio. Life cycle analysis of organic photovoltaic technologies. *Progress in Photovoltaics: Research and Applications*, v. 18, n. 7, p. 535–538, 2010.

GMBH, Greendelta. ecoinvent v.3.3 in openLCA. n. September, p. 1–20, 2016.

GOEDKOOP, Mark; HUIJBREGTS, Mark. ReCiPe 2008 Characterisation. 2013.

GRAFE, Andrea. Request Heliatek Websit [personal message]. Message received by brunosbampato@gmail.com on 4th of September of 2017.

HENGEVOSS, Dirk et al. Life Cycle Assessment and eco-efficiency of prospective, flexible, tandem organic photovoltaic module. Solar Energy, v. 137, p. 317–327, 2016.

INTERGOVERNMENTAL PANEL ON CLIMATE CHANGE. Climate change 2013: The Physical Science Basis. 2013.

JUNQUEIRA, Rafael Coelho. Valoração monetária dos impactos ambientais de usinas fotovoltaicas através de avaliação de ciclo de vida. Belo Horizonte, 2016.

KEITHLEY INSTRUMENTS. Series 2600B System SourceMeter ® Instrument Reference Manual. n. September, 2012.

KEITHLEY INSTRUMENTS. System SourceMeter ® Instruments Quick Start Guide. 2012.

LABORATÓRIO ASSOCIADO DE SENSORES E MATERIAIS. Simulador solar de baixo custo para testes de células solares. 2009.

LIZIN, Sebastien *et al.* Life cycle analyses of organic photovoltaics: a review. *Energy & Environmental Science*, v. 6, n. 11, p. 3136, 2013.

LO, Vivien et al. Manufacturing cost modeling for flexible organic solar cells. Proceedings of Technology Management for Emerging Technologies, p. 2951–2956, 2012.

LOJA ELÉTRICA. Chave 14123 mft1fp1q liga/desliga tecla 15a margirius. 2017. Available on: <http://www.lojaeletrica.com.br/chave-14123-mft1fp1q-ligadesliga-

tecla-15a-margirius,product,2160402310508,dept,12001.aspx>. Accessed on 1st of September of 2017.

LOJA ELÉTRICA. Rolo cabo flexível 750v 1,50mm² 100 metros vermelho. 2017. Available on: <http://www.lojaeletrica.com.br/rolo-cabo-flexivel-750v-150mm2-100-metros-vermelho,product,2180900000930,dept,2004.aspx>. Accessed on 1st of September of 2017.

MACHUI, Florian et al. Cost analysis of roll-to-roll fabricated ITO free single and tandem organic solar modules based on data from manufacture. Energy & Environmental Science, v. 7, n. 9, p. 2792, 2014.

MARKVART, T. AND CASTANER, L. Practical Handbook of Photovoltaics: Fundamentals and Applications. P 1-1015. 2003.

MIRANDA, Raul Figueiredo Carvalho. Análise Da Inserção De Geração Distribuída De Energia Solar Fotovoltaica No Setor Residencial Brasileiro. *Dissertação M. Sc. PPE*, p. 291, 2013.

MULLIGAN, Cara J. et al. A projection of commercial-scale organic photovoltaic module costs. Solar Energy Materials and Solar Cells, v. 120, n. PART A, p. 9–17, 2014.

NATIONAL RENEWABLE ENERGY LABORATORY. Best research-cell efficiencies. 2017. Available on: <https://www.nrel.gov/pv/assets/images/efficiency-chart.png>. Accessed on 19th of September of 2017.

NATIONAL RENEWABLE ENERGY LABORATORY. Levelized Cost of Energy. 2017. Available on: <https://www.nrel.gov/analysis/sam/help/html-php/index.html?mtf_lcoe.htm>. Accessed on 1st of August of 2017.

NDIAYE, Ababacar *et al.* Degradations of silicon photovoltaic modules: A literature review. *Solar Energy*, v. 96, p. 140–151, 2013.

PÄTZOLD, Ralph. Standard Anfrage über opvius.com [personal message]. Message received by brunosbampato@gmail.com on 25th of August of 2017.

ROSA, Carlos Adriano. Análise da capacidade de amortização dos passivos energéticos e ambientais dos painéis fotovoltaicos. v. 19, n. 35, p. 171–194, 2013.

ROSENBAUM, Ralph K. et al. USEtox - The UNEP-SETAC toxicity model: Recommended characterization factors for human toxicity and freshwater ecotoxicity in life cycle impact assessment. International Journal of Life Cycle Assessment, v. 13, n. 7, p. 532–546, 2008.

SANTOS JÚNIOR, Silvio Luís dos Reis. Análise de materiais e técnicas de encapsulamento de módulos fotovoltaicos. Porto Alegre, 2008. p. 1–180, 2011.

SBAMPATO, Bruno De Á. et al. Caracterização elétrica de uma célula fotovoltaica. Congresso Brasileiro de Enegia Solar. p. 1–8, 2016.

SHAHEEN, Sean E.; GINLEY, David S.; JABBOUR, Ghassan E. Organic-Based Photovoltaics: Toward Low-Cost Power Generation. MRS Bull. v. 30, n. January, p. 10–19, 2005.

SUNEW. Proposta de Aplicação [personal message]. Message received by brunosbampato@gmail.com on 24th of August of 2017.

System SourceMeter ® Instruments Quick Start Guide. 2012.

TIAGO Filho, G. L; ROSA, C. A. Análise da capacidade de amortização dos passivos energéticos e ambientais dos painéis fotovoltaicos. Revista Brasileira de Energia, v. 19, n. 1, p 171-194. 2013.

TOM MARKVART AND LUIS CASTANERW. Practical Handbook of Photovoltaics: Fundamentals and applications. *Elsevier*, 2003.

TSANG, Michael. P. Sonnemann, Guido. W. & Bassani, Dario. M. A comparative human health, ecotoxicity, and product environmental assessment on the production of organic and silicon solar cells. *Progress in Photovoltaics,* v. 24, p. 645-655, 2015.

WINTER, Sarah *et al.* openLCA 1.4 Comprehensive User Manual. n. March, p. 1–81, 2015.

YANG, Dong *et al.* Life-cycle assessment of China's multi-crystalline silicon photovoltaic modules considering international trade. *Journal of Cleaner Production*, v. 94, p. 35–45, 2015.

YUE, Dajun *et al.* Deciphering the uncertainties in life cycle energy and environmental analysis of organic photovoltaics. *Energy & Environmental Science*, v. 5, n. 11, p. 9163, 2012.